Received: 15 February 2024 | Revised: 28 June 2024 | Accepted: 7 July 2024

DOI: 10.1111/bph.17317

INVITED REVIEW

Advancing the field of viroporins—Structure, function and pharmacology: IUPHAR Review 39

Kira Devantier[1,2] | Viktoria M. S. Kjær[1] | Stephen Griffin[3,4] | Birthe B. Kragelund[2] | Mette M. Rosenkilde[1]

[1]Molecular and Translational Pharmacology, Department of Biomedical Sciences, University of Copenhagen, Copenhagen, Denmark

[2]Structural Biology and NMR Laboratory, Department of Biology, University of Copenhagen, Copenhagen, Denmark

[3]Leeds Institute of Medical Research, St James' University Hospital, School of Medicine, Faculty of Medicine and Health, University of Leeds, Leeds, UK

[4]Astbury Centre for Structural Molecular Biology, University of Leeds, Leeds, UK

Correspondence
Mette M. Rosenkilde, Molecular and Translational Pharmacology, Department of Biomedical Sciences, University of Copenhagen, Blegdamsvej 3B, Copenhagen 2200, Denmark.
Email: rosenkilde@sund.ku.dk

Funding information
Danish Council for Independent Research|Medical Sciences, Grant/Award Number: DFF1: 6110-00688B; European Research Council, Grant/Award Number: Grant agreement 682549; donation from deceased Valter Alex Torbjørn Eichmuller, Grant/Award Number: 2020-117043; Lundbeck Foundation, Grant/Award Number: R242-2017-409; Novo Nordisk Fonden, Grant/Award Numbers: NNF18OC0033926, NNF20OC0062899

[Correction added on 9 September 2024, after first online publication: The 'X' in the article title has been updated with the corresponding IUPHAR Review number in this version.]

Viroporins possess important potential as antiviral targets due to their critical roles during virus life cycles, spanning from virus entry to egress. Although the antiviral amantadine targets the M2 viroporin of influenza A virus, successful progression of other viroporin inhibitors into clinical use remains challenging. These challenges relate in varying proportions to a lack of reliable full-length 3D-structures, difficulties in functionally characterising individual viroporins, and absence of verifiable direct binding between inhibitor and viroporin. This review offers perspectives to help overcome these challenges. We provide a comprehensive overview of the viroporin family, including their structural and functional features, highlighting the moldability of their energy landscapes and actions. To advance the field, we suggest a list of best practices to aspire towards unambiguous viroporin identification and characterisation, along with considerations of potential pitfalls. Finally, we present current and future scenarios of, and prospects for, viroporin targeting drugs.

KEYWORDS
antiviral drug, membrane protein, viroporin

Abbreviations: $2B_{CVB3}$, coxsackievirus B3 2B; $2B_{HAV}$, hepatitis A virus 2B; $2B_{PV}$, poliovirus 2B; $3a_{SARS\text{-}CoV\text{-}2}$, SARS-CoV-2 3a; $6K_{CHIKV}$, chikungunya virus 6K; $6K_{RRV}$, Ross river virus 6K; CD-$M2_{IAV}$, conductance domain $M2_{IAV}$; $E5_{HPV}$, human papillomavirus E5; $E_{SARS\text{-}CoV\text{-}1}$, severe acute respiratory coronavirus 1 E protein; $E_{SARS\text{-}CoV\text{-}2}$, severe acute respiratory coronavirus 2 E protein; HMA, hexamethylene amiloride; IAV, influenza A virus; $Kcv_{PBCV\text{-}1}$, *Paramecium bursaria* chlorella virus 1 Kcv; $M2_{IAV}$, influenza A virus M2; $M2_{IBV}$, influenza B virus M2; M_{DENV}, dengue virus M; M_{WNV}, West Nile virus; M_{ZIKV}, Zika virus M; $NS2B_{DV}$, dengue virus NS2B; $NS3_{BTV}$, blue tongue virus NS3; $NS7a_{PDCoV}$, porcine delta coronavirus NS7a; $p7_{CSFV}$, classical swine fever virus p7; $p7_{HCV}$, hepatitis C virus p7; PDB, Protein Data Bank; SH_{HMPV}, human metapneumovirus SH protein; SH_{hRSV}, human respiratory syncytial virus SH protein; ssNMR, solid state NMR; $Vpu_{HIV\text{-}1}$, human immunodeficiency virus 1 Vpu; XP_{HAstV}, human astrovirus protein X.

Kira Devantier and Viktoria M. S. Kjær contributed equally.

1 | INTRODUCTION

A key feature of viruses is their ability to implement complex host cell rearrangements essential for productive viral infection (Kellermann et al., 2021). This includes changes to the ion gradients across both viral and host membranes (Carrasco, 1978; Liu et al., 2016; Wozniak et al., 2010). Viral membrane proteins capable of increasing membrane permeability to ions and other small solutes are termed 'viroporins'; they carry out critical functions during virus life cycles and are continuously identified in a growing number of viruses (Nieva et al., 2012; Scott & Griffin, 2015). Thus, blocking the channel function of viroporins provides strategies to alleviate virus-mediated pathology and to suppress infection. Novel, re-emerging and endemic viruses are a significant source of human and animal disease and death worldwide (Baker et al., 2022). For most viruses, effective preventative measures, that is, vaccines, and antiviral therapeutics are lacking (De Clercq & Li, 2016; Tannock et al., 2020). Thus, a critical demand exists for new antivirals to target known and future emerging viruses.

Membrane proteins comprise one-third of all human drug targets, with ion channels specifically accounting for ~20% (Santos et al., 2017). About half of the currently marketed small molecule drugs target membrane proteins, reflecting their ease of accessibility and excellent druggability (Santos et al., 2017). By contrast, most small molecule drugs targeting viral proteins target soluble, primarily enzymatic, components of viral replicase complexes (De Clercq & Li, 2016). This discrepancy suggests that antiviral development opportunities are being under-utilised. With the influenza A virus (IAV) drugs **amantadine** and rimantadine as proof of concept, viroporins constitute a class of viral membrane proteins with prospective druggability and, thus, potentially crucial societal impact.

1.1 | History of viroporins

In the 1970s, virus infections were first observed to cause cell membrane permeabilisation to ions and small solutes not otherwise able to penetrate the host cell. It was originally proposed that viral, rather than host, translation was favoured after increased cytoplasmic cation concentration (Carrasco, 1978). A viral gene product was suspected of causing permeabilisation, but it was not until 1995, after the identification of a handful of proteins from RNA viruses responsible for such effects, that Louis Carrasco grouped and coined the term 'viroporins' (Carrasco, 1995). Although most (~90%, Table 1) of the accepted, or potential, viroporins are encoded by RNA viruses, there are also examples of viroporins or prospective viroporins in DNA viruses (Table 1) (Royle et al., 2015). The full extent to which viruses encode viroporins is still uncertain, because new candidate viroporins are continually reported. Some viruses may even encode more than one viroporin (Table 1), although the reason for such potential functional redundancy is unknown, leading to controversy and debate (Lamb & Pinto, 1997; Toft-Bertelsen et al., 2022).

There has been consistently growing insight into viroporin function in recent years, requiring constantly updated contemporary overviews of current knowledge. This review provides a comprehensive introduction to viroporins as a protein family, as well as highlighting the challenges in the field. We propose definitions and a range of best practices for viroporin identification, followed by an overview of the structural and functional characteristics of the family. This provides a basis for understanding how viroporins can be exploited for antiviral treatments, how this has progressed to date and what therapeutic possibilities the future may hold.

2 | PROPOSED BEST PRACTICE FOR DEFINING, IDENTIFYING AND CHARACTERISING VIROPORINS

The definition of viroporins is virus-encoded transmembrane (TM) proteins that, through homo-oligomerisation, form pores in membranes permeating them to ions and small solutes. As an example of functionally convergent evolution, with high sequence and structural diversity, viroporins exist in a continuum ranging from pores that select substrates only by size exclusion to pores that act as selective ion channels (Figure 1a). One viroporin may preferentially adhere to either end of the spectrum but may also adopt alternate characteristics on the spectrum depending on the environmental context. For example, the viroporin p7 from classical swine fever virus ($p7_{CSFV}$) simultaneously forms two subsets of pores, one with a weak anionic selectivity and the other with a weak cationic selectivity (Largo et al., 2016). Further illustrating this functional malleability, the viroporin M2 from IAV ($M2_{IAV}$), known as a highly proton-selective ion channel, allows passage of potassium ions, as well as relatively large molecules such as the anionic carboxyfluorescein with a hydrodynamic diameter of ~5 Å when reconstituted in liposomes (Scott et al., 2020) or hygromycin B when expressed in bacteria (Guinea & Carrasco, 1994). The uncertain mechanism of substrate selectivity could result from missing technical knowledge to study the authentic function of viroporins, rather than viroporins being inherently primitive pores. However, until research can further delineate this functionality, we are limited to such possibly oversimplified understanding.

Viroporins are diverse in their functions, but they all affect host cell membranes. Some viroporins are present only in the host cell following virus gene expression (e.g., non-structural proteins like poliovirus 2B ($2B_{PV}$)), whereas others additionally reside within virions (structural proteins such as $M2_{IAV}$). Although their presence in virions is known for some viroporins, the associated function is less well studied, if at all. Moreover, the picture is further complicated by many viroporins also performing non-pore related functions during infection (Xia, Cheng, et al., 2022).

The high evolutionary rate of many viruses, especially certain RNA virus families (Duffy, 2018), means that viroporins generally exhibit low sequence conservation, making information transfer about a viroporin from one virus to another challenging. As an illustration, the $M2_{IAV}$ forms an ion channel potently inhibited by amantadine, whereas the M2 from influenza B virus ($M2_{IBV}$) is insensitive to

TABLE 1 List of current and suggested viroporins.

Virus family	Virus	Viroporin	Length	Classification	Ion selectivity	Inhibitors	Non-functional mutants	PDB structures
Astroviridae ssRNA	Human astrovirus 1 (HAstV1)	XP (Lulla & Firth, 2020)	112	SP-Type I	-	-	L95T/L98T/L102S/L105T/ L109S (Lulla & Firth, 2020)	-
	Human astrovirus 4 (HAstV4)	XP4 (Lulla & Firth, 2020)	112	-	-	-	-	-
	Canine astrovirus (CaAstV)	CXP (Lulla & Firth, 2020)	91	-	-	-	-	-
	Feline astrovirus (FAstV)	FXP (Lulla & Firth, 2020)	112	-	-	-	-	-
	Porcine astrovirus (PAstV)	PXP (Lulla & Firth, 2020)	75	-	-	-	-	-
Caliciviridae ssRNA	Feline calicivirus	LC (Peñaflor-Téllez et al., 2022)	124	-	-	-	-	-
	Tulane virus (TV)	NS1-2 (Strtak et al., 2019)	254	[a]MP-Type II	-	-	-	-
	Rabbit haemorrhagic disease virus (RHDV)	[b]P23 (Smertina et al., 2022)	224	[a]MP-Type I	-	-	-	-
Coronaviridae ssRNA	Infectious bronchitis virus (IBV)	E (Wilson, Gage, & Ewart, 2006)	109	SP-Type I	$Na^+ > K^+ > Cl^-$ (Wilson et al., 2006)	-	-	-
	Human coronavirus 229E (HCoV-229E)	E (Wilson, Gage, & Ewart, 2006)	77	SP-Type I	$K^+ > Na^+ > > Cl^-$ (Wilson et al., 2006)	HMA (Wilson et al., 2006)	-	-
		ORF4a (Zhang et al., 2014)	133	[a]MP-Type I	$Na^+ = K^+$ (Zhang et al., 2014)	-	-	-
	Human coronavirus OC43 (HCoV-OC43)	ns12.9 (Zhang et al., 2015)	109	SP-Type II	-	-	-	-
		3a (Schwarz et al., 2011)	-	-	-	Emodin (Schwarz et al., 2011)	-	-
	Middle East respiratory syndrome related coronavirus (MERS-CoV)	E (Surya et al., 2015)	82	SP-Type I	-	-	-	-
	Murine hepatitis virus (MHV)	E (Madan et al., 2005; Wilson, Gage, & Ewart, 2006)	83	SP-Type I	$Na^+ >> K^+ > Cl^-$ (Wilson et al., 2006)	HMA (Wilson et al., 2006) [c]E N-term antibody (Wilson et al., 2006)	-	-
	Porcine deltacoronavirus	NS7a (Xia, Fang, et al., 2022)	100	[a]SP-Type I	-	-	-	-

TABLE 1 (Continued)

Virus family	Virus	Viroporin	Length	Classification	Ion selectivity	Inhibitors	Non-functional mutants	PDB structures
	Porcine epidemic diarrhoea virus (PEDV)	ORF3 (Wang et al., 2012)	224	MP-Type I	K^+ (Wang et al., 2012)	-	Y170A (Wang et al., 2012)	-
	Severe acute respiratory syndrome coronavirus 1 (SARS-CoV-1)	3a (Lu et al., 2006)	274	MP-Type I	K^+ (Lu et al., 2006)	Afzelin (Schwarz et al., 2014) Ba^{2+} (Lu et al., 2006) Emodin (Schwarz et al., 2011) Juglanin (Schwarz et al., 2014) **Kaempferol** (Schwarz et al., 2014) Kaempferol-3-O-α-rhamnopyranosyl (1 → 2) [α-rhamnopyranosyl (1 → 6)]-β-glucopyranoside (Schwarz et al., 2014) Tiliroside (Schwarz et al., 2014)	Y91A (Castaño-Rodriguez et al., 2018) H93A (Castaño-Rodriguez et al., 2018) Y109A (Castaño-Rodriguez et al., 2018) C133A (Lu et al., 2006) Y160A (Chan et al., 2009) E171A/D173A (Chan et al., 2009)	-
		8a (Chen et al., 2011)	39	SP	Cation (Chen et al., 2011)	-	-	-
		E (Liao et al., 2004; Wilson et al., 2004)	76	SP-Type I	Na^+ >> K^+ >> Cl^- (L. Wilson et al., 2006; Wilson et al., 2004)	Amantadine (Torres et al., 2007) **Apigenin** (Breitinger et al., 2021) **EGCG** (Breitinger et al., 2021) **Genistein** (Breitinger et al., 2021) HMA (Pervushin et al., 2009) Kaempferol (Breitinger et al., 2021) **Quercetin** (Breitinger et al., 2021) **Resveratrol** (Breitinger et al., 2021) Rimantadine (Breitinger et al., 2021)	N15A (Torres et al., 2007) V25F (Torres et al., 2007)	2MM4 5X29

(Continues)

TABLE 1 (Continued)

Virus family	Virus	Viroporin	Length	Classification	Ion selectivity	Inhibitors	Non-functional mutants	PDB structures
	Severe acute respiratory syndrome coronavirus 2 (SARS-CoV 2)	E (Singh Tomar & Arkin, 2020; Toft-Bertelsen et al., 2021)	75	SP-Type I	Anions ∼ cations (lipid dependent) (Surya et al., 2023)	Amantadine (Toft-Bertelsen et al., 2021) BE-12 (Xia et al., 2021) [c]BE-30 (Xia et al., 2021) [c]BE-31 (Xia et al., 2021) [c]BE-32 (Xia et al., 2021) [c]BE-33 (Xia et al., 2021) BIT225 (Ewart et al., 2023) Emodin (Toft-Bertelsen et al., 2021) Gliclazide (Singh Tomar & Arkin, 2020) HMA (Toft-Bertelsen et al., 2021) **Memantine** (Singh Tomar & Arkin, 2020) Xanthene (Toft-Bertelsen et al., 2021)	F4A (Xia et al., 2021) T11A (Xia et al., 2021)	7K3G 8SUZ 8U1T
		3a (Toft-Bertelsen et al., 2021)	275	MP-Type I	$Ca^{2+} > K^{+} > Na^{+}$ (Kern et al., 2021)	Amantadine (Fam et al., 2023) **Capreomycin** (Tomar et al., 2021) **Curcumin** (Fam et al., 2023) **Darapladib** (Tomar et al., 2021) EGCG (Fam et al., 2023) Emodin (Yu et al., 2021) **Floxuridine** (Tomar et al., 2021) **Fludarabine** (Tomar et al., 2021) **Flumbatinib** (Tomar et al., 2021) Kaempferol (Fam et al., 2023) Kasugamycin (Tomar et al., 2021) Litronesib (Tomar et al., 2021) **Nobiletin** (Fam et al., 2023)	Q57E (Kern et al., 2021) S58L/Q116L (Kern et al., 2021)	8EQJ 8EQS 8EQT 8EQU 6XDC 7KJR

TABLE 1 (Continued)

Virus family	Virus	Viroporin	Length	Classification	Ion selectivity	Inhibitors	Non-functional mutants	PDB structures
						Pentamidine (Tomar et al., 2021) **Plerixafor** (Tomar et al., 2021) Quercetin (Fam et al., 2023) Resveratrol (Fam et al., 2023) Rimantadine (Fam et al., 2023) **Spectinomycin** (Tomar et al., 2021) Xanthene (Toft-Bertelsen et al., 2021)		
		ORF7b (Toft-Bertelsen et al., 2021)	43	[a]SP-Type I	-	Emodin (Toft-Bertelsen et al., 2021) Xanthene (Toft-Bertelsen et al., 2021)	-	-
		ORF10 (Toft-Bertelsen et al., 2021, 2022)	38	[a]SP-Type I	-	Amantadine (Toft-Bertelsen et al., 2021)	-	-
Filoviridae ssRNA	Zaire ebolavirus (EBOV)	Delta peptide (He et al., 2017)	40	SP-Type I	[a]Cl^- (Pokhrel et al., 2019)	-	-	-
		GP2 (Han et al., 2007)	174	SP-Type I	-	-	-	-
Flaviviridae ssRNA	Bovine viral diarrhoea virus (BVDV)	p7 (Griffin et al., 2004)	69	MP-Type I	-	BIT225 (Luscombe et al., 2010)	-	-
	Classical swine fever virus (CSFV)	p7 (Gladue et al., 2012; Largo et al., 2016)	69	MP-Type I	Two subpopulations: 1. cations > anions 2. anions > cations (Largo et al., 2016)	Amantadine (Gladue et al., 2012) **Verapamil** (Gladue et al., 2012)	F46A/H47A (Largo et al., 2018)	-
	Dengue virus (DENV)	M (Lahiri & Arkin, 2022; Premkumar et al., 2005) Opposing data (Wong et al., 2011)	75	[d]MP-type I	$Na^+ = K^+ > Cl^- > Ca^{2+}$ (Premkumar et al., 2005)	Amantadine (Premkumar et al., 2005) **CI-1040** (Lahiri & Arkin, 2022) **Glecaprevir** (Lahiri & Arkin, 2022) HMA (Premkumar et al., 2005) Kasugamycin mesna (Lahiri & Arkin, 2022)	-	-

(Continues)

TABLE 1 (Continued)

Virus family	Virus	Viroporin	Length	Classification	Ion selectivity	Inhibitors	Non-functional mutants	PDB structures
						Plerixafor (Lahiri & Arkin, 2022) **Streptomycin** (Lahiri & Arkin, 2022) **Tranexamic acid** (Lahiri & Arkin, 2022)		
		NS2A (Shrivastava et al., 2017)	218	MP-Type I	-	-	-	-
		NS2B (León-Juárez et al., 2016)	130	MP-Type I	-	-	-	-
	Hepatitis C virus (HCV)	E1 (Ciccaglione et al., 1998)	191	SP-Type I	-	-	-	-
		NS4A (Madan et al., 2008)	53	-	-	-	-	-
		p7 (Griffin et al., 2003; Montserret et al., 2010; Pavlović et al., 2003; Premkumar, Wilson, et al., 2004)	63	MP-Type I	$Na^+ = K^+ > Cl^-$ (Premkumar, Wilson, et al., 2004)	Amantadine (genotype dependent) (Griffin et al., 2003; Montserret et al., 2010) BIT225 (Luscombe et al., 2010) [c]CD (Foster et al., 2011) Cu^{2+} (Chew et al., 2009) [c]GSK-2 (StGelais et al., 2007) HMA (Montserret et al., 2010; Premkumar, Wilson, et al., 2004) [c]JK3/32 (Shaw et al., 2020) [c]LDS19 (Foster et al., 2014) [c]LDS21 (Foster et al., 2014) NN-DGJ (Pavlović et al., 2003) NN-DNJ (Pavlović et al., 2003) N-7-oxanonyl-6-deoxy-DGJ (Pavlović et al., 2003) Rimantadine (Foster et al., 2014)	H17A (genotype dependent) (Chew et al., 2009; StGelais et al., 2009) G39A (StGelais et al., 2009) P49A (StGelais et al., 2009)	2MTS 2M6X 3ZD0 2K8J

TABLE 1 (Continued)

Virus family	Virus	Viroporin	Length	Classification	Ion selectivity	Inhibitors	Non-functional mutants	PDB structures
	Japanese encephalitis virus (JEV)	NS2A (Chang et al., 1999)	226	-	-	-	-	-
		NS2B (Chang et al., 1999)	131	-	-	-	-	-
		NS4B (Chang et al., 1999)	125	-	-	-	-	-
	West Nile virus (WNV)	M (Lahiri & Arkin, 2022)	75	[a]SP-Type I	-	**5-Azacytidine** (Lahiri & Arkin, 2022) Benzbromarone (Lahiri & Arkin, 2022) Idasanutlin (Lahiri & Arkin, 2022) Plerixafor (Lahiri & Arkin, 2022)	-	-
	Zika virus (ZIKV)	M (Tomar et al., 2022)	75	MP-type I	K^+ (Tomar et al., 2022) H^+ (Tomar et al., 2022)	5-Azacytidine (Tomar et al., 2022) Floxuridine (Tomar et al., 2022) Kasugamycin (Tomar et al., 2022) Pentamidine (Tomar et al., 2022)	G54A (Tomar et al., 2022) Q59A (Tomar et al., 2022)	-
Hepadnaviridae pdsDNA	Hepatitis B virus (HBV)	X (Lee et al., 2018)	154	SP	Ca^{2+} (Casciano & Bouchard, 2018)	NN-DNJ (Lee et al., 2018)		-
Herpesviridae dsDNA	Human cytomegalovirus (HCMV)	US21 (Luganini et al., 2018)	243	MP-Type 2	Ca^{2+} (Luganini et al., 2018)	-	D201N (Luganini et al., 2018)	-
Orthomyxoviridae ssRNA	Influenza A virus (IAV)	M2 (Pinto et al., 1992)	97	SP-Type I	H^+ >>> K^+ > Na^+ (Chizhmakov et al., 1996; Tosteson et al., 1994)	[c]3-Azaspiro[5,5]undecane (Wang, Cady, et al., 2009) Amantadine (Balannik, Carnevale, et al., 2010; Pinto et al., 1992) [c]BL-1743 (Kurtz et al., 1995; Wang, Cady, et al., 2009) [c]M2JW332 (Wang et al., 2013) NN-DNJ (Scott et al., 2020) Rimantadine (Pielak et al., 2009)	V27F (Balannik, Carnevale, et al., 2010) A30F (Balannik, Carnevale, et al., 2010) S31F (Balannik, Carnevale, et al., 2010) G34F/V/L (Balannik, Carnevale, et al., 2010) H37A/E/G (pH sensitivity lost) (Pinto et al., 1992; Wang et al., 1995)	6OUG 6NV16MJH 6US8 6US9 6BKK 6BKL 6BOC 6BMZ 2RLF 2KQT 2LY0 2MUV 2MUW 2KIH 4QK7 4QKC 4QKL 4QKM 2KAD 5C02 3LBW

(Continues)

TABLE 1 (Continued)

Virus family	Virus	Viroporin	Length	Classification	Ion selectivity	Inhibitors	Non-functional mutants	PDB structures
						[c]Spiroadamantane 9 (Wang et al., 2011)		2KWX 4RWB 4RWC 6MPL 6MPM 6MPN 2L0J 2N70 5JOO 5TTC 5UM1 3C9J 3BKD
		PB1-F2 (Henkel et al., 2010)	90	SP	Cation ~ anion (Henkel et al., 2010)	-	-	-
	Influenza B virus (IBV)	BM2 (Mould et al., 2003)	109	SP-Type I	H^+ (Mould et al., 2003)	-	H19C (Mould et al., 2003)	6PVR 6PVT 2KJ1 2KIX
		NB (Fischer et al., 2001; Sunstrom et al., 1996)	100	SP-Type I	$Na^+ > cl^-$	Amantadine (Fischer et al., 2001; Sunstrom et al., 1996) [c]NB antibody (Sunstrom et al., 1996)	S20A (Premkumar, Ewart, et al., 2004)	-
	Influenza C virus (ICV)	CM2 (Hongo et al., 2003)	115	SP-Type I	$Cl^- > Na^+ = K^+$ (Hongo et al., 2003)	DIDS (Hongo et al., 2003)	-	-
	Influenza D virus (IDV)	DM2 (Kesinger et al., 2018)	152	SP-Type I	Cl^- (Kesinger et al., 2018)	DIDS (Kesinger et al., 2018)	-	-
Papillomaviridae dsDNA	Human papillomavirus (HPV)	E5 (Wetherill et al., 2012)	83	MP-Type I	-	[c]MV006 (Wetherill et al., 2012) Rimantadine (Wetherill et al., 2012)	-	-
Paramyxoviridae ssRNA	Human metaneumovirus (HMPV)	SH (Masante et al., 2014)	179	SP-Type II	-	-	-	-
	Human respiratory syncytial virus (HRSV)	SH (Gan et al., 2008)	64	SP-Type II	Cations > anions (high pH) Anions > cations (low pH) (Li et al., 2014)	Pyronin B (Li et al., 2014)	I21F (Li et al., 2014)	2NB7 2NB8
Phycodnaviridae dsDNA	ATCV-1	Kcv (Gazzarrini et al., 2009)	82	MP	$K^+ >> Na^+$ (Gazzarrini et al., 2009)	Ba^{2+} (Gazzarrini et al., 2009)	-	-
	MT325	Kcv (Gazzarrini et al., 2006)	95	MP	$K^+ >>> Na^+$ (Gazzarrini et al., 2006)	Ba^{2+} (Gazzarrini et al., 2006)	-	-
	Paramecium bursaria chlorella virus 1 (PBCV-1)	Kcv (Plugge et al., 2000)	94	MP-Type II	$K^+ > Na^+$ (Plugge et al., 2000)	Amantadine (Plugge et al., 2000) Ba^{2+} (Plugge et al., 2000)	-	-

TABLE 1 (Continued)

Virus family	Virus	Viroporin	Length	Classification	Ion selectivity	Inhibitors	Non-functional mutants	PDB structures
Picornaviridae ssRNA	Duck hepatitis A virus (DHAV)	2B (Liu et al., 2021)	119	SP-Type I	Ca^{2+} (Liu et al., 2021)	-	-	-
	Encephalomyocarditis virus (EMCV)	2B (Ito et al., 2012)	151	MP	Ca^{2+} (Jong et al., 2008)	-	-	-
	Enterovirus 71 (EV71)	2B (Xie et al., 2011)	99	MP	Cl^{-} (Xie et al., 2011)	**DIDS** (Xie et al., 2011)	-	-
	Foot-and-mouth disease virus (FMDV)	2B (Ao et al., 2015; Gladue et al., 2018)	154	MP-Type II	Ca^{2+} (Ao et al., 2015)	-	R68A/L69A/S70A (Gladue et al., 2018) G132LA/L133A (Gladue et al., 2018)	-
	Hepatitis A virus (HAV)	2B (Shukla et al., 2015)	251	MP-Type II	-			-
	Human rhinovirus 14 (HRV14)	2B (Jong et al., 2008)	97	MP	Ca^{2+} (Jong et al., 2008)	-	-	-
	Human rhinovirus 16 (HRV-16)	VP4 (Panjwani et al., 2014)	68	SP	-	-	-	-
	Poliovirus (PV)	2B (Agirre et al., 2002; Aldabe et al., 1996; Lama & Carrasco, 1992)	97	MP-Type II	Ca^{2+} (Jong et al., 2008)	-	K39E/K42E/K46E (Agirre et al., 2002) V52D/I54K (Agirre et al., 2002; Aldabe et al., 1996) A69E/I71E (Agirre et al., 2002)	-
		3A (Lama & Carrasco, 1992)	86	SP-Type II	-	-	-	-
	Coxsackievirus B3 (CVB3)	2B (van Kuppeveld, Hoenderop, et al., 1997; van Kuppeveld, Melchers, et al., 1997)	99	MP	Ca^{2+}, H^{+} (de Jong et al., 2006)	-	K41E/K44E/K48E (van Kuppeveld, Hoenderop, et al., 1997; van Kuppeveld, Melchers, et al., 1997) I64S/V66S (van Kuppeveld, Hoenderop, et al., 1997; van Kuppeveld, Melchers, et al., 1997) A71E (van Kuppeveld, Melchers, et al., 1997)	-
Polyomaviridae dsDNA	Simian virus 40 (SV40)	VP4 (Raghava et al., 2011)	62	SP	-	-	P70A (Giorda Kristina et al., 2012)	-
	JC polyomavirus (JCPyV)	Agnoprotein (Suzuki et al., 2010)	71	SP-Type II	Ca^{2+} (Suzuki et al., 2010)	-	-	-

(Continues)

TABLE 1 (Continued)

Virus family	Virus	Viroporin	Length	Classification	Ion selectivity	Inhibitors	Non-functional mutants	PDB structures
Potyviridae	Turnip mosaic virus (TuMV)	6K1 (Chai et al., 2024)	52	MP-Type II	-	-	K33D/K37A/K39D (Chai et al., 2024)	-
	Potato virus Y (PVY)	6K1 (Chai et al., 2024)	51	[d]MP	-	-	K33D/K37A/K39D (Chai et al., 2024)	-
Poxviridae dsDNA	Monkeypox virus (hMPXV)	A15.5L (Basu et al., 2023)	53	SP	K^+, H^+ (Basu et al., 2023)	-	-	-
Rhabdoviridae ssRNA	Bovine ephemeral fever virus (BEVF)	α1 (Joubert et al., 2014)	88	SP-Type I	-	-	-	-
Reoviridae dsRNA	Avian orthoreovirus	p10 (Bodelón et al., 2002) Opposing data (Salsman et al., 2005)	98	SP-Type I	-	-	-	-
	Blue tongue virus (BTV)	NS3 (Han & Harty, 2004)	229	MP-Type II	-	-	A131E/L132E/L133E (Han & Harty, 2004)	-
	Rotavirus	NSP4 (Hyser et al., 2010; Pham et al., 2017)	175	MP	$Ca^{2+} = K^+ >> Cl^-$ (Pham et al., 2017)	-	75IFNTLL80 to ASDASA (Hyser et al., 2010; Pham et al., 2017)	-
Retroviridae ssRNA	Human immunodeficiency virus 1 (HIV-1)	Vpr (Piller et al., 1996)	96	-	$Na^+ > Cl^-$ (Piller et al., 1996)	[c]Vpr C-term antibody (Piller et al., 1996)	-	-
		Vpu (Ewart et al., 1996; Schubert et al., 1996)	81	SP-Type I	$Na^+ = K^+ > Cl^-$ (Ewart et al., 1996)	Ba^{2+} (Sauter et al., 2014) BIT225 (Khoury et al., 2010) DMA (Ewart et al., 2002) Genistein (Sauter et al., 2014) HMA (Ewart et al., 2002)	S24L (Mehnert et al., 2008)	1VPU 2N29 2N28 2K7Y 1PI7 1PI8 1PJE 2JPX 2GOF 2GOH
	Human T-lymphotropic virus 1 (HTLV-1)	p13 (D'Agostino et al., 2002)	87	SP-Type I	Cations (D'Agostino et al., 2002)	-	-	-
	Simian immunodeficiency virus (SIV)	Vpu (Greiner et al., 2016)	81	SP-Type I	-	-	-	-
Togaviridae ssRNA	Barmah Forest virus (BFV)	6K (Melton et al., 2002)	60	[d]SP-Type I	$Na^+ = K^+ > Ca^{2+} > Cl^-$ (Melton et al., 2002)	[c]6K antibody (Melton et al., 2002)	-	-
	Chikungunya virus (CHIKV)	6K (Dey et al., 2019)	60	[d]SP-Type I	-	Amantadine (Dey et al., 2019)	-	-

TABLE 1 (Continued)

Virus family	Virus	Viroporin	Length	Classification	Ion selectivity	Inhibitors	Non-functional mutants	PDB structures
	Eastern equine encephalitis virus (EEEV)	6K (Tomar et al., 2019)	55	[a]MP-Type I	H^+ (Tomar et al., 2019)	-	-	-
	Semliki Forest virus (SFV)	6K (Sanz et al., 1994)	59	SP	-	-	-	-
		E1 (Nieva et al., 2004)	437	[a]SP	-	-	-	-
	Sindbis virus	6K (Sanz et al., 2003) Opposing data (Antoine et al., 2007)	54	[d]MP-Type I	-	-	9YLW11xAAA/18FWV20xAAA (Sanz et al., 2003)	-
	Ross River virus (RRV)	6K (Melton et al., 2002)	62	[d]SP-Type I	$Na^+ = K^+ > Ca^{2+} > Cl^-$ (Melton et al., 2002)	[c]6K antibody (Melton et al., 2002)	-	-

Note: - = information not available. > = permeability ratio of less than 10. >> = permeability ratio of 10 or more. >>> = permeability ratio of hundred or more.
[a]Predicted information.
[b]Pore function was not confirmed.
[c]Inhibitor was optimised or designed specifically for this viroporin.
[d]Disputed if single pass or multipass.

amantadine (Mould et al., 2003). The two proteins exhibit low sequence homology outside of the functional HXXXW motif in the TM helix (TMH) suggested to be sufficient for $M2_{IBV}$ to complement $M2_{IAV}$ during IAV infection functionally (Wanitchang et al., 2016). Within a virus family, there can be sequence conservation of the complete viroporin, of specific domains or sequence motifs, and the degree of conservation will depend on the size and diversity of the group in question. For example, **E proteins** from the *Coronaviridae* family exhibit some sequence conservation that decreases with increasing evolutionary distance, meaning only three residues are ubiquitously conserved across the seven viruses that infect humans (Duart et al., 2020). However, with SARS-CoV-2 and related *Sarbecoviruses*, conservation of protein E remains very high across individually sampled sequences (Troyano-Hernáez et al., 2021). As a precaution, given that considerable variation in sequence and function can exist (Breitinger et al., 2016; Griffin et al., 2008), it is important to investigate viroporins individually and not assume a protein must be a viroporin based solely on comparative analyses. Importantly, generic naming and numbering, such as ORF1 for 'open reading frame 1', NSP2 for 'non-structural protein 2' or "E" for envelope, are often used for viral proteins, some of which are viroporins. Consequently, overlap in names across families exists without necessarily referring to the functional or structural relatedness of those proteins.

The viroporin field lacks criteria for defining a viroporin, and because not all viroporins have been fully characterised following initial identification, many are described as viroporin-like, for example, human astrovirus protein X (XP_{HAstV}), NS7a from porcine delta coronavirus ($NS7a_{PDCoV}$) and NS3 from blue tongue virus ($NS3_{BTV}$) (Han & Harty, 2004; Lulla & Firth, 2020; Xia, Fang, et al., 2022). Based on current literature and status of the field, we here put forward some important considerations towards experimentally working with viroporins and propose a checklist of best practices for guidance in identifying and further characterising viroporins (Figure 1b).

The first task of the best practice checklist is (a) evidence of integral membrane localisation, meaning the identification of at least one TMH within the protein. Second is (b) evidence that the protein can form a pore, either by having sufficient TMHs in a monomer to do so (b-i) or by the formation of homo-oligomers (b-ii). Alternatively, a good-quality 3D experimental structure of a viroporin can be evidence of pore formation (b-iii). Third is (c) evidence that the viroporin functions as a pore; that is, it functions as an ion channel (c-i) and/or permeabilises membranes to small solutes (c-ii). Fourth is (d) pore function of a viroporin is verified by the ability to disrupt it, meaning that, if available, it can be inhibited by the addition of a generic or specialised viroporin inhibitor or an antibody (d-i) or mutated to abolish its function (d-ii). Finally, to have a full profile of a viroporin, (e) identification of its function within the virus life cycle, to support the characterisation even further. However, given that the roles of viroporins vary and that they may exhibit functions that exceed our current understanding, we suggest this information is desirable but not essential before a viroporin can be classified as belonging to the family.

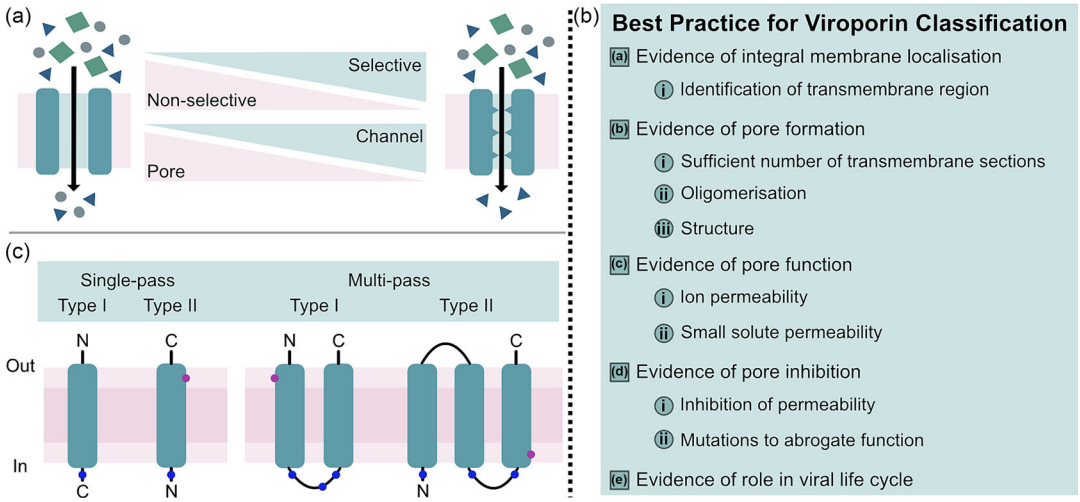

FIGURE 1 Viroporin selectivity and classification. (a) Viroporins exist in a continuum between non-selective pores that filter based on molecular size and physicochemical properties and more specific ion channels that preferentially conduct certain ions over others. The selectivity of a viroporin likely depends on the environment: membrane composition, oligomer formation, electrolyte composition and protein–protein interactions. (b) Viroporin classification best practice checklist. A list of desirable evidence proposed to help classify a viral protein as a viroporin. Each main task (a–d, preferably also e) could be addressed via any or all associated sub-tasks (i, ii or iii). (c) Classification of viroporins according to transmembrane (TM) topology. Viroporins with one TMH are classified as single-pass. If the N-terminus is oriented out (lumen or extracellular) and the C-terminus is oriented in (cytosol), the viroporin is type I. The opposite orientation with C-terminus out and N-terminus in is type II. Viroporins with several TMHs are classified as multi-pass, and types I and II solely distinguish the orientation of the N-terminus (type I: N-terminus out; type II: N-terminus in). Blue circles: basic residues. Magenta circles: aromatic residues.

In Table 1, we list proteins identified as viroporins or potential viroporins. Not all of these follow the best practice checklist that we propose; however, with the considerations provided in this review, the process by which viroporins are characterised can be unified.

2.1 | Key factors affecting viroporin research

When working experimentally with viroporins, some key considerations related to the proposed best practice summarised above exist (Figure 1b). The first is choosing between full-length protein or truncated variants, which, in the most extreme, only covers a single TMH, usually not sensible when investigating a multi-pass viroporin (Section 3.1). The advantage of working with the TMH in isolation is that peptides can be easily synthesised and reconstituted in membrane-mimetics, liposomes or lipid bilayers used in various techniques to determine channel function (Section 4.2) and structure. Several examples, such as the structural characteristics of $M2_{IAV}$ being greatly affected by truncation (Section 3.3), suggest that it cannot readily be assumed that truncated variants behave functionally and structurally like the full-length viroporin. Furthermore, as exemplified by $p7_{CSFV}$, pH-dependency and amantadine sensitivity may only occur if specific extra-membranous residues are included (Largo et al., 2014). Likewise, residues outside the TMH of 2B from coxsackievirus B3 ($2B_{CVB3}$) were found to be important for pore function and membrane targeting (de Jong et al., 2003; van Kuppeveld, Hoenderop, et al., 1997). If the characterisation of a truncated viroporin is done without consideration for the full-length protein, careful interpretation must be made. Apart from the protein variant, the use and placement of fusion partners for solubility or identification can affect cellular location, as seen for XP_{HAstV1} (Lulla & Firth, 2020), or can perturb the protein function as in the case of $p7_{HCV}$, showing increased channel activity upon removal of the solubility tag (Griffin et al., 2003).

Following the observation of viroporin behaviour by either ion conductance or membrane permeabilisation, indirect or non-specific effects must be ruled out. These could be, but are not limited to, cytotoxicity (Madan et al., 2008), dysregulation of endogenous ion channels (Antoine et al., 2007; Shimbo et al., 1995) or artefacts related to the tendency of amphipathic peptides to permeabilise membranes, resulting in false positives (Lear et al., 1988; Tosteson et al., 1988). In addition, it needs to be considered that viruses may encode multiple viroporins (Table 1), which could influence an infected cell in whole-virus systems.

An inhibitor can be confirmed to act directly on a viroporin by isolation from the virus context, and evidence becomes stronger if inhibitor-resistant mutations are identified, although this can be challenging. In addition, direct binding can be substantiated using structurally similar compounds that lack/gain functionality, known as structure–activity relationship (SAR) studies. Viroporin-specific effects may be identified by non-functional mutations of the viroporin (Figure 1b), examples of which can be found in Table 1. However, the collateral impact of mutations designed to abrogate viroporin function may complicate data interpretation. To make pore-specific non-functional viroporin mutants, these must maintain wild-type (WT)-like membrane insertion, localisation and/or expression levels. When

implementing viroporin mutations in virus genomes, potential disruption of non-channel related functions, such as partaking in the virion or directly interacting with the antiviral signalling components of cells, cannot be disregarded. Mutations that solely decrease or block the pore or disrupt oligomerisation are favourable, although not always possible. In the initial identification and characterisation of a viroporin, generic inhibitors (Table 1) can sometimes be useful. However, novel inhibitors with specific inhibition profiles are more convincing because, in combination with resistant viroporin variants, they can be used to rule out off-target effects.

In conclusion, the provided list of best practice for identifying and characterising viroporins, in addition to the concerns of experimentally working with viroporins, should serve to help the field progress in identifying and characterising novel viroporins as well as reaffirming those already identified.

3 | VIROPORINS FORM MEMBRANE PORES THROUGH OLIGOMERISATION

To design viroporin-targeting drugs, high-quality structures can serve as a useful asset in the optimisation process. However, despite their relatively small size, the structures of full-length viroporins have proven difficult to obtain. Accommodating the TMH and establishing the oligomeric state remains challenging, because reconstitution in tractable membrane mimetics, rather than lipid bilayers after purification, can alter their native structure (Majeed et al., 2021). This has left many viroporins characterised only in part, focusing on either the TM or the extra-membranous regions, for example, the TMH structures of $M2_{IBV}$ (Mandala, Loftis, et al., 2020; Wang, Pielak, et al., 2009) and E protein of severe acute respiratory coronavirus 2 ($E_{SARS\text{-}CoV\text{-}2}$) (Mandala, McKay, et al., 2020), the structures of the N- and C-terminal peptides of human respiratory syncytial virus SH protein (SH_{hRSV}) (Li et al., 2014) and the structures of the C-terminal peptide of Vpu from human immunodeficiency virus 1 ($Vpu_{HIV\text{-}1}$) (Willbold et al., 1997; Wittlich et al., 2009). Consequently, interactions between the TMH and extra-membranous regions and the effects that context has on the stability and function of viroporins are understudied. This section will introduce the common structural features of viroporins, such as membrane association and oligomerisation, followed by a comparative analysis of the available viroporin structures. Considerations regarding the experimental conditions and the use of in silico methods such as, for example, AlphaFold, will also be highlighted.

3.1 | Sequence features of viroporins classify them as membrane proteins

Identified viroporins span the size range of 38–437 residues for the monomer, with ~75% having less than 135 residues (Table 1). Some viroporins only span the membrane once, for example, $M2_{IAV}$ (97 residues), $E_{SARS\text{-}CoV\text{-}2}$ (75 residues) or SH_{hRSV} (64 residues), whereas others contain more than one TMH as well as extra-membranous loops and/or tails (Hyser et al., 2010; Lu et al., 2006; Luganini et al., 2018; Shukla et al., 2015). Examples of larger viroporins are protein **3a** from SARS-CoV-2 ($3a_{SARS\text{-}CoV\text{-}2}$) (275 residues) (Kern et al., 2021) and the SH protein from human metapneumovirus (SH_{HMPV}) (179 residues) (Masante et al., 2014), suggesting that viroporins may not be restricted to an upper size limit.

Some viroporins were discovered by bioinformatics analyses of viral genomes, identifying open reading frames containing at least one hydrophobic and often helical segment with an amphipathic character anticipated to be the membrane-spanning region (Dey et al., 2019; Gladue et al., 2012). Membrane insertion of viroporins can be determined using TM predictors, analysing the amino acid sequence for hydrophobic stretches (Guo et al., 2013; Sanz et al., 2003; Ye & Hogue, 2007) or experimentally, for example, by membrane fractionation with alkaline or denaturant wash steps (Guo et al., 2013; Kongpracha et al., 2022; Raghava et al., 2011; Sanz et al., 2003). Worth noting is that algorithms used for the predictors of membrane proteins vary (Bugge et al., 2016), possibly resulting in ambiguity, for example, due to the presence of polar residues towards the lumen-facing side of the pore; thus, gathering consensus from multiple predictors is advantageous.

One way to classify viroporins is via (predicted) structural topology (Nieva et al., 2012). Dividing viroporins into separate classes based on whether they contain one or multiple TMHs and on the orientation of the N-terminus is in keeping with the general classification for integral membrane proteins (Figure 1c) (Hegde & Keenan, 2022). Previously, a classification was constructed for viroporins based on the same principles but with different identifying labels (Nieva et al., 2012). Because the viroporin classification only accounts for viroporins with one or two TMHs, and viroporins with multiple TMHs exist, this previous classification does not otherwise add to the general description of membrane proteins. Thus, until a separate classification based on sequence or functional properties of viroporins can be established, we suggest keeping to the more commonly used integral membrane protein classification (Figure 1c).

Identification of membrane flanking residues can be indicative of the TMH location. For membrane proteins in general, basic residues are often seen bordering the intracellular side of the membrane (Figure 1c), adhering to the *positive-inside rule* (von Heijne, 1989, 2006). This states that integral membrane proteins, such as viroporins, tend to be oriented such that most Arg and Lys residues will be on the side of the membrane facing the cytosol (Baeza-Delgado et al., 2013). Furthermore, basic residues are important in the subcellular targeting of integral membrane proteins (von Heijne, 1989). Single-pass type I viroporins such as E protein of severe acute respiratory coronavirus 1 ($E_{SARS\text{-}CoV\text{-}1}$) and $E_{SARS\text{-}CoV\text{-}2}$, $M2_{IAV}$ and $Vpu_{HIV\text{-}1}$ all contain basic residues following their TMH (Park et al., 2003; Sharma et al., 2010; Surya et al., 2018). In contrast, the single-pass type II viroporin agnoprotein of JC polyomavirus ($agnoprotein_{JCPyV}$) contains more basic residues preceding its TMH (Suzuki et al., 2010). In the case of multi-pass type I viroporin p7 of hepatitis C virus ($p7_{HCV}$), conserved basic residues reside within the cytosolic loop (Griffin et al., 2004; StGelais et al., 2009).

A previously reported characteristic of viroporin primary structure is clustering of aromatic residues (Gonzalez & Carrasco, 2003). Many viroporins contain aromatic residues around the membrane interface (Figure 1c) (Lulla & Firth, 2020; Raghava et al., 2011; Suzuki et al., 2010; Wozniak et al., 2010). Indeed, aromatic residues are often found at the borders of membrane-spanning regions of proteins, where they are located at the water-lipid interface, impacting orientation and functioning as contact points for specific lipids through headgroup interactions (Killian & von Heijne, 2000; Mall et al., 2000). Some viroporins also contain aromatic residues within their pore lumen, where the aromatic residues have been speculated to be involved in channel activity and possible gating (Medeiros-Silva et al., 2023; Tang et al., 2002).

Mutation of basic or aromatic residues in viroporins can alter the orientation and lead to abrogated function (Park et al., 2003; Sharma et al., 2010; Surya et al., 2018). It has yet to be confirmed for all examples whether mutations impact the direct function or if the mutations adversely affect the integration or localisation in the membrane (StGelais et al., 2009). In the case of basic residues and aromatic clusters, there is not much evidence that these are particular features of viroporins but rather more general traits of membrane proteins, securing their placement and orientation in the bilayer.

Finally, palmitoylation sites have been identified in the cytoplasmic regions of several viroporins, such as $M2_{IAV}$ (Holsinger et al., 1995), 6K of Sindbis virus (Gaedigk-Nitschko et al., 1990) and protein E from multiple coronaviruses (Boscarino et al., 2008; Liao et al., 2006; Lopez et al., 2008). Palmitoylation was shown to be involved in membrane anchoring (Liao et al., 2006; Lopez et al., 2008), complex stability (Lopez et al., 2008; Sun et al., 2021) and virus budding (Boscarino et al., 2008; Gaedigk-Nitschko et al., 1990; Lopez et al., 2008) but not necessarily important for viroporin ion channel activity, for example, in $M2_{IAV}$ (Holsinger et al., 1995).

3.2 | The energy landscapes of viroporins allow adoption of variable oligomeric states

One of the main features of viroporins is their ability to homo-oligomerise. Oligomerisation is thought to be advantageous in viruses and is frequently seen for other viral protein families, for example, capsid proteins (Jayaraman et al., 2016). Viruses possess limited genetic coding capacity, requiring the use of alternative strategies such as encoding multifunctional proteins (Faust et al., 2017). Differential homo-oligomerisation can thus enable the production of multiple functional complexes from the same polypeptide.

The nature of oligomerisation varies between different viroporins and within individual viroporins, depending on conditions. This variation stems both from the number of TMHs in the monomeric protein and the oligomeric state, spanning from dimers to heptamers or even larger oligomeric structures reaching up to nm-sized diameters to the pore (Clarke et al., 2006; Griffin et al., 2003; Largo et al., 2021; León-Juárez et al., 2016). Some viroporins, for example, $E_{SARS\text{-}CoV\text{-}2}$, can exist in a broader energy landscape capable of occupying multiple oligomeric states (Surya et al., 2023), whereas others, for example, SH_{hRSV}, preferentially form one (known) oligomeric state (Kochva et al., 2003). Thus, before ascribing a preferential oligomeric state to a viroporin, it should ideally be confirmed using multiple techniques and with consideration of the experimental conditions.

The forces that drive the oligomerisation of viroporins and membrane proteins generally differ from those that drive soluble protein oligomerisation (De Marothy & Elofsson, 2015). For soluble proteins, the electrostatic forces and hydrophobic effect play major roles, whereas van der Waals' forces and lipid entropy optimisation mainly drive the helix–helix interaction of membrane proteins (Corin & Bowie, 2022). For some viroporins, disulphide bridges have been demonstrated to be essential for functional oligomeric assembly, for example, the ebolavirus delta peptide (He et al., 2017; Pokhrel et al., 2019), but these bonds are not a general requirement, because the disulphide bonds formed in $M2_{IAV}$ are nonessential for oligomerisation (Holsinger & Lamb, 1991) or $VPU_{HIV\text{-}1}$, which does not contain any cysteines (Schubert et al., 1996). Unpaired charged residues or polar side chains facing the hydrophobic tails of lipids are generally unfavourable (Mandala, McKay, et al., 2020; Park et al., 2003; Stouffer et al., 2008; Surya et al., 2023); thus, their presence is depleted in the TMHs of viroporins. This does not imply that salt bridges or interhelical hydrogen bonds are neither present nor important, as exemplified by the luminally exposed residues partaking in hydrogen bond-water networks in $M2_{IAV}$ (He et al., 2017; Pokhrel et al., 2019; Smertina et al., 2022; Zhang et al., 2014). Although extra-membranous regions can assist folding, it has been shown for several viroporins that the TMH alone is sufficient for oligomerisation (Mandala, McKay, et al., 2020; Park et al., 2003; Stouffer et al., 2008; Surya et al., 2023), but the degree to which these resemble the full-length protein in terms of structure or stability is not certain.

Structures of viroporins have shown a diversity of states, even when considering a single viroporin (Figure 2a) (Chandler et al., 2012; Moore et al., 1998; Park et al., 2003; StGelais et al., 2009). Whether this diversity is relevant to the viral life cycle and pathogenesis or whether some observed states result from in vitro reconstitution and experimental conditions used to characterise the viroporin, is not known. For many, including $M2_{IAV}$, $p7_{HCV}$ and $p7_{CSFV}$, the choice of lipid, pH, or the protein-to-lipid ratio was shown to affect the distribution of oligomeric states (Clarke et al., 2006; Largo et al., 2021; Oestringer et al., 2018; OuYang et al., 2013; Townsend et al., 2021; Zhou & Cross, 2013), also supported by the existence of specific lipid binding sites in viroporins (Agirre et al., 2002; Campbell & Monje-Galvan, 2023; Verdiá-Báguena et al., 2012). The protein variant can also influence the oligomeric state, as seen for $E_{SARS\text{-}CoV\text{-}2}$, where the TMH-only variant formed either higher-order oligomers compared to the full-length protein or changed the helix packing (Mandala, McKay, et al., 2020; Surya et al., 2018, 2023; Torres et al., 2005); however, the oligomeric state of $E_{SARS\text{-}CoV\text{-}2}$ driving the ion transport has not yet been fully established.

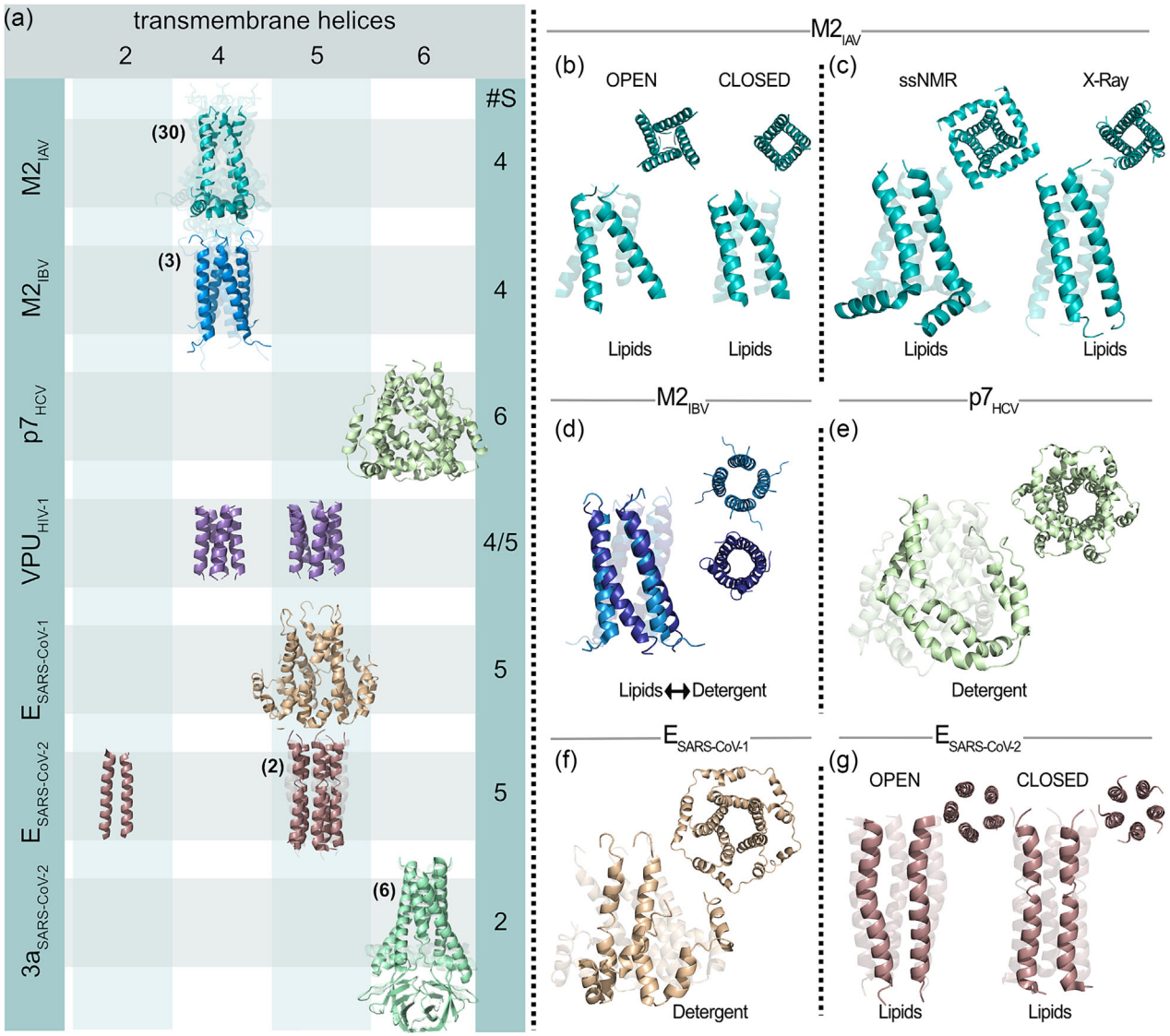

FIGURE 2 Experimentally determined viroporin atomic structures. (a) All current PDB-available oligomeric TMH structures of viroporins. Left panel: virus and protein name. Middle panel: structures sorted by the number of TM helices in the structure. Numbers in parentheses indicate multiple structures, highlighting the number of similar structures in the PDB. Right panel: the number of subunits (#S) in the oligomers. PDB IDs in Table S1. (b) $M2_{IAV}$ in the open, low pH state (PDB ID 4QKM) and the closed, neutral pH state (PDB ID 6NV1). (c) CD-$M2_{IAV}$–structures solved by ssNMR (PDB ID 2L0J) or X-ray crystallography (PDB ID 6OUG). (d) $M2_{IBV}$ structures solved by ssNMR in lipids (light blue, PDB ID 6PVR) or solution NMR in detergent (dark blue, PDB ID 2KIX). (e) $p7_{HCV}$-structure solved by solution NMR in detergent (PDB ID 2M6X). (f) $E_{SARS\text{-}CoV\text{-}1}$-structure solved by solution NMR in detergent (PDB ID 5X29). (g) $E_{SARS\text{-}CoV\text{-}2}$-structure solved by ssNMR in lipids in open, low pH (PDB ID 8SUZ) or closed, neutral pH conformations (PDB ID 7K3G). All structures are shown with the N-terminal to C-terminal in side-view and C-terminal/cytoplasmic top view. For clarity, all structures have all but two chains made transparent.

3.3 | Viroporin structures depend on their environment

So far, despite the classification of 83 proposed viroporins (Table 1), fewer than 80 monomeric and oligomeric 3D-structures pertaining to less than 10 different viroporins have been deposited in the Protein Data Bank (PDB), including structures of fragments (Figure 2a, Table 1). Thus, there is a considerable gap in the molecular understanding of viroporin structures. The current 3D-structures of viroporins have been solved using X-ray crystallography and NMR spectroscopy, both solid state (ssNMR) and solution state, and involving a variety of detergents as lipid mimetics or, more rarely, lipid bilayers.

As one of the larger viroporins, $3a_{SARS\text{-}CoV\text{-}2}$ (62 kDa as a dimer) is the only viroporin whose structure has been determined by cryo-electron microscopy (EM) (Kern et al., 2021; Miller et al., 2023) and one of the few viroporins forming a pore solely by dimerisation (three TMHs per subunit). It is also the best example of a viroporin where most of the extra-membranous regions are structurally resolved, protruding far out of the membrane (Figure 2a) (Kern et al., 2021).

Contrary to multiple previous reports (Chan et al., 2009; Fam et al., 2023; Kern et al., 2021; Lu et al., 2006; Toft-Bertelsen et al., 2021; Yu et al., 2021), Miller et al. (2023) were unable to detect any ion conduction by $3a_{SARS\text{-}CoV\text{-}2}$ and thus concluded that it is not a viroporin, despite never testing an untagged protein (Miller et al., 2023), which may at least in part explain the contradictive results. Most other viroporins are too small for current high-resolution microscopy methods, even in their oligomeric states (Cianfrocco & Kellogg, 2020), but EM can be useful in resolving lower resolution structures of the overall fold, topology and channel size of viroporin complexes, as for example, of the full-length structure of $p7_{HCV}$ (Luik et al., 2009).

More than one-third (30) of the available viroporin structures are of $M2_{IAV}$, comprising both WT and drug-resistant variants, in either a free or drug-bound form. The oligomerisation process for $M2_{IAV}$ has been described as a tandem mechanism going from monomer to dimer, then from dimer to tetramer, leading to the description of $M2_{IAV}$ as dimers-of-dimers (Georgieva et al., 2015). For comparison with the other viroporins, we refer here to $M2_{IAV}$ as a tetramer. All $M2_{IAV}$ structures are tetrameric with left-handed helix crossing angles (Figure 2a). Still, variations between structures exist, stemming from the differences in sequence composition and length. Most $M2_{IAV}$-structures are composed of TMH-only peptides (residues 22–46 or 20–49), and some include the 'conductance domain', with an additional helix after the TMH (CD-$M2_{IAV}$, residues 22–62) (Sharma et al., 2010). By visual inspection of the helix tilt (the angle of the helix axis with respect to the membrane normal), some general observations can be made. The 'open' state, with a wider C-terminal opening, is considered to be induced by lowering the pH (Figure 2b), with evidence suggesting this is caused by a destabilisation of the channel (Schnell & Chou, 2008). However, not all structures with wider C-terminal openings have been solved at low pH (Cady et al., 2009; Stouffer et al., 2008), and not all structures solved at high pH are in the closed state (Thomaston et al., 2015, 2017). Furthermore, all structures solved at low pH were of TMH peptides, without the additional sequence to potentially stabilise the C-terminal (Stouffer et al., 2008; Thomaston et al., 2015, 2018). The presence of a ligand favours the closed state, including structures solved at low pH, but not consistently (Stouffer et al., 2008; Thomaston et al., 2018).

For the three available $M2_{IBV}$-structures that include only the TMHs, a wider pore and a slightly larger helical tilt are seen at low pH compared with neutral pH (Mandala, Loftis, et al., 2020). However, the difference between the observed states is less pronounced for $M2_{IBV}$ than the differences between the states of the $M2_{IAV}$-structures. More evidently, the $M2_{IBV}$-structure in detergent micelles has a much larger helical tilt (~26°) compared with the two structures in a lipid environment (~2°) (Figure 2d) (Mandala, Loftis, et al., 2020; Wang, Pielak, et al., [2009]). Thus, the variances in both $M2_{IAV}$- and $M2_{IBV}$-structures, including in structures using identical length peptides, highlight the large variability in viroporin structures imposed by the experimental conditions.

The CD-$M2_{IAV}$-structures generally display a narrower pore, whereas TMH-only variants tend to splay towards the C-terminus. For the CD-$M2_{IAV}$, an amphipathic helix in the C-terminus, perpendicular to the TMH, is observed for structures determined by NMR, whereas no helix bend is observed by X-ray crystallography, perhaps resulting from crystal packing (Figure 2c) (Thomaston et al., 2020). The structures of $p7_{HCV}$ and $E_{SARS\text{-}CoV\text{-}1}$ (OuYang et al., 2013; Surya et al., 2018) also have the C-terminus folding back and around the first TMH, and in the case of $p7_{HCV}$, forming an entire second TMH (Figure 2e,f). Critically, all structures with a second helix, except one of $M2_{IAV}$ (Sharma et al., 2010), were solved in detergent micelles, where access to the hydrophobic chains is possible. The missing bilayer surface and curvature of the micelle might impact the resulting structures, questioning the presence and/or orientation of the second helix (OuYang et al., 2013; Schnell & Chou, 2008; Surya et al., 2018). Whether a second helix is a general trait of viroporins with extended C-termini is thus not clear. Furthermore, issues have been raised concerning experimental artefacts in the $p7_{HCV}$-structure, as it conflicts with previously determined orientations of important pore facing and terminal residues (Carrère-Kremer et al., 2002; Luik et al., 2009; Oestringer et al., 2018).

Comparing the structures of the longer $E_{SARS\text{-}CoV\text{-}1}$ with the TMH-variant of $E_{SARS\text{-}CoV\text{-}2}$, the most striking differences are variations in helical tilt angle, as well as the right-handedness of $E_{SARS\text{-}CoV\text{-}1}$ not observed for $E_{SARS\text{-}CoV\text{-}2}$, which is less tilted and lacks distinct handedness (Figure 2f,g). The $E_{SARS\text{-}CoV\text{-}1}$ also shows a looser packing of the helices compared with $E_{SARS\text{-}CoV\text{-}2}$ (Mandala, McKay, et al., 2020; Surya et al., 2018). The longer $E_{SARS\text{-}CoV\text{-}1}$-structure is in detergent micelles at low pH, whereas the $E_{SARS\text{-}CoV\text{-}2}$-structure is in lipid bilayers at neutral pH. $E_{SARS\text{-}CoV\text{-}2}$ has also been solved in a low pH state, which is more open compared to the $E_{SARS\text{-}CoV\text{-}2}$-strucure at neutral pH, as well as slightly tilted, but not to the degree of the $E_{SARS\text{-}CoV\text{-}1}$-structure (Figure 2f,g) (Medeiros-Silva et al., 2023). Other studies show the C-terminus of full-length $E_{SARS\text{-}CoV\text{-}2}$ can form concentration dependent β-strands (Dregni et al., 2023; Surya & Torres, 2022), an extra membranous structure also observed for SH_{hRSV} (Gan et al., 2012). Given the identical sequences of the E protein TMH of the SARS-CoV variants, the differences mentioned above likely originate from differences in experimental conditions rather than reflect native variation. Overall, it seems that structures obtained in detergents tend to have larger helical tilts compared with those in lipid bilayers.

Both a tetrameric and a pentameric $Vpu_{HIV\text{-}1}$-structure exist (Figure 2a), but when combining the experimental data with stability calculations from molecular simulations of various $Vpu_{HIV\text{-}1}$ oligomers, $Vpu_{HIV\text{-}1}$ is more widely accepted to form pentamers (Moore et al., 1998; Padhi et al., 2013; Park et al., 2003). Similarly, even though only a hexameric $p7_{HCV}$-structure exists, heptameric $p7_{HCV}$ complexes have been observed experimentally (Chandler et al., 2012; StGelais et al., 2009), highlighting that the oligomeric state may not necessarily be static. It is even possible that the state could vary in differing biological settings.

The above analyses provide an overview of the current structures of viroporins but only information on the overall configurations and not how sidechain orientations vary. The 3D-structures demonstrate how sensitive viroporins are to experimental conditions, even for a single viroporin and a single oligomeric state, and they distinctly

highlight how much remains to be uncovered. While structural differences are observed, the main question remains whether all these structures exist in nature and are relevant to viroporin functions. Even in the case of $M2_{IAV}$, the relevance of the various structures is still debated, arguments emphasising either the use of a more native-like environment of lipid bilayers compared with detergent (Cady et al., 2010) or the effect of using full-length viroporins to obtain the most accurate structures (Pielak et al., 2009; Thomaston et al., 2020). Thus, improving the methods with which viroporin structures are studied, such as including more than the TMH, and using native-like conditions are all crucial to the further disentanglement of the structure–function relationship of viroporins.

3.4 | In silico viroporin models complement experimental data

Although few 3D-structures of intact viroporins exist, the structural properties of selected viroporins have been investigated experimentally, computationally and in combination (Araujo et al., 2016; Dey et al., 2019; Wetherill et al., 2012). Therefore, several models of viroporins and partial structural information exist, but as opposed to the PDB-deposited structures, there is no overview of the available information. In silico modelling, as well as integrative methods, combining experimental data and the computational generation of models, have been used to investigate, for example, $E_{SARS\text{-}CoV\text{-}2}$ and $SH_{hRSV,}$ by incorporating NMR data or $p7_{HCV}$ with incorporated EM data (Dey et al., 2020; Gan et al., 2012; Jalily et al., 2022; Luik et al., 2009). Molecular dynamics simulations have been used to indicate the preferential stoichiometry of viroporins by simulation of various oligomeric states to reveal differences in stability (Padhi et al., 2013; Park et al., 2003) and packing (Torres et al., 2005). In some cases, only marginal differences were seen, such as $E_{SARS\text{-}CoV\text{-}1}$, which was stable as multiple oligomers (Torres et al., 2005). Other viroporins exhibit a clear preference for one state over others; for example, SH_{hRSV} was found most stable as a pentamer (Kochva et al., 2003). As in silico methods for investigating membrane proteins improve (Almeida et al., 2017), their use in studying viroporins, along with integrated experimental data, holds great promise.

3.5 | Advancing prediction of viroporin structures

The revolution within sequence-based structure prediction and artificial intelligence models means that structures that were difficult to determine experimentally are no longer completely inaccessible (Jumper et al., 2021). While predictors work effectively and are under constant improvement, several reasons make confidently predicting the structures of viroporins challenging. Viral proteins have low sequence conservation, even between functionally related proteins (Kuchibhatla et al., 2014; Wilson, Fuentes, et al., 2006), making homology modelling difficult (Perdigão et al., 2015). Another challenge relates to defining the oligomeric state. Programmes that can confidently predict membrane protein multimers exist (Evans et al., 2022), but for viroporins, it is not always evident which oligomeric state(s) are relevant. Additionally, structural evidence suggests that viroporins exist simultaneously in a wider energy landscape of multiple functional oligomeric states, which might not be predictable. It is possible to use sequence-based predictors (Basu et al., 2023) but with a critical approach to assessing the confidence with which the structure model, or regions within it, is produced (Figure S1) (Varadi et al., 2022). For example, when predicting structures with AlphaFold (Jumper et al., 2021) for already characterised viroporins, few of these are predicted confidently (Figure S1). While the TMH is confidently predicted for monomeric $M2_{IAV}$ and $E_{SARS\text{-}COV\text{-}1}$, neither the TMH, the structure of the extra membrane regions, nor the relative orientation of these are reliably predicted for monomeric $p7_{HCV}$ and the majority of the oligomeric models. Thus, while structure prediction accuracy improves at impressive rate, the ensuing structures of viroporins should still be considered with caution unless supported by experimental data.

In conclusion, we argue that the structural classification of viroporins should intuitively follow the general classification for integral membrane proteins. We elucidate some of the common features of viroporins, such as their oligomerisation and the position of their basic residues relative to the membrane. We have shown that even within the limited number of viroporin structures, the amino acid sequence used, and the experimental conditions, impact the resulting structures. Hence, much ambiguity still exists, even for the more well-characterised examples such as $M2_{IAV}$. Lastly, while computational methods are available and should be utilised where possible, the results on viroporins must be compared with experimental data, as these methods are still not optimised for viral proteins.

4 | VIROPORINS PERMEABILISE CELL MEMBRANES AND EXHIBIT PRO-VIRAL FUNCTIONS

Viroporins locate to the virion membrane, the plasma membrane and the membranes of organelles in infected cells, carrying out multiple functions throughout the virus life cycle (Figure 3). Deletion or other mutational disruption of a viroporin seldom affects genome replication but often leads to virus attenuation, including via decreased virus particle production, infectivity and pathogenicity (Bukreyev et al., 1997; Cheung et al., 2005; DeDiego et al., 2007; Gladue et al., 2012; Gonzalez & Carrasco, 2001; Kuo & Masters, 2003; Steinmann, Penin, et al., 2007; Strebel et al., 1988; van Kuppeveld, Hoenderop, et al., 1997; Wang et al., 2012). As proof that viroporins directly contribute to in vivo pathogenesis, mice infected with recombinant SARS-CoV-1 viruses carrying ion-channel-deficient E variants recovered from terminal disease, and the positive outcome was linked to reductions in lung inflammatory cytokines with no difference in virus titre (Nieto-Torres et al., 2014). Despite the lack of sequence homology within the viroporin family, *cis/trans*-complementation experiments suggest a degree of functional similarity between some

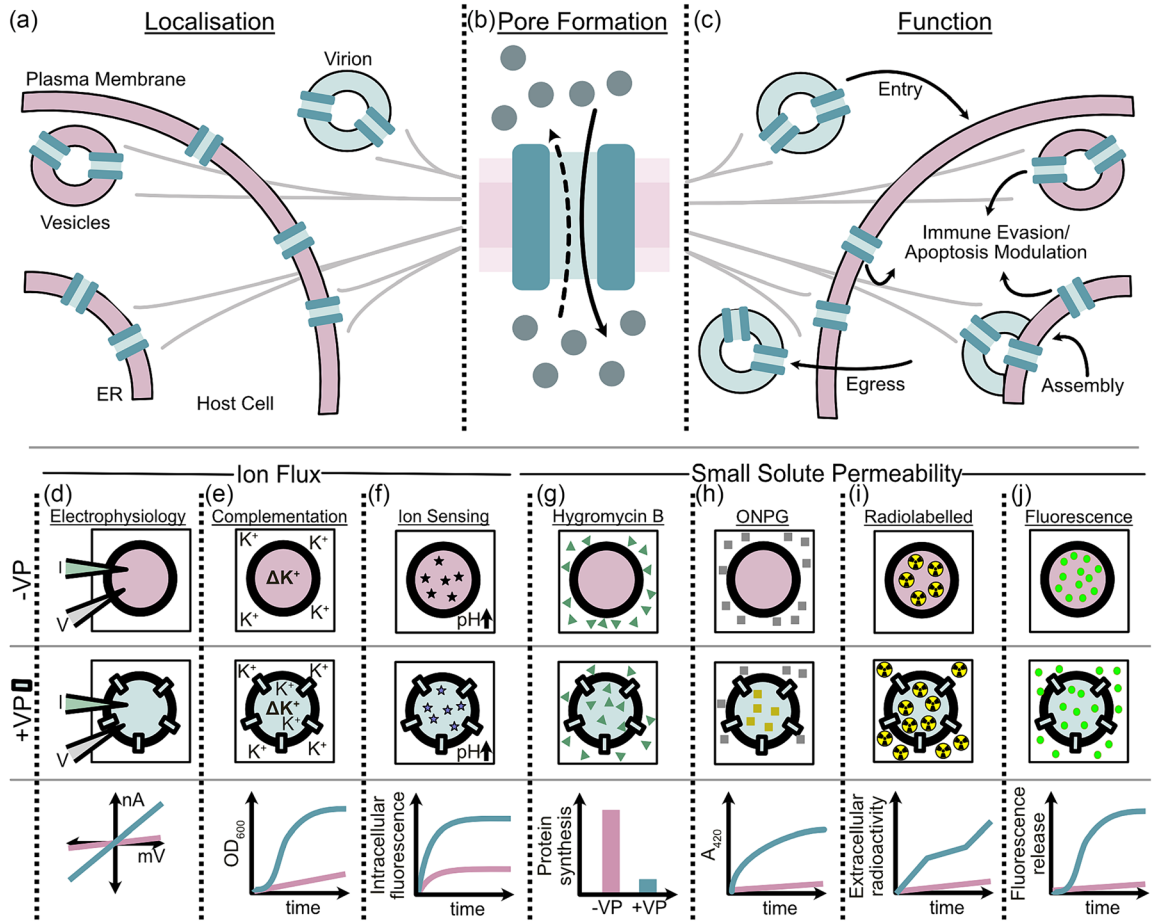

FIGURE 3 Viroporin function and assays for functional determination. (a) Viroporins can localise in the plasma membrane, organelle membranes and/or virions. (b) Pore-forming viroporins allow permeability for ions or small solutes (solid arrow), and some viroporins allow countermovement of ions (dashed arrow). (c) Steps in the viral life cycle where most viroporins function. (d–f) Ion flux assays: (d) electrophysiological; (e) complementation; (f) ion sensing. (g,h) Small solute permeability assays: (g) hygromycin B-based; (h) ONPG. (i) Radiolabelled. (j) Fluorescence. (d–j) Top row: without viroporin (−VP, pink). Middle row: with viroporin (+VP, blue). Bottom row: representative schematic diagrams of data obtained in the above experiment.

viroporins, although rescue is usually inefficient; a genetically modified Sindbis virus with Vpu_{HIV-1} replacing endogenous viroporin 6K was viable, and similarly, HCV with $M2_{IAV}$ expressed in *trans* replaced mutated p7 (Elmasri et al., 2022; Gonzalez & Carrasco, 2001; Wozniak et al., 2010). Complementation is, however, not always possible because $E_{SARS-CoV-2}$ did not complement Vpu-deleted HIV-1, and the Sindbis virus lacking 6K was neither rescued by $M2_{IAV}$ TMH nor $p7_{HCV}$ full-length (Elmasri et al., 2022; Henke et al., 2022). This lack of complementation could be due to differences in ion preference. Still, issues related to efficient expression, processing or localisation cannot be ruled out in these experiments.

The primary function and feature of viroporins that give rise to their name is their ability to form hydrophilic pores and permeabilise cell membranes to small solutes and ions (Figure 3b) (Carrasco, 1995). Ion conductance has been shown for several viroporins to be critical to their function, as elaborated below. However, the permeability to small solutes has not yet been linked to a biological function, and whether this characteristic is merely an inherent side-effect of pore formation remains to be elucidated. The primary role of viroporins in the virus life cycle is the involvement in the entry, assembly and egress of viruses (Figure 3c). Yet, they also exhibit complementary functions, such as those derived from interactions with host proteins.

4.1 | Viroporins facilitate passage of ions across cell membranes

Classical ion channels are highly ion-selective and gated because they would otherwise be detrimental to the cell (Alexander et al., 2023). Viroporins, on the other hand, are more difficult to characterise as ion channels. Apart from the common amphipathic character of the pore, most viroporins have not been characterised in terms of the specific pore-lining residues critical for function. Some exceptions are $M2_{IAV}$, $E_{SARS-CoV}$ and $p7_{HCV}$, where, for example, tryptophan, phenylalanine and asparagine are suggested to be important for defining the pore size to permeants (Ma & Wang, 2018; Medeiros-Silva et al., 2023;

Tang et al., 2002) and histidine has been proposed as a pH sensor (Chew et al., 2009; Ma & Wang, 2018; Pinto et al., 1992).

The ion-selectivity, if any (Henkel et al., 2010; Largo et al., 2016; Surya et al., 2023), of viroporins is generally weak compared to the highly specialised selectivity filters of classical ion channels (Hille, 2001), and a range of viroporins are broadly cation-selective (Ewart et al., 1996; Mehnert et al., 2008; Melton et al., 2002; Piller et al., 1996; Premkumar, Wilson, et al., 2004; Wilson et al., 2004). The ion selectivity in a given environment can be described using permeability ratios, which is the ratio between two ions that permeate the pore (Hille, 2001). Taking $E_{SARS\text{-}CoV\text{-}1}$ as an example, it has an approximate 5 to10-fold preference for Na^+ over K^+ and a 10-fold preference for K^+ over Cl^- (Wilson et al., 2004). $E_{SARS\text{-}CoV\text{-}1}$ and the other cation-selective viroporins such as $p7_{HCV}$ (Premkumar, Wilson, et al., [2004]), $Vpu_{HIV\text{-}1}$ (Ewart et al., 1996) and 6K from Ross river virus ($6K_{RRV}$) (Melton et al., 2002) all exhibit relatively little discrimination between the monovalent cations Na^+ and K^+ (H^+ selectivity was not examined), whereas Cl^- is clearly less preferred. For comparison, the K^+/Na^+ permeability ratio for K^+-channels found in the animal kingdom can be more than 100 and even up to 1000 with complete rejection of anions, thus displaying a well-defined preference even within the monovalent cations (Dudev & Lim, 2009; Hille, 2001).

There are examples of ion-specialised viroporins, such as the H^+-selective $M2_{IAV}$, which prefer H^+ more than 1 million times over Na^+ (Chizhmakov et al., 1996), and the K^+-selective Kcv from *Paramecium bursaria* chlorella virus 1 ($Kcv_{PBCV\text{-}1}$), which prefers K^+ ~9 times more than Na^+ (Plugge et al., 2000). However, given that most viroporins are weakly selective in electrophysiology experiments, it is generally unclear whether the ion selectivity is meaningful to their function during the virus life cycle. Some exceptions exist, where the biological importance of selective ion conductance has been established. $M2_{IAV}$ is a well-studied example, because it facilitates the influx of protons into the viral interior leading to acidification and promotes uncoating of the virus and establishing the infection (Leiding et al., 2010; Stauffer et al., 2014). However, even $M2_{IAV}$ allows the conductance of other ions. To counteract the electrical gradient that arises from H^+ influx into the virus particle, $M2_{IAV}$ allows the exit of cations to restore a balance to the electrochemical potential (Leiding et al., 2010; Stauffer et al., 2014). In other examples of biologically relevant ion-selectivity, H^+ conductance by $p7_{HCV}$ was correlated with productive HCV infection (Wozniak et al., 2010), whereas Ca^{2+} release via $2B_{CVB3}$ from intracellular calcium stores was suggested to facilitate CVB3 release (Frank J.M. van Kuppeveld, Hoenderop, et al., 1997). Outside a cellular context, however, $p7_{HCV}$ and $2B_{CVB3}$ conduct other ions (de Jong et al., 2006; Premkumar, Wilson, et al., 2004; van Kuppeveld, Hoenderop, et al., 1997), potentially alluding to additional roles for these viroporins during virus infection. Identifying the coupling of ion selectivity of individual viroporins to their biological function will be crucial to determine the relevance of ion selectivity observed in electrophysiology systems.

Based on gating preference, ion channels can be grouped into three categories: voltage-gated, ligand-gated or mechanosensitive (Alexander et al., 2023). In the case of viroporins, to our knowledge, no known examples fit into any of these categories. In contrast, most characterised viroporins open and close spontaneously, although many studies report that they exhibit different states of conduction, either corresponding to different conformational states and/or simultaneous opening of multiple channels (Dey et al., 2019; Largo et al., 2016; Surya et al., 2023; Verdiá-Báguena et al., 2013; Whitfield et al., 2011). Lack of gating, however, does not mean that viroporins cannot be regulated or modulated. There are several examples of viroporins being modulated by pH; in some cases, such as $p7_{HCV}$, $E_{SARS\text{-}CoV\text{-}2}$ and $M2_{IAV}$, there is an inverse relationship between ion current and pH (Breitinger et al., 2016; Gan et al., 2012; Largo et al., 2016; Pinto et al., 1992; Xia et al., 2021), and in other cases, such as $E_{SARS\text{-}CoV\text{-}1}$ and SH_{hRSV}, changes in pH can invert the ion selectivity of the viroporin (Gan et al., 2008; Sunstrom et al., 1996; Verdiá-Báguena et al., 2013). Remarkably, once the pH inside $M2_{IAV}$-containing vesicles decreases, $M2_{IAV}$ switches its selectivity from H^+ influx to K^+ and Na^+ efflux allowing it to trap H^+ inside the virus (Leiding et al., 2010). In addition to H^+, specific ions on either membrane side can modulate viroporin activity. For example, high Ca^{2+} concentrations will change the selectivity of $p7_{HCV}$ to be less selective towards monovalent cations over Cl^- (Premkumar, Wilson, et al., 2004), and Na^+ can negatively modulate outward K^+ current via $Kcv_{PBCV\text{-}1}$ (Plugge et al., 2000).

Besides modulation by solute, the lipid environment can affect viroporin ion channel activity. The conductance of $E_{SARS\text{-}CoV\text{-}1}$ varies greatly when reconstituted in neutral versus negatively charged lipids (Verdiá-Báguena et al., 2013), and the ion selectivity changes from non-selective in neutral lipids to a 16-fold preference for cations over anions in negatively charged lipids (Surya et al., 2023). Similarly, $p7_{HCV}$ displays longer opening times in phosphatidylethanolamine-rich bilayers compared to phosphatidylcholine-rich membranes (Whitfield et al., 2011), and conductance of $p7_{CSFV}$ is substantially reduced when the negatively charged lipids are excluded from the lipid composition (Largo et al., 2016).

Besides ions, viroporins also allow the passage of small solutes such as carboxyfluorescein, FITC-dextrans and hygromycin B (Agirre et al., 2002; Aldabe et al., 1996; Bodelón et al., 2002; Ciccaglione et al., 1998; Dey et al., 2019; González & Carrasco, 1998; Guinea & Carrasco, 1994; Han et al., 2007; Liao et al., 2004; Madan et al., 2005; Raghava et al., 2011; StGelais et al., 2007; Wetherill et al., 2012). The functional outcome for the virus of such a feature, if any, is less well understood, but it has been a valuable trait for investigating viroporin function experimentally (Section 4.2). The size of the molecules, whether denoted by hydrodynamic diameter, molecular weight, or Stokes radius, that can penetrate the pore varies between viroporins and likely depends not only on the porin but also on the method used to investigate it. Studies on $2B_{PV}$, 2B from hepatitis A virus ($2B_{HAV}$), $p7_{HCV}$ or $p7_{CSFV}$ determined the size limitation of permeating agents to be 1, 5, 10, and 20 kDa, respectively (Agirre et al., 2002; Largo et al., 2018; Shukla et al., 2015; StGelais et al., 2007). As an example from a DNA virus, E5 from human papillomavirus ($E5_{HPV}$) allows passage of molecules with 0.6-nm Stokes radius and excluded molecules

of ≥1.4 nm (Wetherill et al., 2012). The diameter of selected viroporins has also been experimentally determined using transmission EM, sometimes with fusion proteins, and here, $p7_{HCV}$ forms pores of 2–8 nm in diameter (Luik et al., 2009), whereas pores formed by $E5_{HPV}$ fusion protein and SH_{hRSV} fusion protein are around 1–2 nm in diameter (Carter et al., 2010; Wetherill et al., 2012). Some viroporins can exist in dynamic heterogenous oligomeric populations, and the viroporins $p7_{CSFV}$ and NS2B from dengue virus ($NS2B_{DV}$) pore sizes consequently vary, reaching up to 10–30 nm in diameter (Largo et al., 2021; León-Juárez et al., 2016). However, whether these large structures are generated in the context of infection remains to be elucidated.

As for the ion-channel activity of viroporins, the small solute permeability can be modulated by pH with $M2_{IAV}$, $p7_{HCV}$ and $E5_{HPV}$ displaying increased permeability of a given solute at lower pH (Largo et al., 2016; Scott et al., 2020; Wetherill et al., 2012). Similarly, the lipid environment affects this function, as exemplified with $VP4_{SV40}$ permeabilising well plasma-membrane-like but less nuclear-membrane-like liposomes (Raghava et al., 2011). In addition, the chikungunya virus 6K ($6K_{CHIKV}$) and $2B_{HAV}$ only permeabilise ER-like, not plasma-membrane-like liposomes, although in these cases, lack of viroporin insertion into the latter can be the cause (Dey et al., 2019; Shukla et al., 2015). Because the insertion of viroporin into liposomes may depend on lipid composition, verification of insertion is necessary to truly uncouple this event from the functional readout.

Electrophysiology measurements parallel to solute permeability measurements have rarely been conducted in the same study. One study, however, showed that ion conductance and fluorescence permeability of $p7_{CSFV}$ both depended on the pore-forming domain and were similarly modulated by lipid composition and pH, suggesting that data retrieved via ion conductance measurements may be translated to permeability measurements and vice versa (Largo et al., 2016). Two separate studies on the ion channel and permeability function of $p7_{HCV}$ found that both activities were enhanced at low pH and were blocked by the drug amantadine, again supporting correlation (Griffin et al., 2003; StGelais et al., 2007). Furthermore, the $M2_{IAV}$ proton-selective channel displayed rimantadine resistance in both ion channel and permeability assays upon an S31N mutation (Scott et al., 2020; Wang et al., 2013).

Given the modulation of viroporin function by the lipid environment and the ion composition of the surrounding aqueous solution, care must be taken when applying meaning to ion selectivity or size of the permeating agent in differing environments. Such modulation does, however, render it possible that a viroporin may carry out different functions depending on context. This would align with viroporins being important for multiple steps of the virus life cycle (see Section 4.3).

4.2 | Various techniques can unveil pore function

As a corollary of the channel-pore duality feature of viroporins, the methods for their functional determination can be divided into two categories investigating ion flux and small solute permeability, respectively (Figure 3d–j).

The direct measurement of ion conductance by a viroporin can be done through electrophysiological techniques. These involve the use of microelectrodes that measure the ionic current across a membrane containing the viroporin of interest compared with a membrane that does not (Figure 3d). The techniques can be applied on either whole cell systems, such as *Xenopus laevis* oocytes (Pinto et al., 1992) and mammalian cells (Wang et al., 1994), or on artificial membrane systems such as planar lipid bilayers (Duff & Ashley, 1992; Piller et al., 1996; Saint et al., 2009), solid supported membranes (Balannik, Obrdlik, et al., 2010) or liposomes (Pham et al., 2017; Saint et al., 2009) with reconstituted viroporins. Electrophysiology techniques also allow for determining any potential ion selectivity of a viroporin (Ewart et al., 1996; Plugge et al., 2000). Importantly, when doing electrophysiology on whole cell systems, the dysregulation of endogenous ion channels (Antoine et al., 2007; Ewart et al., 2023; Shimbo et al., 1995) should be considered and, if possible, ruled out, for example, by using inhibitors of endogenous ion channels and conversely addressing if viroporin inhibitors target these channels (Ewart et al., 2023). Ion permeability can also be assessed indirectly. Complementation assays using K^+-uptake-deficient yeast (Wang et al., 2012) or bacteria (Taube et al., 2014) cultured in low K^+ medium have been used to study viroporins (Figure 3e). Under these conditions, cells only grow if they express a viroporin facilitating K^+ influx. As another indirect measurement, the ability of a viroporin to disturb pH can be assessed in a cellular haemadsorption assay, in which pH-dependent hemagglutinin expressed in cells only reaches the cell surface if the pH of secretory vesicles is raised by the presence of an appropriate viroporin (Griffin et al., 2004; Takeuchi & Lamb, 1994). Other types of ion flux assays use redox (Hyser Joseph et al., 2012) or ion-sensitive fluorophores (Griffin et al., 2004; Schroeder et al., 1994; Takeuchi & Lamb, 1994; Wozniak et al., 2010; Yu et al., 2021), for example, cells containing a pH-sensitive fluorophore, like pHluorin, that responds to H^+ flux when expressing a viroporin (Figure 3f) (Breitinger et al., 2016; Santner et al., 2018). Similarly, Ca^{2+}-sensing fluorophores can be used to assess the release from intracellular Ca^{2+}-stores upon expression of viroporins (Hyser et al., 2010; Hyser et al., 2013; van Kuppeveld, Hoenderop, et al., 1997) or the flux of Ca^{2+} into liposomes (Henkel et al., 2010; Pham et al., 2017).

For permeability assays that determine the ability of viroporins to permeabilise membranes to small hydrophilic solutes, hygromycin B-based assays were established early on, and many viroporins have been initially identified using this method (Figure 3g) (Aldabe et al., 1996; Bodelón et al., 2002; Ciccaglione et al., 1998; González & Carrasco, 1998; Han et al., 2007; Liao et al., 2004; Madan et al., 2005). Being a protein translation inhibitor that does not easily cross the membrane over short timescales, hygromycin B will only enter cells and inhibit protein translation if a viroporin can facilitate its entry (Madan et al., 2008). However, permeability may have been indirect for studies where viroporin inhibitors or null-function mutants were not used. Although not a direct measurement of pore function, cytotoxicity induced by expression of a viroporin can lead to growth

retardation in both yeast and bacteria cultures; however, only if growth can be restored by viroporin inhibitors, this suggests pore function (Balgi et al., 2013; Mao et al., 2013; Tomar et al., 2019). Importantly, cytotoxicity derived from functions parallel to pore function should be considered because pore inhibitors in that case would be unlikely to rescue growth. In another assay, the uptake of the β-galactosidase substrate ONPG into *Escherichia coli* can be facilitated by viroporins, and its colorimetric conversion to ONP in cells containing the enzyme can be measured using absorbance (Figure 3h) (Ciccaglione et al., 1998; González & Carrasco, 1998; Lama & Carrasco, 1992; Liao et al., 2004). Similarly, the release of radioactivity from mammalian or bacteria cells preloaded with small, radiolabelled metabolites such as **uridine** and **choline** can increase in viroporin-expressing cells and thus report on viroporin activity (Figure 3i) (Aldabe et al., 1996; Bodelón et al., 2002; González & Carrasco, 1998). The use of red blood cell haemolysis can be employed to measure viroporin activity, because viroporin insertion leads to osmotic lysis and release of haemoglobin (Raghava et al., 2011). Finally, fluorescent molecule release from, or uptake into, liposomes containing viroporins can assay membrane permeability (Figure 3j) (Agirre et al., 2002; Gervais et al., 2011; Largo et al., 2018; Raghava et al., 2011; StGelais et al., 2007).

4.3 | Viroporins influence virus entry, assembly and egress

Viroporins exert functions throughout the viral life cycle, but the most well-described occur during entry, assembly and egress of virus particles. For more in-depth reviews on viroporin function during the viral life cycle, see Scott and Griffin (2015) and Xia, Cheng, et al. (2022). Whether viroporin-mediated functions solely result from pore function, or via interactions with other viral or host proteins, or combinations thereof is not fully understood.

Enveloped viruses enter host cells via the fusion of virus and cell membranes and, in the case of SH_{HMPV}, $M2_{IAV}$ and $6k_{CHIKV}$, these viroporins have been shown to regulate membrane fusogenic processes (Bron et al., 1993; Dey et al., 2019; Masante et al., 2014). More importantly, during the establishment of IAV infection, $M2_{IAV}$ causes acidification of the virion leading to weakening of the interactions of M1 and the ribonucleoprotein (RNP) complexes and an influx of K^+ ions that further destabilises the interaction of RNP components, which after membrane fusion mediated by the HA-protein is released to the cytoplasm (Stauffer et al., 2014). Similarly, as a $p7_{HCV}$ specialised inhibitor reduces the infectivity of a sensitive strain, p7 virion-resident activity seems to be essential for HCV entry (Shaw et al., 2020). Later in the virus life cycle, new virus particles must be assembled inside the host cells. For some viruses, their viroporins may facilitate this process via an increase in cytosolic Ca^{2+} levels, as for the rotavirus viroporin NSP4 and $2B_{CVB3}$ (Hyser et al., 2010; van Kuppeveld, Hoenderop, et al., 1997; Zhou et al., 2009). In addition to these examples, mutation or deletion of E proteins of certain coronaviruses is associated with decreased particle production and/or aberrant virion formation, in some cases with fewer spike proteins, and although the exact mechanism is not determined, part of the effect might be attributed to E protein being a structural protein (DeDiego et al., 2007; Machamer & Youn, 2006; Ye & Hogue, 2007).

In the final part of any virus life cycle, the newly formed virus particles are released from host cells, and viroporins also contribute to this process. Several E proteins of coronaviruses are important for this step (Machamer & Youn, 2006; Ye & Hogue, 2007). The mechanism has been explored for $E_{SARS\text{-}CoV\text{-}2}$ and involves the deacidification of lysosomes and, thus, possibly prevention of particle degradation (Miura et al., 2023). A similar mechanism was shown for $p7_{HCV}$, which deacidifies host cell intracellular compartments, leading to successful virus production and release (Steinmann, Penin, et al., 2007; Wozniak et al., 2010). Likewise, $M2_{IAV}$ deacidifies the *trans*-Golgi network to prevent premature acid-induced fusogenic conformational changes to furin-cleaved hemagglutinin envelope protein (Alvarado-Facundo et al., 2015; Grambas et al., 1992). In addition, $M2_{IAV}$ is involved in the budding of new virus particles by inducing curvature of the membrane and scission of the budding virion in a mechanism independent of its channel function (Rossman et al., 2010).

4.4 | Viroporins can modulate host cell signalling

Viroporins can interact with other proteins encoded by the host or virus genomes and do so either through their TM or extramembranous regions. Interactions with host proteins often serve to inhibit antiviral responses of the infected cell. As an example, **CD4**, the receptor for HIV-1 infection, inhibits the release of progeny HIV-1 virions. To escape this, $Vpu_{HIV\text{-}1}$ interacts with newly synthesised CD4 through cytosolic and TM regions, sequestering it in the ER and sentencing it to degradation, which in addition prevents reinfection of the same cell (Bour et al., 1995; Magadán & Bonifacino, 2012; Willey et al., 1992). In addition, E proteins from both SARS-CoV 1 and 2 have been shown to interact with host proteins through a C-terminal PDZ-binding motif, and in the case of SARS-CoV-1, the motif was shown to be important for viral pathogenesis (Jimenez-Guardeño et al., 2014; Shepley-McTaggart et al., 2021). Viroporins may also antagonise antiviral responses of the innate immune system through direct interactions with mediators thereof. The $2B_{FMDV}$ directly interacts with retinoic acid-inducible gene 1 (**RIG-I**), a pattern recognition receptor sensing viral double stranded (ds)RNA, consequently downregulating RIG-I expression and ultimately its antiviral immune response (Weerawardhana et al., 2022; Zhu et al., 2016). Similarly, E_{PEDV} inhibits the translation of RIG-I associated antiviral proteins, although in this case, a direct interaction was not investigated (Zheng et al., 2022). When investigating immune evading strategies of HCV, one study found that $p7_{HCV}$ interacts with and blocks the function of IFI6-16, an interferon-induced mediator of antiviral responses in the host (Qi et al., 2017), thus exemplifying viroporin-linked immune evasion, although confirmation using an available $p7_{HCV}$ inhibitor (Table 1) is yet to come. An increasing number of studies have suggested that viroporins may activate the inflammasome and thus

mediate inflammatory signals, and although the mechanism behind this remains unknown, it is believed to involve disruption of ion homeostasis (Farag et al., 2020). It should be considered whether the cell lines used for these types of experiments are relevant to the virus infection and future designed viroporin inhibitors will likely help determine the influence of viroporin ion-channel activity for this process.

The induction of apoptosis by some viroporins, such as E_{MVH} and $2B_{PV}$, has been reported in several cases and suggested to be initiated via **caspase**-dependent mechanisms (Aweya et al., 2013; Chan et al., 2009; Cong et al., 2016; Madan et al., 2008; Ren et al., 2020; Yang et al., 2005). The outcome was proposed to help the spread of new virus particles (Madan et al., 2008). Whether apoptosis is a consequence of the permeabilising function of viroporins or happens independently is unclear, and current data are contradictory. For $3a_{SARS\text{-}CoV\text{-}1}$, mutagenesis shows that ion channel activity and apoptosis both decrease when mutating specific residues (Chan et al., 2009); however, collateral damage of these mutations on, for example, loss or gain of interactions cannot be ruled out, and thus, experiments using one of the available $3a_{SARS\text{-}CoV\text{-}1}$ inhibitors (Table 1) would be valuable to answer this question. Oppositely, $p7_{HCV}$ and $M2_{IAV}$ induce apoptosis in a mechanism independent of their ion channel function (Aweya et al., 2013; Gannagé et al., 2009). Of interest, cytosolic Ca^{2+}-increase can induce apoptosis and, thus, is possibly what drives viroporin-induced apoptosis in some cases (Hajnóczky et al., 2003).

Contrary to the pro-apoptotic effects of some viroporins, there are examples of viroporins, such as SH_{hRSV}, $ORF3_{PEDV}$ and $2B_{CVB3}$, that suppress apoptosis (Campanella et al., 2004; Fuentes et al., 2007; Luganini et al., 2018; Si et al., 2020). The manipulation of cell death by a virus during infection likely depends on the virus life cycle stage. Thus, suppression of apoptosis in the early stages of infection to allow replication may be followed by induction of apoptosis at later stages to facilitate egress, specifically of non-enveloped viruses (Roulston et al., 1999). Given the broad actions of viroporins spanning the entire virus life cycle, it is plausible that they participate in either pro- or anti-apoptotic actions depending on context.

In conclusion, although the functions of viroporins vary, they share the trait of forming membrane permeabilising pores. In addition, they are important for at least one part of the virus life cycle, be it entry, assembly, egress, inhibition of host antiviral responses or something else. Lastly, they are heavily modulated by the environment, perhaps owing to their ability to exhibit multiple functions during the virus life cycle, making them complicated to analyse and invoking caution in data interpretation.

5 | VIROPORINS ARE PROMISING DRUG TARGETS

Viroporins are pharmaceutically relevant targets. So far, the approach has largely been based on inhibiting their pore activity by direct or allosteric blockage or disrupting oligomerisation. A broad range of viroporin inhibitors have been discovered, and many are generic, exhibiting promiscuous inhibition of viroporin activity (Table 1). Such non-selective inhibition would be favourable in the case of 'one drug fits all', meaning one inhibitor could be used to treat a variety of virus infections, providing a tool to treat emerging virus diseases of the future. However, unwanted adverse effects caused by drug binding off-target, such as endogenous ion channels, may exist. In addition, most of the generic inhibitors exhibit low potency, making them unsuitable as drugs. In this section, we will describe the past and current efforts and challenges to developing viroporin-targeting drugs, focusing on those that made it to clinical trials, and provide some ideas to move viroporin drug research forward into the future.

5.1 | Clinical trials of viroporin inhibitors are sparse

The in vitro inhibition of virus infection in cell culture by generic or designed viroporin inhibitors has been demonstrated repeatedly using a variety of viruses, emphasising the great potential of viroporins as drug targets (Table 2). However, the only viroporin inhibitors ever marketed are amantadine and its derivative rimantadine (collectively adamantanes), which bind to $M2_{IAV}$, although the molecular target was not initially known (Figure 4a,b) (Hay et al., 1985; Wingfield et al., 1969). Because of widespread resistance (Bright et al., 2005; CDC, 2006) and unwanted side effects, such as effects on the central nervous system and gastrointestinal tract (Hayden et al., 1983), adamantanes are now clinically obsolete for treatment of IAV (Figure 4e). Drug discovery efforts towards identifying compounds that potently inhibit amantadine or rimantadine-resistant IAV strains have been made, either based on adamantyl amines or completely novel scaffolds, but despite successful in vitro studies with compounds showing reduction of virus titre and in some cases improved pharmacokinetics, these have not yet reached the clinic (Hu et al., 2018; Jalily et al., 2020; Rey-Carrizo et al., 2013; Scott et al., 2020; Stampolaki et al., 2023; Wang et al., 2018). One compound, however, showed promising results in mouse studies inhibiting both one amantadine sensitive and one resistant strain carrying the V27A mutation in M2, suggesting that M2 inhibitors against adamantane-resistant IAV strains are a viable antiviral strategy to treat IAV infections (Hu et al., 2017).

In addition to the use of amantadine against IAV, the drug was investigated in human clinical trials for the treatment of an array of different viruses including HCV, and although in vitro data suggested efficacy of amantadine against this virus (Griffin et al., 2008), no significant antiviral effect was observed in clinical trials neither as monotherapy nor in combination with interferon and **ribavirin** (Langlet et al., 2009; Smith et al., 2004). A caveat to these studies is that several HCV strains display an intrinsic amantadine and interferon resistance, explaining in part the negative results (Breitinger et al., 2016; Griffin et al., 2008). Amantadine also was tested in a small-scale case study for the treatment of dengue virus, which encodes an amantadine-sensitive viroporin M (M_{DENV}) (Premkumar et al., 2005). The use of amantadine reduced the disease symptoms of dengue virus patients (Lin & Chen, 2016), consistent with the in vitro activity of

TABLE 2 Viroporin inhibitors with in vitro antiviral efficacy.[a]

Inhibitor	Virus	Assay	Reference
Amantadine	Chikungunya virus (CHIKV)	Plaque assay + PCR	Dey et al. (2019)
	Foot-and-mouth virus (FMDV)	Viral titre	Ao et al. (2015)
	Hepatitis A virus (HAV)	PCR	Sasaki-Tanaka et al. (2022)
	Hepatitis C virus (HCV) (genotype dependent)	Focus forming assay	Griffin et al. (2008)
	Severe acute respiratory syndrome virus 2 (SARS-CoV 2)	Plaque assay + detection of spike protein	Lim et al. (2022)
[b]BE-12 [b]BE-30 [b]BE-31 [b]BE-32 [b]BE-33	Severe acute respiratory syndrome virus 2 (SARS-CoV 2)	PCR	Xia et al. (2021)
BIT225	Bovine viral diarrhoea virus (BVDV)	Inhibition of virus-induced cytopathic effect	Luscombe et al. (2010)
	Hepatitis C virus (HCV)	NS5A quantification	Meredith et al. (2013)
	Human immunodeficiency virus 1 (HIV-1)	Reverse transcriptase activity	Khoury et al. (2010)
	Severe acute respiratory syndrome virus 2 (SARS-CoV 2)	Plaque assay + PCR	Ewart et al. (2023)
DIDS	Enterovirus 71 (EV71)	Plaque assay + PCR	Xie et al. (2011)
[b]DL7	Influenza A virus (IAV)	Plaque assay	Scott et al. (2020)
[b]DP9	Influenza A virus (IAV)	Plaque assay	Scott et al. (2020)
Emodin	HCoV-OC43	Plaque assay + PCR	Schwarz et al. (2011)
HMA	HCoV-229E	Plaque assay	Wilson et al. (2006)
	Human astrovirus 1 (HAstV1)	Virus titre	Lulla & Firth (2020)
	Human astrovirus 4 (HAstV4)	Virus titre	Lulla & Firth (2020)
	Murine hepatitis virus (MHV)	Plaque assay	Wilson et al. (2006); Ye & Hogue (2007)
JK3-32	Hepatitis C virus (HCV)	Focus forming assay	Shaw et al. (2020)
[b]L1.1	Influenza A virus (IAV)	Plaque assay	Scott et al. (2020)
[b]LDS19	Hepatitis C virus (HCV)	Luciferase assay	Foster et al. (2014)
[b]LDS21	Hepatitis C virus (HCV)	Luciferase assay	Foster et al. (2014)
[b]M2WJ332	Influenza A virus (IAV)	Plaque assay	Wang et al. (2013)
NN-DGJ	Hepatitis C virus (HCV)	Luciferase assay	Steinmann, Whitfield, et al. (2007)
NN-DNJ	Hepatitis C virus (HCV)	Luciferase assay	Steinmann, Whitfield, et al. (2007)
	Influenza A virus (IAV)	Plaque assay	Scott et al. (2020)
Rimantadine	Hepatitis A virus (HAV)	PCR	Sasaki-Tanaka et al. (2022)
	Hepatitis C virus (HCV)	Focus forming assay	Griffin et al. (2008)
	Severe acute respiratory syndrome virus 2 (SARS-CoV 2)	Plaque assay + detection of spike protein	Lim et al. (2022)
Spiroadamantane	Influenza A virus (IAV)	Plaque assay	Hu et al. (2017)

[a]The inhibitors listed here were only included if inhibition was also demonstrated on the viroporin pore function directly.
[b]SAR optimised or rationally designed inhibitor.

amantadine (Koff et al., 1980), however, larger studies are needed to strengthen the evidence. The SARS-CoV-2 pandemic, which began in 2019, led to worldwide efforts to repurpose drugs against the viral disease and, again, amantadine was of interest. Amantadine inefficiently inhibited $E_{SARS\text{-}CoV\text{-}2}$ ion channel activity (Toft-Bertelsen et al., 2021), as found in previous studies on $E_{SARS\text{-}CoV\text{-}1}$ (Torres et al., 2007). In vitro SARS-CoV-2 infectivity and virus production was inhibited by amantadine, although again with low potency (Lim et al., 2022), and it failed to exhibit in vivo efficacy in both a mouse model (Lim et al., 2022) and in multiple human clinical trials (Barczyk et al., 2023; Rejdak et al., 2023; Weis et al., 2023).

The only other viroporin inhibitor that has reached human clinical trials is the **amiloride**-derivative BIT225, developed by Biotron (Figure 4c) (Khoury et al., 2010). It was initially developed as a $Vpu_{HIV\text{-}}$

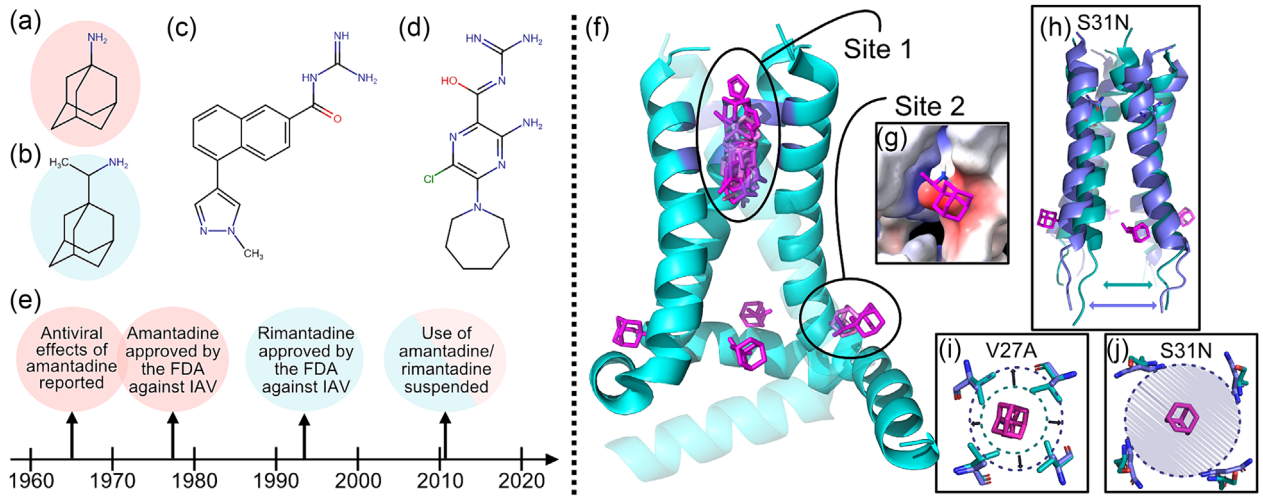

FIGURE 4 Commonly tested inhibitors against viroporins and $M2_{IAV}$ drug binding. (a) Amantadine (pink). (b) Rimantadine (blue). (c) BIT225. (d) Hexamethylene amiloride. (e) Timeline of amantadine and rimantadine use against $M2_{IAV}$. (f) Binding sites one and two on $M2_{IAV}$ (teal) identified by circles, with site two existing in each of the four helix interfaces, front helix made transparent for clarity. All drugs (magenta) from experimentally determined structures of $M2_{IAV}$ displayed on a single structure (PDB ID 2L0J). Purple residues on the structure indicate sites commonly mutated in drug-resistant variants. (g) Site two shown as polar surfaces of the two adjoining helices bound to rimantadine. (h) Side view of S31N mutation, WT (teal); S31N (purple). (i) Top view of V27A mutation, WT (teal); V27A (purple). (j) Top view of S31N mutation, WT (teal); S31N (purple).

$_1$ inhibitor and exhibits efficacy in Vpu ion channel inhibition and anti-HIV-1 effects in macrophages and dendritic cells (Khoury et al., 2010, 2016). In the first trial with HIV-1 infected patients, 400-mg BIT225 twice daily reduced the virus copy number only at day 10 of treatment in 3 out of 6 patients, and in the second trial, BIT225 was investigated in combination with the standard of care three-drug antiretroviral therapy but failed to further reduce the HIV-1 plasma RNA in patients (Luscombe et al., 2020; Wilkinson et al., 2015). The most common side effects observed in monotherapy with BIT225 were headache, nausea and vomiting, and thus, the type of adverse effects caused by BIT225 is reminiscent of those encountered during treatment with amantadine (Hayden et al., 1983; Wilkinson et al., 2015). Since the development of BIT225 as an HIV-1 targeting drug, it has been re-investigated in a pre-clinical mouse model of SARS-CoV-2 infection. Here, BIT225 inhibited $E_{SARS\text{-}CoV\text{-}2}$ ion channel activity in vitro and effectively reduced respiratory tract viral load, inflammatory cytokine production and, critically, lethality in a humanised transgenic mouse model, even when treatment was initiated 48 h post-infection (Ewart et al., 2023). In the same mouse model for SARS-CoV-2 infection, the optimised $E_{SARS\text{-}CoV\text{-}2}$ inhibitor BE-33 was able to after 1 day reduce viral RNA copies and the expression of inflammatory cytokines in lungs when administered either 2 h prophylactically or 2 h post infection (Xia et al., 2021). Furthermore, in a hamster model for SARS-CoV-2, rimantadine, but not amantadine, modestly reduced the lung viral titre, altogether suggesting inhibition of viroporin activity of SARS-CoV-2 as a viable treatment option (Lim et al., 2022).

The human trials administering amantadine and BIT225 to patients to treat various viruses, excluding IAV, lack convincing positive results, contradicting the repeatedly observed efficacy against virus infections in cell culture. This may be explained in part by the shortage of investigation into the target engagement of the viroporin inhibitor. Amantadine and BIT225 must be added at micromolar concentrations to exert their antiviral function in cell cultures. The half maximal effective concentration (EC_{50}) of amantadine against SARS-Cov-2 infectivity is 120 μM, and to inhibit sensitive HCV strains, amantadine is added at 20- to 100-μM concentrations (Griffin et al., 2008; Lim et al., 2022), with rimantadine more potent in both cases (Griffin et al., 2008; Lim et al., 2022). In comparison, the in vitro cell culture EC_{50} of amantadine against a sensitive IAV strain is 0.3 μM (Abed et al., 2005). The in vitro effect of BIT225 against HIV-1 in macrophages and dendritic cells results in an EC_{50} of 2.25 μM and an antiviral effect at 20 μM, respectively (Khoury et al., 2010, 2016). As for other viruses, BIT225 inhibits HCV infectivity and transmission at one concentration tested (30 μM) in Huh7.5 cells (Meredith et al., 2013) and SARS-CoV-2 with an EC_{50} between 2.5 and 7.9 μM depending on the assay, virus genotype and cell type (Ewart et al., 2023). However, there has been some debate regarding the toxicity of BIT225 and, based on analyses done in varying cell types using diverse techniques, the 50% cytotoxic concentration (CC_{50}) was reported to be between 11.6 and 284 μM (Khoury et al., 2010; Luscombe et al., 2010; Meredith et al., 2013; Shaw et al., 2020).

The μM in vitro efficacy of generic viroporin targeting drugs like amantadine and BIT225 suggests room for affinity improvement, and none of the human trial studies have, preceding their initiation, quantified the affinity or stoichiometry of the ligand to the viroporin, nor the specificity of the interaction. Neither have they qualitatively studied the binding mode through mutagenesis or experimental 3D-structures with the ligand, all common endeavours in drug design and molecular pharmacology of membrane proteins. It is likely that the

success rate of clinical trials investigating the efficacy of viroporin inhibitors will increase once a drug–target interaction has been studied in greater depth, possibly coupled to the rational design and optimisation of drugs through SAR studies and structure-guided drug design. The latter has been pursued through a series of studies, mainly focusing on $p7_{HCV}$ and $M2_{IAV}$, and several were successful in designing new and more potent anti-HCV and anti-IAV compounds, respectively (Table 1) (Foster et al., 2014; Scott et al., 2020; Shaw et al., 2020; StGelais et al., 2007; Wang et al., 2013; Wetherill et al., 2012). For example, a structure-guided in silico compound library screening identified two $M2_{IAV}$ inhibitors with novel scaffolds different from amantadine both exhibiting potent anti-IAV effects, resulting in an EC_{50} of around 1.5 μM (Scott et al., 2020). Similar efforts with a $p7_{HCV}$ structure-based channel model as starting point resulted in two novel $p7_{HCV}$ inhibitors, exhibiting antiviral efficacy at a concentration of 400 nM, drastically improved compared with the adamantanes (Foster et al., 2014). Seeing a rationally designed viroporin inhibitor make it further than in vitro cell culture assays will be a true test of the general usefulness of viroporins as drug targets and the biggest advancement in the field since amantadine was identified to target $M2_{IAV}$.

5.2 | The site of viroporin inhibitor binding is not universal

The most well-studied binding mode for an inhibitor-viroporin pair is amantadine with $M2_{IAV}$, where two binding sites have been described (Figure 4f,g). Site one resides inside the pore on the luminal side, around Ser31, facilitating a direct blocking mechanism (Figure 4f,i,j) (Cady et al., 2009, 2010; Stouffer et al., 2008; Wang et al., 2013; Wu et al., 2014). Site two resides in the helix-lipid interface on the cytosolic side of the membrane formed by the interface of two adjacent helixes centred around Asp44 (Figure 4f,g) (Cady et al., 2010; Pielak et al., 2009), functioning allosterically by stabilising the closed state of the pore (Schnell & Chou, 2008).

More structures exist where site one is occupied, and site two can only be occupied in CD-$M2_{IAV}$-structures because this site is incomplete in the shorter TMH peptides (Pielak et al., 2009; Schnell & Chou, 2008). Some argue that site two interacts with ligands due to the high partition coefficient of the amphipathic adamantanes (Cady et al., 2009, 2010; Chew et al., 2008; Schnell & Chou, 2008), making them suited to localise to the membrane surface, without specific binding, especially in cases of high molar excess of the drug (Gu et al., 2011; Konstantinidi et al., 2018, 2020; Thomaston et al., 2021). Besides $M2_{IAV}$, ligand binding at the helix-lipid interface has been observed for other viroporins, including $E_{SARS\text{-}CoV\text{-}2}$ and $p7_{HCV}$ (Foster et al., 2011; Somberg et al., 2023), as well as for other drugs than the adamantanes (Scott et al., 2020; Shaw et al., 2020), showing its generality. Amantadine has been observed to bind with higher affinity to the closed state of the $M2_{IAV}$-tetramer (Cady et al., 2010; Cady & Hong, 2009), adding the additional aspect that potential inhibitors may be capable of binding multiple—or selective—conformations.

While no structures of other drug-bound viroporins are available, the binding modes of other viroporin-inhibitor complexes have been investigated. The binding of various inhibitors to $p7_{HCV}$ has been studied through mutagenesis, determining the binding mode through resistance variants. Rimantadine binds $p7_{HCV}$ at a membrane-exposed binding pocket around Leu20, preventing pH-dependent pore opening (Foster et al., 2011). Similarly, alkylated iminosugars and novelly designed $p7_{HCV}$ inhibitors bind in the protein-lipid interface, around the Leu20-site (Foster et al., 2011; Shaw et al., 2020; Wei et al., 2021). A structural study of $E_{SARS\text{-}CoV\text{-}2}$ and **hexamethylene amiloride** (HMA, Figure 4d) suggested that HMA binds dynamically inside the N-terminal lumen of the pore, with higher drug sensitivity observed in lipid bilayers compared with detergent micelles (Mandala, McKay, et al., 2020). However, new data obtained with a lower HMA concentration indicate that HMA preferably binds $E_{SARS\text{-}CoV\text{-}2}$ with a 1:5 ratio on the outer periphery of the channel (Somberg et al., 2023). HMA and its derivatives have also been shown more broadly to block other viroporins, including $M2_{IAV}$ (Jalily et al., 2016), $Vpu_{HIV\text{-}1}$ (Rosenberg et al., 2016) and $p7_{HCV}$ (Premkumar, Wilson, et al., 2004), although HMA shows high cytotoxicity (Breitinger et al., 2021; Griffin et al., 2008). These observations further support the possibility of ligands binding both luminal and, perhaps preferably, at peripheral membrane-exposed binding sites.

From the wealth of studies on amantadine binding and the general lack of structural information and quantitative measures, this provides a distorted view of viroporin-drug binding. More in-depth studies are clearly warranted, and there is also a need to increase the breadth of the studies to focus beyond $M2_{IAV}$, $p7_{HCV}$ and $E_{SARS\text{-}CoV\text{-}2}$. The overall uncertainty of how inhibitors bind to viroporins and the lack of an inhibition mechanism for most viroporins, coupled to a diverse energy landscape with several possible states, make drug optimisation processes difficult. Hence, while the generic compounds can identify druggable site(s), this information should be exploited to develop more specific and effective drugs.

5.3 | Resistance limits the use of anti-viral drugs

With amantadine and rimantadine as the only marketed viroporin inhibitors, the resistance arising from treating humans exposed to a virus can best be exemplified by IAV. Resistance to adamantanes was detected as early as 1980 (Heider et al., 1981) but was relatively infrequent until the early 2000s (Hussain et al., 2017). In a 4-year period between 2000 and 2004, the resistance rose from 1.1% to 27% among H3N2 isolates from Asia (Bright et al., 2005), whereas, on a global level, the resistance incidents were at 12.3% of circulating IAV H3N2 subtypes (Hussain et al., 2017). In the following period, the global adamantane resistance increased dramatically to 45% among all circulating IAV subtypes by 2013 (Dong et al., 2015). Several mutations in $M2_{IAV}$, including S31N and V27A as the most dominant, caused adamantane resistance (Figure 4f, h–j). S31N, lining the inner pore channel, is the major resistance mutation accounting for 95% of all resistant subtypes and proposed to arise independently at least

11 times in the H3N2 subtype during a 10-year period (Hussain et al., 2017). However, other resistance mutations span the length of the helix, including ones in the helix–helix interface and in a larger region than that occupied by luminally bound drug molecules (Hussain et al., 2017). Therefore, resistance could be more complex than alterations at either binding site, such as the mutations L46P and R45H around site two in $M2_{IAV}$ (Musharrafieh et al., 2019, 2020), impacting folding, lipid interaction, allostery and stabilisation of oligomeric states. Some of the mutations, such as S31N and V27A, lead to destabilisation of the tetramer and an increase in the observed dynamics (Pielak et al., 2009; Pielak & Chou, 2010), which affects drug binding negatively, both in direct blocking of the channel and by allosteric inhibition (Pielak & Chou, 2010; Thomaston et al., 2020).

Only one other example of viroporin drug resistance occurring in the treatment of infected humans exists. During clinical trials investigating amantadine in combination with interferon-α based treatment against HCV, the L20F substitution in p7 of HCV in the amantadine-treated patient group was correlated with non-responders (Mihm et al., 2006). This substitution was later shown to confer amantadine and rimantadine resistance in HCV cell cultures and to inhibit fluorescence release through $p7_{HCV}$ (Foster et al., 2011). Intriguingly, the L20F mutation does not confer resistance to the imino-sugar *N*N-DNJ, and conversely, a rimantadine-sensitive strain with a hyperactivity conferring F25A mutation was resistant to *N*N-DNJ, again pointing to several distinct druggable sites in $p7_{HCV}$ (Foster et al., 2011).

In the absence of human trials, the resistance developed in viruses upon treatment with viroporin inhibitors can be determined in cell cultures by extended exposure that spans several replication cycles. In an attempt to develop inhibitors of the S31N $M2_{IAV}$ variant, it was found that an adamantane-based inhibitor rapidly selected resistant IAV variants, whereas other novel inhibitors did not, suggesting that the drug scaffold could be important to the genetic barrier of resistance development (Scott et al., 2020). In another study, an imino-sugar sensitive HCV strain was efficiently cleared over five passages during exposure to the compounds, suggesting that resistance to these did not occur despite studies having identified naturally occurring resistance mutations (Foster et al., 2011; Steinmann, Whitfield, et al., 2007). However, it cannot be ruled out that in vitro resistance could emerge under different experimental conditions.

The currently known single residue mutations that confer resistance to viroporin inhibitors do not generally decrease the fitness of the virus, meaning that the genetic barrier to resistance development is low (Foster et al., 2011; Scott et al., 2020). In addition, if inhibitors bind within the pore, the homo-oligomeric nature of viroporins means that a single mutation in the primary structure results in an n-fold symmetrical effect in the quaternary structure of nsubunits. Because the only examples of resistance development in humans are cases with amantadine, the general propensity of viruses to become resistant to viroporin inhibitors is difficult to assess. A potential positive prospect is that not all viroporin inhibitors prompt resistance to the same degree (Scott et al., 2020), rendering the design of drugs with less propensity for resistance development possible.

One approach that could be employed to diminish the likelihood of resistance development towards viroporin inhibitors is the co-administration of one or more other antivirals, because the genetic barrier for multiple simultaneous resistance mutations is higher than for single mutations. A prime example of combining several (two or three) antivirals is in the treatment of HIV-1 infections, for which patients need life-long treatment and where mono-therapy inevitably causes resistance (Shyr et al., 2021). In the case of viroporin inhibitors, these may be combined with a different type of antiviral, targeting another viral protein, or they could be supplemented with another viroporin inhibitor that binds the same target but in a different manner. This approach may even result in synergistic effects, such as those achieved by adding either two $M2_{IAV}$ inhibitors or one $M2_{IAV}$ inhibitor along with an IAV protease/neuraminidase inhibitor to cell cultures infected with IAV (Scott et al., 2020).

5.4 | The prospects for viroporin drugs are positive

The fact that amantadine, a more than 40-year-old yet discontinued antiviral drug in the use against IAV, was the chosen viroporin inhibitor candidate for human trials with SARS-CoV-2 demonstrates that antivirals against viroporins are poorly developed. This is paradoxical to the continuous discovery that viroporins are important for multiple steps in the viral life cycle and that inhibitors impede virus infections in cell culture (Table 2). To date, a significant focus has been on building specific amantadine derivatives or compounds with alternative functional groups (Mandour et al., 2018; Shiryaev et al., 2018; Stampolaki et al., 2023) or repurposing of generic inhibitors. However, this approach is narrow and does not allow for the development of novel scaffolds, which is clearly needed. Thus, emphasis must be placed on developing new and more specific viroporin inhibitors.

Such goals can be achieved via rational drug design based on viroporin structures and SAR studies, of which there are a few examples using viroporins (Foster et al., 2014; Scott et al., 2020; Shaw et al., 2020; StGelais et al., 2007; Wetherill et al., 2012). However, viroporin 3D-structures remain sparse, incomplete and sometimes inaccurate, needing a massive recovery effort. In addition, targeting diverse structural states would be ideal but requires fine-tuning of the experimental conditions and high-resolution structures in realistic membrane systems, allowing for more detailed computational analyses, not to forget assigning the function of each state to their biology. Until then, computational screens for potential new drug candidates can be performed by molecular docking of small molecule compounds to models of viroporins. Several such screens have resulted in new compounds and insight into possible binding modes, but some lack the in vitro and in vivo testing necessary to validate any effect of the compound (Jalily et al., 2022; Klimochkin et al., 2016; Lebedeva et al., 2021; Mathew et al., 2015; Wei et al., 2022). Furthermore, in silico screens have been used to test FDA-approved drugs as possible inhibitors for viroporins, and while potential compounds have been suggested, a lack of follow-up testing in vitro and in vivo exists here (Das et al., 2021; Dey et al., 2020; Zeba et al., 2023). These types of inhibitor screens hold

some information, regarding scaffolds and functional groups and can help suggest new targets. However, successful screening depends on a relevant starting model of the viroporin target, and for most viroporins, high-confidence models are still lacking.

Recent years of drug discovery have implemented high-throughput development of peptide drugs, including variations such as cyclic peptides and incorporation of non-native amino acids, for example, through mRNA display systems (Huang et al., 2021; Rogers & Suga, 2015). While mRNA display systems were originally designed for soluble protein and have not yet been applied to viroporins, it has been shown to work for membrane proteins (Stefan et al., 2021) and may thus pose a future strategy for viroporin drugs. Another possible approach not yet extensively explored would be to embark on the already available repertoire of drugs that target ion channels (Harding et al., 2023) or other drug compounds libraries, as such strategy can be used to identify new viroporin inhibitors or new scaffolds for SAR optimisations. Exactly that has been done for the M protein of Zika virus (M_{ZIKV}), West Nile virus (M_{WNV}) and M_{DENV} identifying several drugs inhibiting viroporin function; thus, a next step would be verifying their antiviral potency (Lahiri & Arkin, 2022; Tomar et al., 2022). Despite the few mentioned studies using bacteria-based assays to identify hits in a semi-high-throughput setup, there is a huge need to develop high-throughput methods suitable for screening tens of thousands of inhibitors. The gold standard for viroporin assays is based on electrophysiology or liposome fluorescence release, which require individual measurements and protein synthesis or purification, respectively, making them unsuitable for high-throughput screening. The development of assays that are capable of many parallel measurements with minimum handling will facilitate screening of large libraries, allowing exploration of the chemical space of binding to viroporins and thus be of great value to the viroporin drug field.

To conclude, the lack of successful clinical trials examining the antiviral potency of viroporin inhibitors does not point to it as an unviable strategy but instead reinforces that advancements in drug-target engagements are necessary before proceeding. In addition, the repurposing of adamantanes and BIT225 against other viruses without first optimising drug potency to the novel target will likely result in unsuccessful clinical trials as demonstrated repeatedly. Instead, designing novel drug scaffolds and optimising existing ones through SAR studies or structure-based drug design can, as examples in the literature prove, result in more potent inhibitors, and although none of these have made it to clinical trials, they hold the potential to elevate the outcomes of such studies.

6 | WHAT ARE THE OUTSTANDING QUESTIONS?

Viroporins comprise a diverse family of proteins, both in terms of function and structure. Most viroporins are not essential for viral genome replication when studied in cell cultures and are not limited to one specific function. Consequently, viroporins are easily overlooked, and the exact extent of viroporins is unknown; thus, their impact during infection could be critically underestimated. Currently, most viroporins are from RNA viruses (Table 1), but whether this truly reflects viroporin abundance or if this observation stems from incomplete searching and lack of awareness are unknown. In this review, we discussed the common features of viroporins and proposed best practices for viroporin classification (Figure 1b), increasing the focus on this class of proteins and pushing the field forward.

One clear barrier to understanding viroporins is the lack of complete 3D-structures solved in native or native-like environments. This, combined with the apparent broad energy landscape with diverse states, makes the rational design of novel drugs targeting discrete states possible but difficult. Although computational methods can help close the knowledge gap, as evidenced by several successful examples of rationally designed drugs based on models, the current predicted models of viroporins lack confidence. Therefore, to improve our understanding, there is still a huge need for experimental structural characterisation of viroporins alone and in complex with inhibitors.

Another clear obstacle in furthering the understanding of viroporin function is the shortage of specific and high-affinity inhibitors as well as their quantification in terms of stoichiometry and affinity. Defining novel strategies for developing new inhibitors is encouraged to go beyond the current approach, relying on a restricted portfolio of generic inhibitors as scaffolds. High-throughput screening methods of bigger libraries, like those employed for $M2_{IAV}$ and $p7_{HCV}$, could be helpful to overcome current barriers in discovering high-affinity binders, and such molecules will inevitably further the understanding of viroporin function during the virus life cycle.

The only current classification of viroporins, an iteration of which we present here, is based on their membrane topology. However, as an increasing number of viroporins are identified and our knowledge about them grows, it is possible that sub-classification of the viroporin family, based either on their function or structural aspects, will be needed. With the ambiguous identification and characterisation of novel viroporins, our current understanding of the family is built mainly on the staples in the field, that is, M2 of *Orthomyxoviridae*, p7 of *Flaviviridae*, E protein of *Coronaviridae*, 2B of *Picornaviridae* and 6K of *Togaviridae* (Table 1), some of which are still understudied compared to others. Consequently, there is a huge, untapped source of information in the less characterised viroporins.

With the provided best practices (Figure 1b), which include identifying key structural and functional features as well as non-functional mutations, inhibitors and resistance mutations, ultimately supporting the identification of their role in the virus life cycle, this information can be exposed and contribute to our understanding of viroporins as a protein family and ultimately the design of antivirals targeting viroporins. Advancing the field of viroporins is necessary and will result in a huge societal impact.

NOMENCLATURE OF TARGETS AND LIGANDS

Key protein targets and ligands in this article are hyperlinked to corresponding entries in https://www.guidetopharmacology.org and are permanently archived in the Concise Guide to PHARMACOLOGY 2023/24 (Alexander et al., 2023).

AUTHOR CONTRIBUTIONS

K. Devantier, V.M.S. Kjær, B.B. Kragelund and M.M. Rosenkilde conceived the project. K. Devantier and V.M.S. Kjær wrote first draft. K. Devantier made the figures, and V.M.S. Kjær made the tables. K. Kjær, V.M.S. Kjær, S. Griffin, B.B. Kragelund and M.M. Rosenkilde wrote and edited the manuscript.

ACKNOWLEDGEMENTS

This work was supported by the Novo Nordisk Foundation 'Turning virus survival and defense mechanisms into offensive antiviral therapy' (NNF20OC0062899 to M.M.R), the Danish Council for Independent Research|Medical Sciences (DFF1: 6110-00688B to M.M.R), the European Research Council: VIREX (Grant agreement 682549, Call ERC-2105-CoG to M.M.R), the Lundbeck Foundation (large project grant - R242-2017-409 to M.M.R), donation from deceased Valter Alex Torbjørn Eichmuller (2020-117043 to M.M.R), the Novo Nordisk Foundation challenge grant REPIN, rethinking protein interactions (NNF18OC0033926 to B.B.K.) and UKRI Impact Accelerator funding award to S.G.

CONFLICT OF INTEREST STATEMENT

The authors declare no conflict of interest.

DECLARATION OF TRANSPARENCY AND SCIENTIFIC RIGOUR

This declaration acknowledges that this paper adheres to the principles for transparent reporting and scientific rigour of preclinical research as stated in the BJP guidelines for Design and Analysis and as recommended by funding agencies, publishers and other organisations engaged with supporting research.

ORCID

Kira Devantier https://orcid.org/0009-0002-4200-4707
Mette M. Rosenkilde https://orcid.org/0000-0001-9600-3254

REFERENCES

Abed, Y., Goyette, N., & Boivin, G. (2005). Generation and characterization of recombinant influenza A (H1N1) viruses harboring amantadine resistance mutations. *Antimicrobial Agents and Chemotherapy*, *49*(2), 556–559. https://doi.org/10.1128/aac.49.2.556-559.2005

Agirre, A., Barco, A., Carrasco, L., & Nieva, J. L. (2002). Viroporin-mediated membrane permeabilization: Pore formation by nonstructural poliovirus 2B protein*. *Journal of Biological Chemistry*, *277*(43), 40434–40441. https://doi.org/10.1074/jbc.M205393200

Aldabe, R., Barco, A., & Carrasco, L. (1996). Membrane permeabilization by poliovirus proteins 2B and 2BC*. *Journal of Biological Chemistry*, *271*(38), 23134–23137. https://doi.org/10.1074/jbc.271.38.23134

Alexander, S. P. H., Mathie, A., Peters, J. A., Veale, E. L., Striessnig, J., Kelly, E., Armstrong, J. F., Faccenda, E., Harding, S. D., Pawson, A. J., Sharman, J. L., Southan, C., Davies, J. A., & Collaborators, C. (2023). The concise guide to pharmacology 2023/24: Ion channels. *British Journal of Pharmacology*, *180*, S145–S222. https://doi.org/10.1111/bph.16178

Almeida, J. G., Preto, A. J., Koukos, P. I., Bonvin, A., & Moreira, I. S. (2017). Membrane proteins structures: A review on computational modeling tools. *Biochimica et Biophysica Acta - Biomembranes*, *1859*(10), 2021–2039. https://doi.org/10.1016/j.bbamem.2017.07.008

Alvarado-Facundo, E., Gao, Y., Ribas-Aparicio, R. M., Jiménez-Alberto, A., Weiss, C. D., & Wang, W. (2015). Influenza virus M2 protein Ion channel activity helps to maintain pandemic 2009 H1N1 virus hemagglutinin fusion competence during transport to the cell surface. *Journal of Virology*, *89*(4), 1975–1985. https://doi.org/10.1128/jvi.03253-14

Antoine, A.-F., Montpellier, C., Cailliau, K., Browaeys-Poly, E., Vilain, J.-P., & Dubuisson, J. (2007). The alphavirus 6K protein activates endogenous ionic conductances when expressed in Xenopus oocytes. *Journal of Membrane Biology*, *215*(1), 37–48. https://doi.org/10.1007/s00232-007-9003-6

Ao, D., Guo, H.-C., Sun, S.-Q., Sun, D.-H., Fung, T. S., Wei, Y.-Q., Han, S.-C., Yao, X.-P., Cao, S.-Z., Liu, D. X., & Liu, X.-T. (2015). Viroporin activity of the foot-and-mouth disease virus non-structural 2B protein. *PLoS ONE*, *10*(5), e0125828. https://doi.org/10.1371/journal.pone.0125828

Araujo, G. C., Silva, R. H., Scott, L. P., Araujo, A. S., Souza, F. P., & de Oliveira, R. J. (2016). Structure and functional dynamics characterization of the ion channel of the human respiratory syncytial virus (hRSV) small hydrophobic protein (SH) transmembrane domain by combining molecular dynamics with excited normal modes. *Journal of Molecular Modeling*, *22*(12), 286. https://doi.org/10.1007/s00894-016-3150-6

Aweya, J. J., Mak, T. M., Lim, S. G., & Tan, Y.-J. (2013). The p7 protein of the hepatitis C virus induces cell death differently from the influenza A virus viroporin M2. *Virus Research*, *172*(1), 24–34. https://doi.org/10.1016/j.virusres.2012.12.005

Baeza-Delgado, C., Marti-Renom, M. A., & Mingarro, I. (2013). Structure-based statistical analysis of transmembrane helices. *European Biophysics Journal*, *42*(2–3), 199–207. https://doi.org/10.1007/s00249-012-0813-9

Baker, R. E., Mahmud, A. S., Miller, I. F., Rajeev, M., Rasambainarivo, F., Rice, B. L., Takahashi, S., Tatem, A. J., Wagner, C. E., Wang, L. F., Wesolowski, A., & Metcalf, C. J. E. (2022). Infectious disease in an era of global change. *Nature Reviews. Microbiology*, *20*(4), 193–205. https://doi.org/10.1038/s41579-021-00639-z

Balannik, V., Carnevale, V., Fiorin, G., Levine, B. G., Lamb, R. A., Klein, M. L., DeGrado, W. F., & Pinto, L. H. (2010). Functional studies and modeling of pore-lining residue mutants of the influenza a virus M2 ion channel. *Biochemistry*, *49*(4), 696–708. https://doi.org/10.1021/bi901799k

Balannik, V., Obrdlik, P., Inayat, S., Steensen, C., Wang, J., Rausch, J. M., DeGrado, W. F., Kelety, B., & Pinto, L. H. (2010). Solid-supported membrane technology for the investigation of the influenza A virus M2 channel activity. *Pflügers Archiv - European Journal of Physiology*, *459*(4), 593–605. https://doi.org/10.1007/s00424-009-0760-1

Balgi, A. D., Wang, J., Cheng, D. Y. H., Ma, C., Pfeifer, T. A., Shimizu, Y., Anderson, H. J., Pinto, L. H., Lamb, R. A., DeGrado, W. F., & Roberge, M. (2013). Inhibitors of the influenza A virus M2 proton channel discovered using a high-throughput yeast growth restoration assay. *PLoS ONE*, *8*(2), e55271. https://doi.org/10.1371/journal.pone.0055271

Barczyk, A., Czajkowska-Malinowska, M., Farnik, M., Barczyk, M., Boda, Ł., Cofta, S., Duława, J., Dyrbuś, M., Harat, R., Huk, M., Kotecka, S., Nahorecki, A., Nasiłowski, J., Naumnik, W., Przybylski, G., Słaboń-Willand, M., Skoczyński, S., Wita, K., Zioło, G., & Kuna, P. (2023). Efficacy of oral amantadine among patients hospitalised with COVID-19: A randomised, double-blind, placebo-controlled, multicentre study. *Respiratory Medicine*, *212*, 107198. https://doi.org/10.1016/j.rmed.2023.107198

Basu, K., Krugliak, M., & Arkin, I. T. (2023). Viroporins of Mpox virus. *International Journal of Molecular Sciences*, *24*(18), 13828. https://doi.org/10.3390/ijms241813828

Bodelón, G., Labrada, L.a., Martínez-Costas, J., & Benavente, J. (2002). Modification of late membrane permeability in avian Reovirus-infected

cells: Viroporin activity of the S1-encoded nonstructural p10 protein*. *Journal of Biological Chemistry*, *277*(20), 17789–17796. https://doi.org/10.1074/jbc.M202018200

Boscarino, J. A., Logan, H. L., Lacny, J. J., & Gallagher, T. M. (2008). Envelope protein palmitoylations are crucial for murine coronavirus assembly. *Journal of Virology*, *82*(6), 2989–2999. https://doi.org/10.1128/jvi.01906-07

Bour, S., Schubert, U., & Strebel, K. (1995). The human immunodeficiency virus type 1 Vpu protein specifically binds to the cytoplasmic domain of CD4: Implications for the mechanism of degradation. *Journal of Virology*, *69*(3), 1510–1520. https://doi.org/10.1128/jvi.69.3.1510-1520.1995

Breitinger, U., Ali, N. K. M., Sticht, H., & Breitinger, H.-G. (2021). Inhibition of SARS CoV envelope protein by flavonoids and classical viroporin inhibitors [original research]. *Frontiers in Microbiology*, *12*, 692423. https://doi.org/10.3389/fmicb.2021.692423

Breitinger, U., Farag, N. S., Ali, N. K. M., & Breitinger, H.-G. A. (2016). Patch-clamp study of hepatitis C p7 channels reveals genotype-specific sensitivity to inhibitors. *Biophysical Journal*, *110*(11), 2419–2429. https://doi.org/10.1016/j.bpj.2016.04.018

Bright, R. A., Medina, M. J., Xu, X., Perez-Oronoz, G., Wallis, T. R., Davis, X. M., Povinelli, L., Cox, N. J., & Klimov, A. I. (2005). Incidence of adamantane resistance among influenza A (H3N2) viruses isolated worldwide from 1994 to 2005: A cause for concern. *Lancet*, *366*(9492), 1175–1181. https://doi.org/10.1016/s0140-6736(05)67338-2

Bron, R., Kendal, A. P., Klenk, H. D., & Wilschut, J. (1993). Role of the M2 protein in influenza virus membrane fusion: Effects of amantadine and monensin on fusion kinetics. *Virology*, *195*(2), 808–811. https://doi.org/10.1006/viro.1993.1435

Bugge, K., Lindorff-Larsen, K., & Kragelund, B. B. (2016). Understanding single-pass transmembrane receptor signaling from a structural viewpoint—What are we missing? *The FEBS Journal*, *283*(24), 4424–4451. https://doi.org/10.1111/febs.13793

Bukreyev, A., Whitehead, S. S., Murphy, B. R., & Collins, P. L. (1997). Recombinant respiratory syncytial virus from which the entire SH gene has been deleted grows efficiently in cell culture and exhibits site-specific attenuation in the respiratory tract of the mouse. *Journal of Virology*, *71*(12), 8973–8982. https://doi.org/10.1128/jvi.71.12.8973-8982.1997

Cady, S. D., & Hong, M. (2009). Effects of amantadine on the dynamics of membrane-bound influenza A M2 transmembrane peptide studied by NMR relaxation. *Journal of Biomolecular NMR*, *45*(1–2), 185–196. https://doi.org/10.1007/s10858-009-9352-9

Cady, S. D., Mishanina, T. V., & Hong, M. (2009). Structure of amantadine-bound M2 transmembrane peptide of influenza A in lipid bilayers from magic-angle-spinning solid-state NMR: The role of Ser31 in amantadine binding. *Journal of Molecular Biology*, *385*(4), 1127–1141. https://doi.org/10.1016/j.jmb.2008.11.022

Cady, S. D., Schmidt-Rohr, K., Wang, J., Soto, C. S., Degrado, W. F., & Hong, M. (2010). Structure of the amantadine binding site of influenza M2 proton channels in lipid bilayers. *Nature*, *463*(7281), 689–692. https://doi.org/10.1038/nature08722

Campanella, M., de Jong, A. S., Lanke, K. W. H., Melchers, W. J. G., Willems, P. H. G. M., Pinton, P., Rizzuto, R., & van Kuppeveld, F. J. M. (2004). The Coxsackievirus 2B protein suppresses apoptotic host cell responses by manipulating intracellular Ca2+ homeostasis*. *Journal of Biological Chemistry*, *279*(18), 18440–18450. https://doi.org/10.1074/jbc.M309494200

Campbell, O., & Monje-Galvan, V. (2023). Lipid composition modulates interactions of p7 viroporin during membrane insertion. *Journal of Structural Biology*, *215*(3), 108013. https://doi.org/10.1016/j.jsb.2023.108013

Carrasco, L. (1978). Membrane leakiness after viral infection and a new approach to the development of antiviral agents. *Nature*, *272*(5655), 694–699. https://doi.org/10.1038/272694a0

Carrasco, L. (1995). Modification of membrane permeability by animal viruses. In K. Maramorosch, F. A. Murphy, & A. J. Shatkin (Eds.), *Advances in virus research* (Vol. 45, pp. 61–112). Academic Press. https://doi.org/10.1016/S0065-3527(08)60058-5

Carrère-Kremer, S., Montpellier-Pala, C., Cocquerel, L., Wychowski, C., Penin, F., & Dubuisson, J. (2002). Subcellular localization and topology of the p7 polypeptide of hepatitis C virus. *Journal of Virology*, *76*(8), 3720–3730. https://doi.org/10.1128/jvi.76.8.3720-3730.2002

Carter, S. D., Dent, K. C., Atkins, E., Foster, T. L., Verow, M., Gorny, P., Harris, M., Hiscox, J. A., Ranson, N. A., Griffin, S., & Barr, J. N. (2010). Direct visualization of the small hydrophobic protein of human respiratory syncytial virus reveals the structural basis for membrane permeability. *FEBS Letters*, *584*(13), 2786–2790. https://doi.org/10.1016/j.febslet.2010.05.006

Casciano, J. C., & Bouchard, M. J. (2018). Hepatitis B virus X protein modulates cytosolic Ca2+ signaling in primary human hepatocytes. *Virus Research*, *246*, 23–27. https://doi.org/10.1016/j.virusres.2018.01.001

Castaño-Rodriguez, C., Honrubia, J. M., Gutiérrez-Álvarez, J., DeDiego, M. L., Nieto-Torres, J. L., Jimenez-Guardeño, J. M., Regla-Nava, J. A., Fernandez-Delgado, R., Verdia-Báguena, C., Queralt-Martín, M., Kochan, G., Perlman, S., Aguilella, V. M., Sola, I., & Enjuanes, L. (2018). Role of severe acute respiratory syndrome coronavirus viroporins E, 3a, and 8a in replication and pathogenesis. *MBio*, *9*(3). https://doi.org/10.1128/mbio.02325-17

CDC. (2006). High levels of adamantane resistance among influenza A (H3N2) viruses and interim guidelines for use of antiviral agents—United States, 2005-06 influenza season. *MMWR. Morbidity and Mortality Weekly Report*, *55*(2), 44–46.

Chai, M., Li, L., Li, Y., Yang, Y., Wang, Y., Jiang, X., Luan, Y., Li, F., Cui, H., Wang, A., Xiang, W., Wu, X., & Cheng, X. (2024). The 6-kilodalton peptide 1 in plant viruses of the family Potyviridae is a viroporin. *Proceedings of the National Academy of Sciences*, *121*(21), e2401748121. https://doi.org/10.1073/pnas.2401748121

Chan, C.-M., Tsoi, H., Chan, W.-M., Zhai, S., Wong, C.-O., Yao, X., Chan, W.-Y., Tsui, S. K.-W., & Chan, H. Y. E. (2009). The ion channel activity of the SARS-coronavirus 3a protein is linked to its pro-apoptotic function. *The International Journal of Biochemistry & Cell Biology*, *41*(11), 2232–2239. https://doi.org/10.1016/j.biocel.2009.04.019

Chandler, D. E., Penin, F., Schulten, K., & Chipot, C. (2012). The p7 protein of hepatitis C virus forms structurally plastic, minimalist ion channels. *PLoS Computational Biology*, *8*(9), e1002702. https://doi.org/10.1371/journal.pcbi.1002702

Chang, Y. S., Liao, C. L., Tsao, C. H., Chen, M. C., Liu, C. I., Chen, L. K., & Lin, Y. L. (1999). Membrane permeabilization by small hydrophobic nonstructural proteins of Japanese encephalitis virus. *Journal of Virology*, *73*(8), 6257–6264. https://doi.org/10.1128/jvi.73.8.6257-6264.1999

Chen, C.-C., Krüger, J., Sramala, I., Hsu, H.-J., Henklein, P., Chen, Y.-M. A., & Fischer, W. B. (2011). ORF8a of SARS-CoV forms an ion channel: Experiments and molecular dynamics simulations. *Biochimica et Biophysica Acta (BBA) Biomembranes*, *1808*(2), 572–579. https://doi.org/10.1016/j.bbamem.2010.08.004

Cheung, T. K. W., Guan, Y., Ng, S. S. F., Chen, H., Wong, C. H. K., Peiris, J. S. M., & Poon, L. L. M. (2005). Generation of recombinant influenza A virus without M2 ion-channel protein by introduction of a point mutation at the 5′ end of the viral intron. *Journal of General Virology*, *86*(5), 1447–1454. https://doi.org/10.1099/vir.0.80727-0

Chew, C. F., Guy, A., & Biggin, P. C. (2008). Distribution and dynamics of adamantanes in a lipid bilayer. *Biophysical Journal*, *95*(12), 5627–5636. https://doi.org/10.1529/biophysj.108.139477

Chew, C. F., Vijayan, R., Chang, J., Zitzmann, N., & Biggin, P. C. (2009). Determination of pore-lining residues in the hepatitis C virus p7 protein. *Biophysical Journal*, *96*(2), L10–L12. https://doi.org/10.1016/j.bpj.2008.10.004

Chizhmakov, I. V., Geraghty, F. M., Ogden, D. C., Hayhurst, A., Antoniou, M., & Hay, A. J. (1996). Selective proton permeability and pH regulation of the influenza virus M2 channel expressed in mouse erythroleukaemia cells. *The Journal of Physiology*, *494*(2), 329–336. https://doi.org/10.1113/jphysiol.1996.sp021495

Cianfrocco, M. A., & Kellogg, E. H. (2020). What could go wrong? A practical guide to single-particle Cryo-EM: From biochemistry to atomic models. *Journal of Chemical Information and Modeling*, *60*(5), 2458–2469. https://doi.org/10.1021/acs.jcim.9b01178

Ciccaglione, A. R., Marcantonio, C., Costantino, A., Equestre, M., Geraci, A., & Rapicetta, M. (1998). Hepatitis C virus E1 protein induces modification of membrane permeability in *E. coli* cells. *Virology*, *250*(1), 1–8. https://doi.org/10.1006/viro.1998.9380

Clarke, D., Griffin, S., Beales, L., Gelais, C. S., Burgess, S., Harris, M., & Rowlands, D. (2006). Evidence for the formation of a heptameric ion channel complex by the hepatitis C virus P7 protein in vitro *. *The Journal of Biological Chemistry*, *281*(48), 37057–37068. https://doi.org/10.1074/jbc.M602434200

Cong, H., Du, N., Yang, Y., Song, L., Zhang, W., & Tien, P. (2016). Enterovirus 71 2B induces cell apoptosis by directly inducing the conformational activation of the proapoptotic protein Bax. *Journal of Virology*, *90*(21), 9862–9877. https://doi.org/10.1128/jvi.01499-16

Corin, K., & Bowie, J. U. (2022). How physical forces drive the process of helical membrane protein folding. *EMBO Reports*, *23*(3), e53025. https://doi.org/10.15252/embr.202153025

D'Agostino, D. M., Ranzato, L., Arrigoni, G., Cavallari, I., Belleudi, F., Torrisi, M. R., Silic-Benussi, M., Ferro, T., Petronilli, V., Marin, O., Chieco-Bianchi, L., Bernardi, P., & Ciminale, V. (2002). Mitochondrial alterations induced by the p13II protein of human T-cell leukemia virus type 1: Critical role of arginine residues*. *Journal of Biological Chemistry*, *277*(37), 34424–34433. https://doi.org/10.1074/jbc.M203023200

Das, G., Das, T., Chowdhury, N., Chatterjee, D., Bagchi, A., & Ghosh, Z. (2021). Repurposed drugs and nutraceuticals targeting envelope protein: A possible therapeutic strategy against COVID-19. *Genomics*, *113*(1 Pt 2), 1129–1140. https://doi.org/10.1016/j.ygeno.2020.11.009

de Clercq, E., & Li, G. (2016). Approved antiviral drugs over the past 50 years. *Clinical Microbiology Reviews*, *29*(3), 695–747. https://doi.org/10.1128/cmr.00102-15

de Jong, A. S., Visch, H.-J., de Mattia, F., van Dommelen, M. M., Swarts, H. G., Luyten, T., Callewaert, G., Melchers, W. J., Willems, P. H., & van Kuppeveld, F. J. (2006). The Coxsackievirus 2B protein increases efflux of ions from the endoplasmic reticulum and Golgi, thereby inhibiting protein trafficking through the Golgi*. *Journal of Biological Chemistry*, *281*(20), 14144–14150. https://doi.org/10.1074/jbc.M511766200

de Jong, A. S., Wessels, E., Dijkman, H. B. P. M., Galama, J. M. D., Melchers, W. J. G., Willems, P. H. G. M., & van Kuppeveld, F. J. M. (2003). Determinants for membrane association and permeabilization of the Coxsackievirus 2B protein and the identification of the Golgi complex as the target organelle*. *Journal of Biological Chemistry*, *278*(2), 1012–1021. https://doi.org/10.1074/jbc.M207745200

de Marothy, M. T., & Elofsson, A. (2015). Marginally hydrophobic transmembrane α-helices shaping membrane protein folding. *Protein Science*, *24*(7), 1057–1074. https://doi.org/10.1002/pro.2698

DeDiego, M. L., Álvarez, E., Almazán, F., Rejas, M. T., Lamirande, E., Roberts, A., Shieh, W.-J., Zaki, S. R., Subbarao, K., & Enjuanes, L. (2007). A severe acute respiratory syndrome coronavirus that lacks the E gene is attenuated in vitro and in vivo. *Journal of Virology*, *81*(4), 1701–1713. https://doi.org/10.1128/jvi.01467-06

Dey, D., Borkotoky, S., & Banerjee, M. (2020). In silico identification of Tretinoin as a SARS-CoV-2 envelope (E) protein ion channel inhibitor. *Computers in Biology and Medicine*, *127*, 104063. https://doi.org/10.1016/j.compbiomed.2020.104063

Dey, D., Siddiqui, S. I., Mamidi, P., Ghosh, S., Kumar, C. S., Chattopadhyay, S., Ghosh, S., & Banerjee, M. (2019). The effect of amantadine on an ion channel protein from chikungunya virus. *PLoS Neglected Tropical Diseases*, *13*(7), e0007548. https://doi.org/10.1371/journal.pntd.0007548

Dong, G., Peng, C., Luo, J., Wang, C., Han, L., Wu, B., Ji, G., & He, H. (2015). Adamantane-resistant influenza a viruses in the world (1902–2013): Frequency and distribution of M2 gene mutations. *PLoS One*,*10*(3), e0119115. https://doi.org/10.1371/journal.pone.0119115

Dregni, A. J., McKay, M. J., Surya, W., Queralt-Martin, M., Medeiros-Silva, J., Wang, H. K., Aguilella, V., Torres, J., & Hong, M. (2023). The cytoplasmic domain of the SARS-CoV-2 envelope protein assembles into a β-sheet bundle in lipid bilayers. *Journal of Molecular Biology*, *435*(5), 167966. https://doi.org/10.1016/j.jmb.2023.167966

Duart, G., García-Murria, M. J., Grau, B., Acosta-Cáceres, J. M., Martínez-Gil, L., & Mingarro, I. (2020). SARS-CoV-2 envelope protein topology in eukaryotic membranes. *Open Biology*, *10*(9), 200209. https://doi.org/10.1098/rsob.200209

Dudev, T., & Lim, C. (2009). Determinants of K+ vs Na+ selectivity in potassium channels. *Journal of the American Chemical Society*, *131*(23), 8092–8101. https://doi.org/10.1021/ja900168k

Duff, K. C., & Ashley, R. H. (1992). The transmembrane domain of influenza A M2 protein forms amantadine-sensitive proton channels in planar lipid bilayers. *Virology*, *190*(1), 485–489. https://doi.org/10.1016/0042-6822(92)91239-Q

Duffy, S. (2018). Why are RNA virus mutation rates so damn high? *PLoS Biology*, *16*(8), e3000003. https://doi.org/10.1371/journal.pbio.3000003

Elmasri, Z., Negi, V., Kuhn, R. J., & Jose, J. (2022). Requirement of a functional ion channel for Sindbis virus glycoprotein transport, CPV-II formation, and efficient virus budding. *PLoS Pathogens*, *18*(10), e1010892. https://doi.org/10.1371/journal.ppat.1010892

Evans, R., O'Neill, M., Pritzel, A., Antropova, N., Senior, A., Green, T., Žídek, A., Bates, R., Blackwell, S., Yim, J., Ronneberger, O., Bodenstein, S., Zielinski, M., Bridgland, A., Potapenko, A., Cowie, A., Tunyasuvunakool, K., Jain, R., Clancy, E., Kohli, P., Jumper, J., & Hassabis, D. (2022). Protein complex prediction with AlphaFold-Multimer. *bioRxiv*, 2021.2010.2004.463034. https://doi.org/10.1101/2021.10.04.463034

Ewart, G., Bobardt, M., Bentzen, B. H., Yan, Y., Thomson, A., Klumpp, K., Becker, S., Rosenkilde, M. M., Miller, M., & Gallay, P. (2023). Post-infection treatment with the E protein inhibitor BIT225 reduces disease severity and increases survival of K18-hACE2 transgenic mice infected with a lethal dose of SARS-CoV-2. *PLoS Pathogens*, *19*(8), e1011328. https://doi.org/10.1371/journal.ppat.1011328

Ewart, G. D., Mills, K., Cox, G. B., & Gage, P. W. (2002). Amiloride derivatives block ion channel activity and enhancement of virus-like particle budding caused by HIV-1 protein Vpu. *European Biophysics Journal*, *31*(1), 26–35. https://doi.org/10.1007/s002490100177

Ewart, G. D., Sutherland, T., Gage, P. W., & Cox, G. B. (1996). The Vpu protein of human immunodeficiency virus type 1 forms cation-selective ion channels. *Journal of Virology*, *70*(10), 7108–7115. https://doi.org/10.1128/jvi.70.10.7108-7115.1996

Fam, M. S., Sedky, C. A., Turky, N. O., Breitinger, H.-G., & Breitinger, U. (2023). Channel activity of SARS-CoV-2 viroporin ORF3a inhibited by adamantanes and phenolic plant metabolites. *Scientific Reports*, *13*(1), 5328. https://doi.org/10.1038/s41598-023-31764-9

Farag, N. S., Breitinger, U., Breitinger, H. G., & El Azizi, M. A. (2020). Viroporins and inflammasomes: A key to understand virus-induced inflammation. *The International Journal of Biochemistry & Cell Biology*, *122*, 105738. https://doi.org/10.1016/j.biocel.2020.105738

Faust, T. B., Binning, J. M., Gross, J. D., & Frankel, A. D. (2017). Making sense of multifunctional proteins: Human immunodeficiency virus type 1 accessory and regulatory proteins and connections to transcription.

Annual Review of Virology, *4*(1), 241–260. https://doi.org/10.1146/annurev-virology-101416-041654

Fischer, W., Pitkeathly, M., & Sansom, M. (2001). Amantadine blocks channel activity of the transmembrane segment of the NB protein from influenza B. *European Biophysics Journal*, *30*(6), 416–420. https://doi.org/10.1007/s002490100157

Foster, T. L., Thompson, G. S., Kalverda, A. P., Kankanala, J., Bentham, M., Wetherill, L. F., Thompson, J., Barker, A. M., Clarke, D., Noerenberg, M., Pearson, A. R., Rowlands, D. J., Homans, S. W., Harris, M., Foster, R., & Griffin, S. (2014). Structure-guided design affirms inhibitors of hepatitis C virus p7 as a viable class of antivirals targeting virion release. *Hepatology*, *59*(2), 408–422. https://doi.org/10.1002/hep.26685

Foster, T. L., Verow, M., Wozniak, A. L., Bentham, M. J., Thompson, J., Atkins, E., Weinman, S. A., Fishwick, C., Foster, R., Harris, M., & Griffin, S. (2011). Resistance mutations define specific antiviral effects for inhibitors of the hepatitis C virus p7 ion channel. *Hepatology*, *54*(1), 79–90. https://doi.org/10.1002/hep.24371

Fuentes, S., Tran, K. C., Luthra, P., Teng, M. N., & He, B. (2007). Function of the respiratory syncytial virus small hydrophobic protein. *Journal of Virology*, *81*(15), 8361–8366. https://doi.org/10.1128/jvi.02717-06

Gaedigk-Nitschko, K., Ding, M. X., Levy, M. A., & Schlesinger, M. J. (1990). Site-directed mutations in the Sindbis virus 6K protein reveal sites for fatty acylation and the underacylated protein affects virus release and virion structure. *Virology*, *175*(1), 282–291. https://doi.org/10.1016/0042-6822(90)90210-i

Gan, S. W., Ng, L., Lin, X., Gong, X., & Torres, J. (2008). Structure and ion channel activity of the human respiratory syncytial virus (hRSV) small hydrophobic protein transmembrane domain. *Protein Science*, *17*(5), 813–820. https://doi.org/10.1110/ps.073366208

Gan, S.-W., Tan, E., Lin, X., Yu, D., Wang, J., Tan, G. M.-Y., Vararattanavech, A., Yeo, C. Y., Soon, C. H., Soong, T. W., Pervushin, K., & Torres, J. (2012). The small hydrophobic protein of the human respiratory syncytial virus forms pentameric ion channels*. *Journal of Biological Chemistry*, *287*(29), 24671–24689. https://doi.org/10.1074/jbc.M111.332791

Gannagé, M., Dormann, D., Albrecht, R., Dengjel, J., Torossi, T., Rämer, P. C., Lee, M., Strowig, T., Arrey, F., Conenello, G., Pypaert, M., Andersen, J., García-Sastre, A., & Münz, C. (2009). Matrix protein 2 of influenza a virus blocks autophagosome fusion with lysosomes. *Cell Host & Microbe*, *6*(4), 367–380. https://doi.org/10.1016/j.chom.2009.09.005

Gazzarrini, S., Kang, M., Abenavoli, A., Romani, G., Olivari, C., Gaslini, D., Ferrara, G., van Etten, J. L., Kreim, M., Kast, S. M., Thiel, G., & Moroni, A. (2009). Chlorella virus ATCV-1 encodes a functional potassium channel of 82 amino acids. *Biochemical Journal*, *420*(2), 295–305. https://doi.org/10.1042/bj20090095

Gazzarrini, S., Kang, M., Epimashko, S., van Etten, J. L., Dainty, J., Thiel, G., & Moroni, A. (2006). Chlorella virus MT325 encodes water and potassium channels that interact synergistically. *Proceedings of the National Academy of Sciences*, *103*(14), 5355–5360. https://doi.org/10.1073/pnas.0600848103

Georgieva, E. R., Borbat, P. P., Norman, H. D., & Freed, J. H. (2015). Mechanism of influenza A M2 transmembrane domain assembly in lipid membranes. *Scientific Reports*, *5*, 11757. https://doi.org/10.1038/srep11757

Gervais, C., Dô, F., Cantin, A., Kukolj, G., White, P. W., Gauthier, A., & Vaillancourt, F. H. (2011). Development and validation of a high-throughput screening assay for the hepatitis C virus p7 Viroporin. *SLAS. Discovery*, *16*(3), 363–369. https://doi.org/10.1177/1087057110396215

Giorda Kristina, M., Raghava, S., & Hebert Daniel, N. (2012). The simian virus 40 late viral protein VP4 disrupts the nuclear envelope for viral release. *Journal of Virology*, *86*(6), 3180–3192. https://doi.org/10.1128/jvi.07047-11

Gladue, D. P., Holinka, L. G., Largo, E., Sainz, I. F., Carrillo, C., O'Donnell, V., Baker-Branstetter, R., Lu, Z., Ambroggio, X., Risatti, G. R., Nieva, J. L., & Borca, M. V. (2012). Classical swine fever virus p7 protein is a viroporin involved in virulence in swine. *Journal of Virology*, *86*(12), 6778–6791. https://doi.org/10.1128/jvi.00560-12

Gladue, D. P., Largo, E., de la Arada, I., Aguilella, V. M., Alcaraz, A., Arrondo, J. L. R., Holinka, L. G., Brocchi, E., Ramirez-Medina, E., Vuono, E. A., Berggren, K. A., Carrillo, C., Nieva, J. L., & Borca, M. V. (2018). Molecular characterization of the viroporin function of foot-and-mouth disease virus nonstructural protein 2B. *Journal of Virology*, *92*(23). https://doi.org/10.1128/jvi.01360-18

González, M. E., & Carrasco, L. (1998). The human immunodeficiency virus type 1 Vpu protein enhances membrane permeability. *Biochemistry*, *37*(39), 13710–13719. https://doi.org/10.1021/bi981527f

Gonzalez, M. E., & Carrasco, L. (2001). Human immunodeficiency virus type 1 VPU protein affects Sindbis virus glycoprotein processing and enhances membrane permeabilization. *Virology*, *279*(1), 201–209. https://doi.org/10.1006/viro.2000.0708

Gonzalez, M. E., & Carrasco, L. (2003). Viroporins. *FEBS Letters*, *552*(1), 28–34. https://doi.org/10.1016/S0014-5793(03)00780-4

Grambas, S., Bennett, M. S., & Hay, A. J. (1992). Influence of amantadine resistance mutations on the pH regulatory function of the M2 protein of influenza a viruses. *Virology*, *191*(2), 541–549. https://doi.org/10.1016/0042-6822(92)90229-I

Greiner, T., Bolduan, S., Hertel, B., Groß, C., Hamacher, K., Schubert, U., Moroni, A., & Thiel, G. (2016). Ion channel activity of Vpu proteins is conserved throughout evolution of HIV-1 and SIV. *Viruses*, *8*(12), 325. https://doi.org/10.3390/v8120325

Griffin, S., StGelais, C., Owsianka, A. M., Patel, A. H., Rowlands, D., & Harris, M. (2008). Genotype-dependent sensitivity of hepatitis C virus to inhibitors of the p7 ion channel. *Hepatology*, *48*(6), 1779–1790. https://doi.org/10.1002/hep.22555

Griffin, S. D. C., Beales, L. P., Clarke, D. S., Worsfold, O., Evans, S. D., Jaeger, J., Harris, M. P. G., & Rowlands, D. J. (2003). The p7 protein of hepatitis C virus forms an ion channel that is blocked by the antiviral drug, amantadine. *FEBS Letters*, *535*(1–3), 34–38. https://doi.org/10.1016/S0014-5793(02)03851-6

Griffin, S. D. C., Harvey, R., Clarke, D. S., Barclay, W. S., Harris, M., & Rowlands, D. J. (2004). A conserved basic loop in hepatitis C virus p7 protein is required for amantadine-sensitive ion channel activity in mammalian cells but is dispensable for localization to mitochondria. *Journal of General Virology*, *85*(2), 451–461. https://doi.org/10.1099/vir.0.19634-0

Gu, R. X., Liu, L. A., Wei, D. Q., Du, J. G., Liu, L., & Liu, H. (2011). Free energy calculations on the two drug binding sites in the M2 proton channel. *Journal of the American Chemical Society*, *133*(28), 10817–10825. https://doi.org/10.1021/ja1114198

Guinea, R., & Carrasco, L. (1994). Influenza virus M2 protein modifies membrane permeability in *E. coli* cells. *FEBS Letters*, *343*(3), 242–246. https://doi.org/10.1016/0014-5793(94)80564-4

Guo, H. C., Sun, S. Q., Sun, D. H., Wei, Y. Q., Xu, J., Huang, M., Liu, X. T., Liu, Z. X., Luo, J. X., Yin, H., & Liu, D. X. (2013). Viroporin activity and membrane topology of classic swine fever virus p7 protein. *The International Journal of Biochemistry & Cell Biology*, *45*(7), 1186–1194. https://doi.org/10.1016/j.biocel.2013.03.021

Hajnóczky, G., Davies, E., & Madesh, M. (2003). Calcium signaling and apoptosis. *Biochemical and Biophysical Research Communications*, *304*(3), 445–454. https://doi.org/10.1016/S0006-291X(03)00616-8

Han, Z., & Harty, R. N. (2004). The NS3 protein of bluetongue virus exhibits viroporin-like properties*. *Journal of Biological Chemistry*, *279*(41), 43092–43097. https://doi.org/10.1074/jbc.M403663200

Han, Z., Licata, J. M., Paragas, J., & Harty, R. N. (2007). Permeabilization of the plasma membrane by Ebola virus GP2. *Virus Genes*, *34*(3), 273–281. https://doi.org/10.1007/s11262-006-0009-4

Harding, S. D., Armstrong, J. F., Faccenda, E., Southan, C., Alexander, S. P. H., Davenport, A. P., Spedding, M., & Davies, J. A. (2023). The IUPHAR/BPS guide to pharmacology in 2024. *Nucleic Acids Research*, *52*(D1), D1438–D1449. https://doi.org/10.1093/nar/gkad944

Hay, A. J., Wolstenholme, A. J., Skehel, J. J., & Smith, M. H. (1985). The molecular basis of the specific anti-influenza action of amantadine. *The EMBO Journal*, *4*(11), 3021–3024. https://doi.org/10.1002/j.1460-2075.1985.tb04038.x

Hayden, F. G., Hoffman, H. E., & Spyker, D. A. (1983). Differences in side effects of amantadine hydrochloride and rimantadine hydrochloride relate to differences in pharmacokinetics. *Antimicrobial Agents and Chemotherapy*, *23*(3), 458–464. https://doi.org/10.1128/aac.23.3.458

He, J., Melnik, L. I., Komin, A., Wiedman, G., Fuselier, T., Morris, C. F., Starr, C. G., Searson, P. C., Gallaher, W. R., Hristova, K., Garry, R. F., & Wimley, W. C. (2017). Ebola virus delta peptide is a viroporin. *Journal of Virology*, *91*(16). https://doi.org/10.1128/jvi.00438-17

Hegde, R. S., & Keenan, R. J. (2022). The mechanisms of integral membrane protein biogenesis. *Nature Reviews. Molecular Cell Biology*, *23*(2), 107–124. https://doi.org/10.1038/s41580-021-00413-2

Heider, H., Adamczyk, B., Presber, H. W., Schroeder, C., Feldblum, R., & Indulen, M. K. (1981). Occurrence of amantadine- and rimantadine-resistant influenza A virus strains during the 1980 epidemic. *Acta Virologica*, *25*(6), 395–400.

Henke, W., Waisner, H., Arachchige, S. P., Kalamvoki, M., & Stephens, E. (2022). The envelope proteins from SARS-CoV-2 and SARS-CoV potently reduce the infectivity of human immunodeficiency virus type 1 (HIV-1). *Retrovirology*, *19*(1), 25. https://doi.org/10.1186/s12977-022-00611-6

Henkel, M., Mitzner, D., Henklein, P., Meyer-Almes, F. J., Moroni, A., Difrancesco, M. L., Henkes, L. M., Kreim, M., Kast, S. M., Schubert, U., & Thiel, G. (2010). The proapoptotic influenza A virus protein PB1-F2 forms a nonselective ion channel. *PLoS ONE*, *5*(6), e11112. https://doi.org/10.1371/journal.pone.0011112

Hille, B. (2001). *Ion channels of excitable membranes* (Third ed.). Oxford Universitiy Press.

Holsinger, L. J., & Lamb, R. A. (1991). Influenza virus M2 integral membrane protein is a homotetramer stabilized by formation of disulfide bonds. *Virology*, *183*(1), 32–43. https://doi.org/10.1016/0042-6822(91)90115-r

Holsinger, L. J., Shaughnessy, M. A., Micko, A., Pinto, L. H., & Lamb, R. A. (1995). Analysis of the posttranslational modifications of the influenza virus M2 protein. *Journal of Virology*, *69*(2), 1219–1225. https://doi.org/10.1128/jvi.69.2.1219-1225.1995

Hongo, S., Ishii, K., Mori, K., Takashita, E., Muraki, Y., Matsuzaki, Y., & Sugawara, K. (2003). Detection of ion channel activity in Xenopus laevis oocytes expressing influenza C virus CM2 protein. *Archives of Virology*, *149*(1), 35–50. https://doi.org/10.1007/s00705-003-0209-3

Hu, Y., Hau, R. K., Wang, Y., Tuohy, P., Zhang, Y., Xu, S., Ma, C., & Wang, J. (2018). Structure–property relationship studies of influenza A virus AM2-S31N Proton Channel blockers. *ACS Medicinal Chemistry Letters*, *9*(11), 1111–1116. https://doi.org/10.1021/acsmedchemlett.8b00336

Hu, Y., Musharrafieh, R., Ma, C., Zhang, J., Smee, D. F., DeGrado, W. F., & Wang, J. (2017). An M2-V27A channel blocker demonstrates potent in vitro and in vivo antiviral activities against amantadine-sensitive and -resistant influenza A viruses. *Antiviral Research*, *140*, 45–54. https://doi.org/10.1016/j.antiviral.2017.01.006

Huang, Y., Meng, L., Nie, Q., Zhou, Y., Chen, L., Yang, S., Fung, Y. M. E., Li, X., Huang, C., Cao, Y., Li, Y., & Li, X. (2021). Selection of DNA-encoded chemical libraries against endogenous membrane proteins on live cells. *Nature Chemistry*, *13*(1), 77–88. https://doi.org/10.1038/s41557-020-00605-x

Hussain, M., Galvin, H. D., Haw, T. Y., Nutsford, A. N., & Husain, M. (2017). Drug resistance in influenza A virus: The epidemiology and management. *Infection and Drug Resistance*, *10*, 121–134. https://doi.org/10.2147/idr.S105473

Hyser, J. M., Collinson-Pautz, M. R., Utama, B., & Estes, M. K. (2010). Rotavirus disrupts calcium homeostasis by NSP4 viroporin activity. *MBio*, *1*(5). https://doi.org/10.1128/mbio.00265-10

Hyser, J. M., Utama, B., Crawford, S. E., Broughman, J. R., & Estes, M. K. (2013). Activation of the endoplasmic reticulum calcium sensor STIM1 and store-operated calcium entry by rotavirus requires NSP4 viroporin activity. *Journal of Virology*, *87*(24), 13579–13588. https://doi.org/10.1128/jvi.02629-13

Hyser Joseph, M., Utama, B., Crawford Sue, E., & Estes Mary, K. (2012). Genetic divergence of rotavirus nonstructural protein 4 results in distinct serogroup-specific viroporin activity and intracellular punctate structure morphologies. *Journal of Virology*, *86*(9), 4921–4934. https://doi.org/10.1128/jvi.06759-11

Ito, M., Yanagi, Y., & Ichinohe, T. (2012). Encephalomyocarditis virus viroporin 2B activates NLRP3 inflammasome. *PLoS Pathogens*, *8*(8), e1002857. https://doi.org/10.1371/journal.ppat.1002857

Jalily, P. H., Duncan, M. C., Fedida, D., Wang, J., & Tietjen, I. (2020). Put a cork in it: Plugging the M2 viral ion channel to sink influenza. *Antiviral Research*, *178*, 104780. https://doi.org/10.1016/j.antiviral.2020.104780

Jalily, P. H., Eldstrom, J., Miller, S. C., Kwan, D. C., Tai, S. S., Chou, D., Niikura, M., Tietjen, I., & Fedida, D. (2016). Mechanisms of action of novel influenza A/M2 viroporin inhibitors derived from hexamethylene amiloride. *Molecular Pharmacology*, *90*(2), 80–95. https://doi.org/10.1124/mol.115.102731

Jalily, P. H., Jalily Hasani, H., & Fedida, D. (2022). In silico evaluation of hexamethylene amiloride derivatives as potential luminal inhibitors of SARS-CoV-2 E protein. *International Journal of Molecular Sciences*, *23*(18), 10647. https://doi.org/10.3390/ijms231810647

Jayaraman, B., Smith, A. M., Fernandes, J. D., & Frankel, A. D. (2016). Oligomeric viral proteins: Small in size, large in presence. *Critical Reviews in Biochemistry and Molecular Biology*, *51*(5), 379–394. https://doi.org/10.1080/10409238.2016.1215406

Jimenez-Guardeño, J. M., Nieto-Torres, J. L., DeDiego, M. L., Regla-Nava, J. A., Fernandez-Delgado, R., Castaño-Rodriguez, C., & Enjuanes, L. (2014). The PDZ-binding motif of severe acute respiratory syndrome coronavirus envelope protein is a determinant of viral pathogenesis. *PLoS Pathogens*, *10*(8), e1004320. https://doi.org/10.1371/journal.ppat.1004320

Jong, A. S.d., Mattia, F.d., Dommelen, M. M. V., Lanke, K., Melchers, W. J. G., Willems, P. H. G. M., & Kuppeveld, F. J. M.v. (2008). Functional analysis of picornavirus 2B proteins: Effects on calcium homeostasis and intracellular protein trafficking. *Journal of Virology*, *82*(7), 3782–3790. https://doi.org/10.1128/jvi.02076-07

Joubert, D. A., Blasdell, K. R., Audsley, M. D., Trinidad, L., Monaghan, P., Dave, K. A., Lieu, K. G., Amos-Ritchie, R., Jans, D. A., Moseley, G. W., Gorman, J. J., & Walker, P. J. (2014). Bovine ephemeral fever rhabdovirus α1 protein has viroporin-like properties and binds importin β1 and importin 7. *Journal of Virology*, *88*(3), 1591–1603. https://doi.org/10.1128/jvi.01812-13

Jumper, J., Evans, R., Pritzel, A., Green, T., Figurnov, M., Ronneberger, O., Tunyasuvunakool, K., Bates, R., Žídek, A., Potapenko, A., Bridgland, A., Meyer, C., Kohl, S. A. A., Ballard, A. J., Cowie, A., Romera-Paredes, B., Nikolov, S., Jain, R., Adler, J., … Hassabis, D. (2021). Highly accurate protein structure prediction with AlphaFold. *Nature*, *596*(7873), 583–589. https://doi.org/10.1038/s41586-021-03819-2

Kellermann, M., Scharte, F., & Hensel, M. (2021). Manipulation of host Cell organelles by intracellular pathogens. *International Journal of Molecular Sciences*, *22*(12), 6484. https://doi.org/10.3390/ijms22126484

Kern, D. M., Sorum, B., Mali, S. S., Hoel, C. M., Sridharan, S., Remis, J. P., Toso, D. B., Kotecha, A., Bautista, D. M., & Brohawn, S. G. (2021). Cryo-EM structure of SARS-CoV-2 ORF3a in lipid nanodiscs. *Nature*

Structural & Molecular Biology, *28*(7), 573–582. https://doi.org/10.1038/s41594-021-00619-0

Kesinger, E., Liu, J., Jensen, A., Chia, C. P., Demers, A., & Moriyama, H. (2018). Influenza D virus M2 protein exhibits ion channel activity in Xenopus laevis oocytes. *PLoS ONE*, *13*(6), e0199227. https://doi.org/10.1371/journal.pone.0199227

Khoury, G., Ewart, G., Luscombe, C., Miller, M., & Wilkinson, J. (2010). Antiviral efficacy of the novel compound BIT225 against HIV-1 release from human macrophages. *Antimicrobial Agents and Chemotherapy*, *54*(2), 835–845. https://doi.org/10.1128/aac.01308-09

Khoury, G., Ewart, G., Luscombe, C., Miller, M., & Wilkinson, J. (2016). The antiviral compound BIT225 inhibits HIV-1 replication in myeloid dendritic cells. *AIDS Research and Therapy*, *13*(1), 7. https://doi.org/10.1186/s12981-016-0093-z

Killian, J. A., & von Heijne, G. (2000). How proteins adapt to a membrane-water interface. *Trends in Biochemical Sciences*, *25*(9), 429–434. https://doi.org/10.1016/s0968-0004(00)01626-1

Klimochkin, Y. N., Shiryaev, V. A., Petrov, P. V., Radchenko, E. V., Palyulin, V. A., & Zefirov, N. S. (2016). Design of Broad-Spectrum Inhibitors of influenza A virus M2 proton channels: A molecular modeling approach. *Current Computer-Aided Drug Design*, *12*(2), 154–164. https://doi.org/10.2174/1573409912666160505113408

Kochva, U., Leonov, H., & Arkin, I. T. (2003). Modeling the structure of the respiratory syncytial virus small hydrophobic protein by silent-mutation analysis of global searching molecular dynamics. *Protein Science*, *12*(12), 2668–2674. https://doi.org/10.1110/ps.03151103

Koff, W. C., Elm, J. L., & Halstead, S. B. (1980). Inhibition of dengue virus replication by amantadine hydrochloride. *Antimicrobial Agents and Chemotherapy*, *18*(1), 125–129. https://doi.org/10.1128/aac.18.1.125

Kongpracha, P., Wiriyasermkul, P., Isozumi, N., Moriyama, S., Kanai, Y., & Nagamori, S. (2022). Simple but efficacious enrichment of integral membrane proteins and their interactions for in-depth membrane proteomics. *Molecular & Cellular Proteomics*, *21*(5), 100206. https://doi.org/10.1016/j.mcpro.2022.100206

Konstantinidi, A., Chountoulesi, M., Naziris, N., Sartori, B., Amenitsch, H., Mali, G., Čendak, T., Plakantonaki, M., Triantafyllakou, I., Tselios, T., Demetzos, C., Busath, D. D., Mavromoustakos, T., & Kolocouris, A. (2020). The boundary lipid around DMPC-spanning influenza A M2 transmembrane domain channels: Its structure and potential for drug accommodation. *Biochimica et Biophysica Acta - Biomembranes*, *1862*(3), 183156. https://doi.org/10.1016/j.bbamem.2019.183156

Konstantinidi, A., Naziris, N., Chountoulesi, M., Kiriakidi, S., Sartori, B., Kolokouris, D., Amentisch, H., Mali, G., Ntountaniotis, D., Demetzos, C., Mavromoustakos, T., & Kolocouris, A. (2018). Comparative perturbation effects exerted by the influenza A M2 WT protein inhibitors amantadine and the spiro[pyrrolidine-2,2′-adamantane] variant AK13 to membrane bilayers studied using biophysical experiments and molecular dynamics simulations. *The Journal of Physical Chemistry. B*, *122*(43), 9877–9895. https://doi.org/10.1021/acs.jpcb.8b07071

Kuchibhatla, D. B., Sherman, W. A., Chung, B. Y., Cook, S., Schneider, G., Eisenhaber, B., & Karlin, D. G. (2014). Powerful sequence similarity search methods and in-depth manual analyses can identify remote homologs in many apparently "orphan" viral proteins. *Journal of Virology*, *88*(1), 10–20. https://doi.org/10.1128/jvi.02595-13

Kuo, L., & Masters, P. S. (2003). The small envelope protein E is not essential for murine coronavirus replication [article]. *Journal of Virology*, *77*(8), 4597–4608. https://doi.org/10.1128/JVI.77.8.4597-4608.2003

Kurtz, S., Luo, G., Hahnenberger, K. M., Brooks, C., Gecha, O., Ingalls, K., Numata, K., & Krystal, M. (1995). Growth impairment resulting from expression of influenza virus M2 protein in Saccharomyces cerevisiae: Identification of a novel inhibitor of influenza virus. *Antimicrobial Agents and Chemotherapy*, *39*(10), 2204–2209. https://doi.org/10.1128/aac.39.10.2204

Lahiri, H., & Arkin, I. T. (2022). Searching for blockers of dengue and West Nile virus viroporins. *Viruses*, *14*(8), 1750. https://doi.org/10.3390/v14081750

Lama, J., & Carrasco, L. (1992). Expression of poliovirus nonstructural proteins in *Escherichia coli* cells. Modification of membrane permeability induced by 2B and 3A. *Journal of Biological Chemistry*, *267*(22), 15932–15937. https://doi.org/10.1016/S0021-9258(19)49623-3

Lamb, R. A., & Pinto, L. H. (1997). Do Vpu and Vpr of human immunodeficiency virus type 1 and NB of influenza B virus have ion channel activities in the viral life cycles? *Virology*, *229*(1), 1–11. https://doi.org/10.1006/viro.1997.8451

Langlet, P., D'Heygere, F., Henrion, J., Adler, M., Delwaide, J., van Vlierberghe, H., Mulkay, J. P., Lasser, L., Brenard, R., Horsmans, Y., Michielsen, P., Laureys, A., & Nevens, F. (2009). Clinical trial: A randomized trial of pegylated-interferon-alpha-2a plus ribavirin with or without amantadine in treatment-naïve or relapsing chronic hepatitis C patients. *Alimentary Pharmacology & Therapeutics*, *30*(4), 352–363. https://doi.org/10.1111/j.1365-2036.2009.04052.x

Largo, E., Gladue, D. P., Huarte, N., Borca, M. V., & Nieva, J. L. (2014). Pore-forming activity of pestivirus p7 in a minimal model system supports genus-specific viroporin function. *Antiviral Research*, *101*, 30–36. https://doi.org/10.1016/j.antiviral.2013.10.015

Largo, E., Gladue, D. P., Torralba, J., Aguilella, V. M., Alcaraz, A., Borca, M. V., & Nieva, J. L. (2018). Mutation-induced changes of transmembrane pore size revealed by combined ion-channel conductance and single vesicle permeabilization analyses. *Biochimica et Biophysica Acta (BBA) Biomembranes*, *1860*(5), 1015–1021. https://doi.org/10.1016/j.bbamem.2018.01.012

Largo, E., Queralt-Martín, M., Carravilla, P., Nieva, J. L., & Alcaraz, A. (2021). Single-molecule conformational dynamics of viroporin ion channels regulated by lipid-protein interactions. *Bioelectrochemistry*, *137*, 107641. https://doi.org/10.1016/j.bioelechem.2020.107641

Largo, E., Verdiá-Báguena, C., Aguilella, V. M., Nieva, J. L., & Alcaraz, A. (2016). Ion channel activity of the CSFV p7 viroporin in surrogates of the ER lipid bilayer. *Biochimica et Biophysica Acta (BBA) - Biomembranes*, *1858*(1), 30–37. https://doi.org/10.1016/j.bbamem.2015.10.007

Lear, J. D., Wasserman, Z. R., & DeGrado, W. F. (1988). Synthetic amphiphilic peptide models for protein ion channels. *Science*, *240*(4856), 1177–1181. https://doi.org/10.1126/science.2453923

Lebedeva, N. S., Gubarev, Y. A., Mamardashvili, G. M., Zaitceva, S. V., Zdanovich, S. A., Malyasova, A. S., Romanenko, J. V., Koifman, M. O., & Koifman, O. I. (2021). Theoretical and experimental study of interaction of macroheterocyclic compounds with ORF3a of SARS-CoV-2. *Scientific Reports*, *11*(1), 19481. https://doi.org/10.1038/s41598-021-99072-8

Lee, H. R., Cho, Y. Y., Lee, G. Y., You, D. G., Yoo, Y. D., & Kim, Y. J. (2018). A direct role for hepatitis B virus X protein in inducing mitochondrial membrane permeabilization. *Journal of Viral Hepatitis*, *25*(4), 412–420. https://doi.org/10.1111/jvh.12831

Leiding, T., Wang, J., Martinsson, J., DeGrado, W. F., & Årsköld, S. P. (2010). Proton and cation transport activity of the M2 proton channel from influenza A virus. *Proceedings of the National Academy of Sciences*, *107*(35), 15409–15414. https://doi.org/10.1073/pnas.1009997107

León-Juárez, M., Martínez-Castillo, M., Shrivastava, G., García-Cordero, J., Villegas-Sepulveda, N., Mondragón-Castelán, M., Mondragón-Flores, R., & Cedillo-Barrón, L. (2016). Recombinant dengue virus protein NS2B alters membrane permeability in different membrane models. *Virology Journal*, *13*(1), 1. https://doi.org/10.1186/s12985-015-0456-4

Li, Y., To, J., Verdià-Baguena, C., Dossena, S., Surya, W., Huang, M., Paulmichl, M., Liu, D. X., Aguilella, V. M., & Torres, J. (2014). Inhibition of the human respiratory syncytial virus small hydrophobic protein and

structural variations in a bicelle environment. *Journal of Virology*, *88*(20), 11899–11914. https://doi.org/10.1128/jvi.00839-14

Liao, Y., Lescar, J., Tam, J. P., & Liu, D. X. (2004). Expression of SARS-coronavirus envelope protein in *Escherichia coli* cells alters membrane permeability. *Biochemical and Biophysical Research Communications*, *325*(1), 374–380. https://doi.org/10.1016/j.bbrc.2004.10.050

Liao, Y., Yuan, Q., Torres, J., Tam, J. P., & Liu, D. X. (2006). Biochemical and functional characterization of the membrane association and membrane permeabilizing activity of the severe acute respiratory syndrome coronavirus envelope protein. *Virology*, *349*(2), 264–275. https://doi.org/10.1016/j.virol.2006.01.028

Lim, S. Y., Guo, Z., Liu, P., McKay, L. G. A., Storm, N., Griffiths, A., Qu, M. D., Finberg, R. W., Somasundaran, M., & Wang, J. P. (2022). Anti-SARS-CoV-2 activity of adamantanes in vitro and in animal models of infection. *Covid*, *2*(11), 1551–1563. https://doi.org/10.3390/covid2110111

Lin, C.-C., & Chen, W.-C. (2016). Treatment effectiveness of amantadine against dengue virus infection. *American Journal of Case Reports*, *17*, 921–924. https://doi.org/10.12659/ajcr.901014

Liu, H., Maruyama, H., Masuda, T., Honda, A., & Arai, F. (2016). The influence of virus infection on the extracellular pH of the host cell detected on cell membrane [original research]. *Frontiers in Microbiology*, *7*, 1127. https://doi.org/10.3389/fmicb.2016.01127

Liu, Z., Ye, Q., Cheng, A., Ou, X., Mao, S., Sun, D., Zhang, S., Zhao, X., Yang, Q., Wu, Y., Huang, J., Gao, Q., Tian, B., & Wang, M. (2021). A viroporin-like 2B protein of duck hepatitis A virus 1 that induces incomplete autophagy in DEF cells. *Poultry Science*, *100*(10), 101331. https://doi.org/10.1016/j.psj.2021.101331

Lopez, L. A., Riffle, A. J., Pike, S. L., Gardner, D., & Hogue, B. G. (2008). Importance of conserved cysteine residues in the coronavirus envelope protein. *Journal of Virology*, *82*(6), 3000–3010. https://doi.org/10.1128/jvi.01914-07

Lu, W., Zheng, B.-J., Xu, K., Schwarz, W., Du, L., Wong, C. K. L., Chen, J., Duan, S., Deubel, V., & Sun, B. (2006). Severe acute respiratory syndrome-associated coronavirus 3a protein forms an ion channel and modulates virus release. *Proceedings of the National Academy of Sciences*, *103*(33), 12540–12545. https://doi.org/10.1073/pnas.0605402103

Luganini, A., di Nardo, G., Munaron, L., Gilardi, G., Fiorio Pla, A., & Gribaudo, G. (2018). Human cytomegalovirus US21 protein is a viroporin that modulates calcium homeostasis and protects cells against apoptosis. *Proceedings of the National Academy of Sciences*, *115*(52), E12370–E12377. https://doi.org/10.1073/pnas.1813183115

Luik, P., Chew, C., Aittoniemi, J., Chang, J., Wentworth, P., Dwek, R. A., Biggin, P. C., Vénien-Bryan, C., & Zitzmann, N. (2009). The 3-dimensional structure of a hepatitis C virus p7 ion channel by electron microscopy. *Proceedings of the National Academy of Sciences*, *106*(31), 12712–12716. https://doi.org/10.1073/pnas.0905966106

Lulla, V., & Firth, A. E. (2020). A hidden gene in astroviruses encodes a viroporin. *Nature Communications*, *11*(1), 4070. https://doi.org/10.1038/s41467-020-17906-x

Luscombe, C. A., Avihingsanon, A., Supparatpinyo, K., Gatechompol, S., Han, W. M., Ewart, G. D., Thomson, A. S., Miller, M., Becker, S., & Murphy, R. L. (2020). Human immunodeficiency virus type 1 Vpu inhibitor, BIT225, in combination with 3-Drug antiretroviral therapy: Inflammation and immune cell modulation. *The Journal of Infectious Diseases*, *223*(11), 1914–1922. https://doi.org/10.1093/infdis/jiaa635

Luscombe, C. A., Huang, Z., Murray, M. G., Miller, M., Wilkinson, J., & Ewart, G. D. (2010). A novel hepatitis C virus p7 ion channel inhibitor, BIT225, inhibits bovine viral diarrhea virus in vitro and shows synergism with recombinant interferon-α-2b and nucleoside analogues. *Antiviral Research*, *86*(2), 144–153. https://doi.org/10.1016/j.antiviral.2010.02.312

Ma, C., & Wang, J. (2018). Functional studies reveal the similarities and differences between AM2 and BM2 proton channels from influenza viruses. *Biochimica et Biophysica Acta - Biomembranes*, *1860*(2), 272–280. https://doi.org/10.1016/j.bbamem.2017.10.026

Machamer, C. E., & Youn, S. (2006). The transmembrane domain of the infectious bronchitis virus E protein is required for efficient virus release. *Advances in Experimental Medicine and Biology*, *581*, 193–198. https://doi.org/10.1007/978-0-387-33012-9_33

Madan, V., Castelló, A., & Carrasco, L. (2008). Viroporins from RNA viruses induce caspase-dependent apoptosis. *Cellular Microbiology*, *10*(2), 437–451. https://doi.org/10.1111/j.1462-5822.2007.01057.x

Madan, V., García, M.d J., Sanz, M. A., & Carrasco, L. (2005). Viroporin activity of murine hepatitis virus E protein. *FEBS Letters*, *579*(17), 3607–3612. https://doi.org/10.1016/j.febslet.2005.05.046

Magadán, J. G., & Bonifacino, J. S. (2012). Transmembrane domain determinants of CD4 downregulation by HIV-1 Vpu. *Journal of Virology*, *86*(2), 757–772. https://doi.org/10.1128/jvi.05933-11

Majeed, S., Ahmad, A. B., Sehar, U., & Georgieva, E. R. (2021). Lipid membrane mimetics in functional and structural studies of integral membrane proteins. *Membranes (Basel)*, *11*(9), 685. https://doi.org/10.3390/membranes11090685

Mall, S., Broadbridge, R., Sharma, R. P., Lee, A. G., & East, J. M. (2000). Effects of aromatic residues at the ends of transmembrane alpha-helices on helix interactions with lipid bilayers. *Biochemistry*, *39*(8), 2071–2078. https://doi.org/10.1021/bi992205u

Mandala, V. S., Loftis, A. R., Shcherbakov, A. A., Pentelute, B. L., & Hong, M. (2020). Atomic structures of closed and open influenza B M2 proton channel reveal the conduction mechanism. *Nature Structural & Molecular Biology*, *27*(2), 160–167. https://doi.org/10.1038/s41594-019-0371-2

Mandala, V. S., McKay, M. J., Shcherbakov, A. A., Dregni, A. J., Kolocouris, A., & Hong, M. (2020). Structure and drug binding of the SARS-CoV-2 envelope protein transmembrane domain in lipid bilayers. *Nature Structural & Molecular Biology*, *27*(12), 1202–1208. https://doi.org/10.1038/s41594-020-00536-8

Mandour, Y. M., Breitinger, U., Ma, C., Wang, J., Boeckler, F. M., Breitinger, H. G., & Zlotos, D. P. (2018). Symmetric dimeric adamantanes for exploring the structure of two viroporins: Influenza virus M2 and hepatitis C virus p7. *Drug Design, Development and Therapy*, *12*, 1019–1031. https://doi.org/10.2147/dddt.S157104

Mao, L., Wang, J., DeGrado, W. F., & Inouye, M. (2013). An assay suitable for high throughput screening of anti-influenza drugs. *PLoS ONE*, *8*(1), e54070. https://doi.org/10.1371/journal.pone.0054070

Masante, C., Najjar, F. E., Chang, A., Jones, A., Moncman, C. L., & Dutch, R. E. (2014). The human metapneumovirus small hydrophobic protein has properties consistent with those of a viroporin and can modulate viral fusogenic activity. *Journal of Virology*, *88*(11), 6423–6433. https://doi.org/10.1128/jvi.02848-13

Mathew, S., Fatima, K., Fatmi, M. Q., Archunan, G., Ilyas, M., Begum, N., Azhar, E., Damanhouri, G., & Qadri, I. (2015). Computational docking study of p7 Ion channel from HCV genotype 3 and genotype 4 and its interaction with natural compounds. *PLoS ONE*, *10*(6), e0126510. https://doi.org/10.1371/journal.pone.0126510

Medeiros-Silva, J., Dregni, A. J., Somberg, N. H., Duan, P., & Hong, M. (2023). Atomic structure of the open SARS-CoV-2 E viroporin. *Science Advances*, *9*(41), eadi9007. https://doi.org/10.1126/sciadv.adi9007

Mehnert, T., Routh, A., Judge, P. J., Lam, Y. H., Fischer, D., Watts, A., & Fischer, W. B. (2008). Biophysical characterization of Vpu from HIV-1 suggests a channel-pore dualism. *Proteins: Structure, Function, and Bioinformatics*, *70*(4), 1488–1497. https://doi.org/10.1002/prot.21642

Melton, J. V., Ewart, G. D., Weir, R. C., Board, P. G., Lee, E., & Gage, P. W. (2002). Alphavirus 6K proteins form ion channels*. *Journal of Biological Chemistry*, *277*(49), 46923–46931. https://doi.org/10.1074/jbc.M207847200

Meredith, L. W., Zitzmann, N., & McKeating, J. A. (2013). Differential effect of p7 inhibitors on hepatitis C virus cell-to-cell transmission.

Antiviral Research, *100*(3), 636–639. https://doi.org/10.1016/j.antiviral.2013.10.006

Mihm, U., Grigorian, N., Welsch, C., Herrmann, E., Kronenberger, B., Teuber, G., von Wagner, M., Hofmann, W. P., Albrecht, M., Lengauer, T., Zeuzem, S., & Sarrazin, C. (2006). Amino acid variations in hepatitis C virus p7 and sensitivity to antiviral combination therapy with amantadine in chronic hepatitis C. *Antiviral Therapy*, *11*(4), 507–519. https://doi.org/10.1177/135965350601100408

Miller, A. N., Houlihan, P. R., Matamala, E., Cabezas-Bratesco, D., Lee, G. Y., Cristofori-Armstrong, B., Dilan, T. L., Sanchez-Martinez, S., Matthies, D., Yan, R., Yu, Z., Ren, D., Brauchi, S. E., & Clapham, D. E. (2023). The SARS-CoV-2 accessory protein Orf3a is not an ion channel, but does interact with trafficking proteins. *eLife*, *12*, e84477. https://doi.org/10.7554/eLife.84477

Miura, K., Suzuki, Y., Ishida, K., Arakawa, M., Wu, H., Fujioka, Y., Emi, A., Maeda, K., Hamajima, R., Nakano, T., Tenno, T., Hiroaki, H., & Morita, E. (2023). Distinct motifs in the E protein are required for SARS-CoV-2 virus particle formation and lysosomal deacidification in host cells. *Journal of Virology*, *97*(10), e00426-23. https://doi.org/10.1128/jvi.00426-23

Montserret, R., Saint, N., Vanbelle, C., Salvay, A. G., Simorre, J.-P., Ebel, C., Sapay, N., Renisio, J.-G., Böckmann, A., Steinmann, E., Pietschmann, T., Dubuisson, J., Chipot, C., & Penin, F. (2010). NMR structure and ion channel activity of the p7 protein from hepatitis C virus*. *Journal of Biological Chemistry*, *285*(41), 31446–31461. https://doi.org/10.1074/jbc.M110.122895

Moore, P. B., Zhong, Q., Husslein, T., & Klein, M. L. (1998). Simulation of the HIV-1 Vpu transmembrane domain as a pentameric bundle. *FEBS Letters*, *431*(2), 143–148. https://doi.org/10.1016/s0014-5793(98)00714-5

Mould, J. A., Paterson, R. G., Takeda, M., Ohigashi, Y., Venkataraman, P., Lamb, R. A., & Pinto, L. H. (2003). Influenza B virus BM2 protein has Ion channel activity that conducts protons across membranes. *Developmental Cell*, *5*(1), 175–184. https://doi.org/10.1016/S1534-5807(03)00190-4

Musharrafieh, R., Lagarias, P., Ma, C., Hau, R., Romano, A., Lambrinidis, G., Kolocouris, A., & Wang, J. (2020). Investigation of the drug resistance mechanism of M2-S31N channel blockers through biomolecular simulations and viral passage experiments. *ACS Pharmacology & Translational Science*, *3*(4), 666–675. https://doi.org/10.1021/acsptsci.0c00018

Musharrafieh, R., Lagarias, P. I., Ma, C., Tan, G. S., Kolocouris, A., & Wang, J. (2019). The L46P mutant confers a novel allosteric mechanism of resistance toward the influenza A virus M2 S31N proton channel blockers. *Molecular Pharmacology*, *96*(2), 148–157. https://doi.org/10.1124/mol.119.116640

Nieto-Torres, J. L., DeDiego, M. L., Verdiá-Báguena, C., Jimenez-Guardeño, J. M., Regla-Nava, J. A., Fernandez-Delgado, R., Castaño-Rodriguez, C., Alcaraz, A., Torres, J., Aguilella, V. M., & Enjuanes, L. (2014). Severe acute respiratory syndrome coronavirus envelope protein ion channel activity promotes virus fitness and pathogenesis. *PLoS Pathogens*, *10*(5), e1004077. https://doi.org/10.1371/journal.ppat.1004077

Nieva, J. L., Madan, V., & Carrasco, L. (2012). Viroporins: Structure and biological functions. *Nature Reviews Microbiology*, *10*(8), 563–574. https://doi.org/10.1038/nrmicro2820

Nieva, J. L., Sanz, M. A., & Carrasco, L. (2004). Membrane-permeabilizing motif in Semliki forest virus E1 glycoprotein. *FEBS Letters*, *576*(3), 417–422. https://doi.org/10.1016/j.febslet.2004.09.061

Oestringer, B. P., Bolivar, J. H., Hensen, M., Claridge, J. K., Chipot, C., Dehez, F., Holzmann, N., Zitzmann, N., & Schnell, J. R. (2018). Re-evaluating the p7 viroporin structure. *Nature*, *562*(7727), E8–e18. https://doi.org/10.1038/s41586-018-0561-9

OuYang, B., Xie, S., Berardi, M. J., Zhao, X., Dev, J., Yu, W., Sun, B., & Chou, J. J. (2013). Unusual architecture of the p7 channel from hepatitis C virus. *Nature*, *498*(7455), 521–525. https://doi.org/10.1038/nature12283

Padhi, S., Khan, N., Jameel, S., & Priyakumar, U. D. (2013). Molecular dynamics simulations reveal the HIV-1 Vpu transmembrane protein to form stable pentamers. *PLoS ONE*, *8*(11), e79779. https://doi.org/10.1371/journal.pone.0079779

Panjwani, A., Strauss, M., Gold, S., Wenham, H., Jackson, T., Chou, J. J., Rowlands, D. J., Stonehouse, N. J., Hogle, J. M., & Tuthill, T. J. (2014). Capsid protein VP4 of human rhinovirus induces membrane permeability by the formation of a size-selective multimeric pore. *PLoS Pathogens*, *10*(8), e1004294. https://doi.org/10.1371/journal.ppat.1004294

Park, S. H., Mrse, A. A., Nevzorov, A. A., Mesleh, M. F., Oblatt-Montal, M., Montal, M., & Opella, S. J. (2003). Three-dimensional structure of the channel-forming trans-membrane domain of virus protein "u" (Vpu) from HIV-1. *Journal of Molecular Biology*, *333*(2), 409–424. https://doi.org/10.1016/j.jmb.2003.08.048

Pavlović, D., Neville, D. C. A., Argaud, O., Blumberg, B., Dwek, R. A., Fischer, W. B., & Zitzmann, N. (2003). The hepatitis C virus p7 protein forms an ion channel that is inhibited by long-alkyl-chain iminosugar derivatives. *Proceedings of the National Academy of Sciences*, *100*(10), 6104–6108. https://doi.org/10.1073/pnas.1031527100

Peñaflor-Téllez, Y., Chávez-Munguía, B., Lagunes-Guillén, A., Salazar-Villatoro, L., & Gutiérrez-Escolano, A. L. (2022). The feline calicivirus leader of the capsid protein has the functional characteristics of a viroporin. *Viruses*, *14*(3), 635. https://doi.org/10.3390/v14030635

Perdigão, N., Heinrich, J., Stolte, C., Sabir, K. S., Buckley, M. J., Tabor, B., Signal, B., Gloss, B. S., Hammang, C. J., Rost, B., Schafferhans, A., & O'Donoghue, S. I. (2015). Unexpected features of the dark proteome. *Proceedings of the National Academy of Sciences of the United States of America*, *112*(52), 15898–15903. https://doi.org/10.1073/pnas.1508380112

Pervushin, K., Tan, E., Parthasarathy, K., Lin, X., Jiang, F. L., Yu, D., Vararattanavech, A., Soong, T. W., Liu, D. X., & Torres, J. (2009). Structure and inhibition of the SARS coronavirus envelope protein ion channel. *PLoS Pathogens*, *5*(7), e1000511. https://doi.org/10.1371/journal.ppat.1000511

Pham, T., Perry, J. L., Dosey, T. L., Delcour, A. H., & Hyser, J. M. (2017). The rotavirus NSP4 Viroporin domain is a calcium-conducting ion channel. *Scientific Reports*, *7*(1), 43487. https://doi.org/10.1038/srep43487

Pielak, R. M., & Chou, J. J. (2010). Solution NMR structure of the V27A drug resistant mutant of influenza a M2 channel. *Biochemical and Biophysical Research Communications*, *401*(1), 58–63. https://doi.org/10.1016/j.bbrc.2010.09.008

Pielak, R. M., Schnell, J. R., & Chou, J. J. (2009). Mechanism of drug inhibition and drug resistance of influenza A M2 channel. *Proceedings of the National Academy of Sciences*, *106*(18), 7379–7384. https://doi.org/10.1073/pnas.0902548106

Piller, S. C., Ewart, G. D., Premkumar, A., Cox, G. B., & Gage, P. W. (1996). Vpr protein of human immunodeficiency virus type 1 forms cation-selective channels in planar lipid bilayers. *Proceedings of the National Academy of Sciences of the United States of America*, *93*(1), 111–115. https://doi.org/10.1073/pnas.93.1.111

Pinto, L. H., Holsinger, L. J., & Lamb, R. A. (1992). Influenza virus M2 protein has ion channel activity. *Cell*, *69*(3), 517–528. https://doi.org/10.1016/0092-8674(92)90452-I

Plugge, B., Gazzarrini, S., Nelson, M., Cerana, R., Van, J. L., Derst, C., DiFrancesco, D., Moroni, A., & Thiel, G. (2000). A potassium channel protein encoded by chlorella virus PBCV-1. *Science*, *287*(5458), 1641–1644. https://doi.org/10.1126/science.287.5458.1641

Pokhrel, R., Pavadai, E., Gerstman, B. S., & Chapagain, P. P. (2019). Membrane pore formation and ion selectivity of the Ebola virus delta peptide. *Physical Chemistry Chemical Physics*, *21*(10), 5578–5585. https://doi.org/10.1039/c8cp07323f

Premkumar, A., Ewart, G. D., Cox, G. B., & Gage, P. W. (2004). An amino-acid substitution in the influenza-B NB protein affects ion-channel gating. *The Journal of Membrane Biology*, *197*(3), 135–143. https://doi.org/10.1007/s00232-004-0648-0

Premkumar, A., Horan, C. R., & Gage, P. W. (2005). Dengue virus M protein C-terminal peptide (DVM-C) forms ion channels. *The Journal of Membrane Biology*, *204*(1), 33–38. https://doi.org/10.1007/s00232-005-0744-9

Premkumar, A., Wilson, L., Ewart, G. D., & Gage, P. W. (2004). Cation-selective ion channels formed by p7 of hepatitis C virus are blocked by hexamethylene amiloride. *FEBS Letters*, *557*(1–3), 99–103. https://doi.org/10.1016/S0014-5793(03)01453-4

Qi, H., Chu, V., Wu, N. C., Chen, Z., Truong, S., Brar, G., Su, S.-Y., Du, Y., Arumugaswami, V., Olson, C. A., Chen, S.-H., Lin, C.-Y., Wu, T.-T., & Sun, R. (2017). Systematic identification of anti-interferon function on hepatitis C virus genome reveals p7 as an immune evasion protein. *Proceedings of the National Academy of Sciences*, *114*(8), 2018–2023. https://doi.org/10.1073/pnas.1614623114

Raghava, S., Giorda, K. M., Romano, F. B., Heuck, A. P., & Hebert, D. N. (2011). The SV40 late protein VP4 is a viroporin that forms pores to disrupt membranes for viral release. *PLoS Pathogens*, *7*(6), e1002116. https://doi.org/10.1371/journal.ppat.1002116

Rejdak, K., Fiedor, P., Bonek, R., Łukasiak, J., Chełstowski, W., Kiciak, S., Dąbrowski, P., Gala-Błądzińska, A., Dec, M., Papuć, E., Zasybska, A., Kaczor, M., & Grieb, P. (2023). Amantadine in unvaccinated patients with early, mild to moderate COVID-19: A randomized, placebo-controlled, double-blind trial. *European Journal of Neurology*, *31*, e16045. https://doi.org/10.1111/ene.16045

Ren, Y., Shu, T., Wu, D., Mu, J., Wang, C., Huang, M., Han, Y., Zhang, X.-Y., Zhou, W., Qiu, Y., & Zhou, X. (2020). The ORF3a protein of SARS-CoV-2 induces apoptosis in cells. *Cellular & Molecular Immunology*, *17*(8), 881–883. https://doi.org/10.1038/s41423-020-0485-9

Rey-Carrizo, M., Torres, E., Ma, C., Barniol-Xicota, M., Wang, J., Wu, Y., Naesens, L., DeGrado, W. F., Lamb, R. A., Pinto, L. H., & Vázquez, S. (2013). 3-Azatetracyclo[5.2.1.1.0(5,8).0(1,5)]undecane derivatives: From wild-type inhibitors of the M2 ion channel of influenza A virus to derivatives with potent activity against the V27A mutant. *Journal of Medicinal Chemistry*, *56*(22), 9265–9274. https://doi.org/10.1021/jm401340p

Rogers, J. M., & Suga, H. (2015). Discovering functional, non-proteinogenic amino acid containing, peptides using genetic code reprogramming. *Organic & Biomolecular Chemistry*, *13*(36), 9353–9363. https://doi.org/10.1039/c5ob01336d

Rosenberg, M. R., Weaver, L. M., & Casarotto, M. G. (2016). Probing interactions of Vpu from HIV-1 with amiloride-based compounds. *Biochimica et Biophysica Acta*, *1858*(4), 733–739. https://doi.org/10.1016/j.bbamem.2015.12.028

Rossman, J. S., Jing, X., Leser, G. P., & Lamb, R. A. (2010). Influenza virus M2 protein mediates ESCRT-independent membrane scission. *Cell*, *142*(6), 902–913. https://doi.org/10.1016/j.cell.2010.08.029

Roulston, A., Marcellus, R. C., & Branton, P. E. (1999). Viruses and apoptosis. *Annual Review of Microbiology*, *53*(1), 577–628. https://doi.org/10.1146/annurev.micro.53.1.577

Royle, J., Dobson, S. J., Müller, M., & Macdonald, A. (2015). Emerging roles of viroporins encoded by DNA viruses: Novel targets for antivirals? *Viruses*, *7*(10), 5375–5387. https://doi.org/10.3390/v7102880

Saint, N., Montserret, R., Chipot, C., & Penin, F. (2009). Structural and functional analysis of the HCV p7 protein. In H. Tang (Ed.), *Hepatitis C: Methods and protocols* (pp. 125–143). Humana Press. https://doi.org/10.1007/978-1-59745-394-3_10

Salsman, J., Top, D., Boutilier, J., & Duncan, R. (2005). Extensive syncytium formation mediated by the reovirus FAST proteins triggers apoptosis-induced membrane instability. *Journal of Virology*, *79*(13), 8090–8100. https://doi.org/10.1128/jvi.79.13.8090-8100.2005

Santner, P., Martins, J. M.d S., Laursen, J. S., Behrendt, L., Riber, L., Olsen, C. A., Arkin, I. T., Winther, J. R., Willemoës, M., & Lindorff-Larsen, K. (2018). A robust proton flux (pHlux) assay for studying the function and inhibition of the influenza a M2 proton channel. *Biochemistry*, *57*(41), 5949–5956. https://doi.org/10.1021/acs.biochem.8b00721

Santos, R., Ursu, O., Gaulton, A., Bento, A. P., Donadi, R. S., Bologa, C. G., Karlsson, A., Al-Lazikani, B., Hersey, A., Oprea, T. I., & Overington, J. P. (2017). A comprehensive map of molecular drug targets. *Nature Reviews. Drug Discovery*, *16*(1), 19–34. https://doi.org/10.1038/nrd.2016.230

Sanz, M. A., Madan, V., Carrasco, L., & Nieva, J. L. (2003). Interfacial domains in Sindbis virus 6K protein: Detection and functional characterization*. *Journal of Biological Chemistry*, *278*(3), 2051–2057. https://doi.org/10.1074/jbc.M206611200

Sanz, M. A., Pérez, L., & Carrasco, L. (1994). Semliki Forest virus 6K protein modifies membrane permeability after inducible expression in *Escherichia coli* cells. *Journal of Biological Chemistry*, *269*(16), 12106–12110. https://doi.org/10.1016/S0021-9258(17)32687-X

Sasaki-Tanaka, R., Shibata, T., Moriyama, M., Okamoto, H., Kogure, H., & Kanda, T. (2022). Amantadine and Rimantadine inhibit hepatitis a virus replication through the induction of autophagy. *Journal of Virology*, *96*(18), e00646-22. https://doi.org/10.1128/jvi.00646-22

Sauter, D., Schwarz, S., Wang, K., Zhang, R., Sun, B., & Schwarz, W. (2014). Genistein as antiviral drug against HIV ion channel. *Planta Medica*, *80*(08/09), 682–687. https://doi.org/10.1055/s-0034-1368583

Schnell, J. R., & Chou, J. J. (2008). Structure and mechanism of the M2 proton channel of influenza A virus. *Nature*, *451*(7178), 591–595. https://doi.org/10.1038/nature06531

Schroeder, C., Ford, C. M., Wharton, S. A., & Hay, A. J. (1994). Functional reconstitution in lipid vesicles of influenza virus M2 protein expressed by baculovirus: Evidence for proton transfer activity. *Journal of General Virology*, *75*(12), 3477–3484. https://doi.org/10.1099/0022-1317-75-12-3477

Schubert, U., Ferrer-Montiel, A. V., Oblatt-Montal, M., Henklein, P., Strebel, K., & Montal, M. (1996). Identification of an ion channel activity of the Vpu transmembrane domain and its involvement in the regulation of virus release from HIV-1-infected cells. *FEBS Letters*, *398*(1), 12–18. https://doi.org/10.1016/S0014-5793(96)01146-5

Schwarz, S., Sauter, D., Wang, K., Zhang, R., Sun, B., Karioti, A., Bilia, A. R., Efferth, T., & Schwarz, W. (2014). Kaempferol derivatives as antiviral drugs against the 3a channel protein of coronavirus. *Planta Medica*, *80*(02/03), 177–182. https://doi.org/10.1055/s-0033-1360277

Schwarz, S., Wang, K., Yu, W., Sun, B., & Schwarz, W. (2011). Emodin inhibits current through SARS-associated coronavirus 3a protein. *Antiviral Research*, *90*(1), 64–69. https://doi.org/10.1016/j.antiviral.2011.02.008

Scott, C., & Griffin, S. (2015). Viroporins: Structure, function and potential as antiviral targets. *Journal of General Virology*, *96*(8), 2000–2027. https://doi.org/10.1099/vir.0.000201

Scott, C., Kankanala, J., Foster, T. L., Goldhill, D. H., Bao, P., Simmons, K., Pingen, M., Bentham, M., Atkins, E., Loundras, E., Elderfield, R., Claridge, J. K., Thompson, J., Stilwell, P. R., Tathineni, R., McKimmie, C. S., Targett-Adams, P., Schnell, J. R., Cook, G. P., … Griffin, S. (2020). Site-directed M2 proton channel inhibitors enable synergistic combination therapy for rimantadine-resistant pandemic influenza. *PLoS Pathogens*, *16*(8), e1008716. https://doi.org/10.1371/journal.ppat.1008716

Sharma, M., Yi, M., Dong, H., Qin, H., Peterson, E., Busath, D. D., Zhou, H. X., & Cross, T. A. (2010). Insight into the mechanism of the influenza A proton channel from a structure in a lipid bilayer. *Science*, *330*(6003), 509–512. https://doi.org/10.1126/science.1191750

Shaw, J., Gosain, R., Kalita, M. M., Foster, T. L., Kankanala, J., Mahato, D. R., Abas, S., King, B. J., Scott, C., Brown, E., Bentham, M. J., Wetherill, L., Bloy, A., Samson, A., Harris, M., Mankouri, J., Rowlands, D. J., Macdonald, A., Tarr, A. W., … Griffin, S. (2020).

Rationally derived inhibitors of hepatitis C virus (HCV) p7 channel activity reveal prospect for bimodal antiviral therapy. *eLife*, *9*, e52555. https://doi.org/10.7554/eLife.52555

Shepley-McTaggart, A., Sagum, C. A., Oliva, I., Rybakovsky, E., DiGuilio, K., Liang, J., Bedford, M. T., Cassel, J., Sudol, M., Mullin, J. M., & Harty, R. N. (2021). SARS-CoV-2 envelope (E) protein interacts with PDZ-domain-2 of host tight junction protein ZO1. *PLoS ONE*, *16*(6), e0251955. https://doi.org/10.1371/journal.pone.0251955

Shimbo, K., Brassard, D. L., Lamb, R. A., & Pinto, L. H. (1995). Viral and cellular small integral membrane proteins can modify ion channels endogenous to Xenopus oocytes. *Biophysical Journal*, *69*(5), 1819–1829. https://doi.org/10.1016/s0006-3495(95)80052-4

Shiryaev, V. A., Radchenko, E. V., Palyulin, V. A., Zefirov, N. S., Bormotov, N. I., Serova, O. A., Shishkina, L. N., Baimuratov, M. R., Bormasheva, K. M., Gruzd, Y. A., Ivleva, E. A., Leonova, M. V., Lukashenko, A. V., Osipov, D. V., Osyanin, V. A., Reznikov, A. N., Shadrikova, V. A., Sibiryakova, A. E., Tkachenko, I. M., & Klimochkin, Y. N. (2018). Molecular design, synthesis and biological evaluation of cage compound-based inhibitors of hepatitis C virus p7 ion channels. *European Journal of Medicinal Chemistry*, *158*, 214–235. https://doi.org/10.1016/j.ejmech.2018.08.009

Shrivastava, G., García-Cordero, J., León-Juárez, M., Oza, G., Tapia-Ramírez, J., Villegas-Sepulveda, N., & Cedillo-Barrón, L. (2017). NS2A comprises a putative viroporin of dengue virus 2. *Virulence*, *8*(7), 1450–1456. https://doi.org/10.1080/21505594.2017.1356540

Shukla, A., Dey, D., Banerjee, K., Nain, A., & Banerjee, M. (2015). The C-terminal region of the non-structural protein 2B from hepatitis a virus demonstrates lipid-specific viroporin-like activity. *Scientific Reports*, *5*(1), 15884. https://doi.org/10.1038/srep15884

Shyr, Z. A., Cheng, Y. S., Lo, D. C., & Zheng, W. (2021). Drug combination therapy for emerging viral diseases. *Drug Discovery Today*, *26*(10), 2367–2376. https://doi.org/10.1016/j.drudis.2021.05.008

Si, F., Hu, X., Wang, C., Chen, B., Wang, R., Dong, S., Yu, R., & Li, Z. (2020). Porcine epidemic diarrhea virus (PEDV) ORF3 enhances viral proliferation by inhibiting apoptosis of infected cells. *Viruses*, *12*(2), 214. https://doi.org/10.3390/v12020214

Singh Tomar, P. P., & Arkin, I. T. (2020). SARS-CoV-2 E protein is a potential ion channel that can be inhibited by Gliclazide and Memantine. *Biochemical and Biophysical Research Communications*, *530*(1), 10–14. https://doi.org/10.1016/j.bbrc.2020.05.206

Smertina, E., Carroll, A. J., Boileau, J., Emmott, E., Jenckel, M., Vohra, H., Rolland, V., Hands, P., Hayashi, J., Neave, M. J., Liu, J.-W., Hall, R. N., Strive, T., & Frese, M. (2022). Lagovirus non-structural protein p23: A putative viroporin that interacts with heat shock proteins and uses a disulfide bond for dimerization [original research]. *Frontiers in Microbiology*, *13*, 923256. https://doi.org/10.3389/fmicb.2022.923256

Smith, J. P., Riley, T. R. 3rd, Devenyi, A., Bingaman, S. I., & Kunselman, A. (2004). Amantadine therapy for chronic hepatitis C. *Journal of General Internal Medicine*, *19*(6), 662–668. https://doi.org/10.1111/j.1525-1497.2004.30057.x

Somberg, N. H., Medeiros-Silva, J., Jo, H., Wang, J., DeGrado, W. F., & Hong, M. (2023). Hexamethylene amiloride binds the SARS-CoV-2 envelope protein at the protein-lipid interface. *Protein Science*, *32*(10), e4755. https://doi.org/10.1002/pro.4755

Stampolaki, M., Hoffmann, A., Tekwani, K., Georgiou, K., Tzitzoglaki, C., Ma, C., Becker, S., Schmerer, P., Döring, K., Stylianakis, I., Turcu, A. L., Wang, J., Vázquez, S., Andreas, L. B., Schmidtke, M., & Kolocouris, A. (2023). A study of the activity of Adamantyl amines against mutant influenza a M2 channels identified a polycyclic cage amine triple blocker, explored by molecular dynamics simulations and solid-state NMR**. *ChemMedChem*, *18*(16), e202300182. https://doi.org/10.1002/cmdc.202300182

Stauffer, S., Feng, Y., Nebioglu, F., Heilig, R., Picotti, P., & Helenius, A. (2014). Stepwise priming by acidic pH and a high K+ concentration is required for efficient uncoating of influenza a virus cores after penetration. *Journal of Virology*, *88*(22), 13029–13046. https://doi.org/10.1128/jvi.01430-14

Stefan, E., Obexer, R., Hofmann, S., Vu Huu, K., Huang, Y., Morgner, N., Suga, H., & Tampé, R. (2021). De novo macrocyclic peptides dissect energy coupling of a heterodimeric ABC transporter by multimode allosteric inhibition. *eLife*, *10*, e67732. https://doi.org/10.7554/eLife.67732

Steinmann, E., Penin, F., Kallis, S., Patel, A. H., Bartenschlager, R., & Pietschmann, T. (2007). Hepatitis C virus p7 protein is crucial for assembly and release of infectious virions. *PLoS Pathogens*, *3*(7), e103. https://doi.org/10.1371/journal.ppat.0030103

Steinmann, E., Whitfield, T., Kallis, S., Dwek, R. A., Zitzmann, N., Pietschmann, T., & Bartenschlager, R. (2007). Antiviral effects of amantadine and iminosugar derivatives against hepatitis C virus. *Hepatology*, *46*(2), 330–338. https://doi.org/10.1002/hep.21686

StGelais, C., Foster, T. L., Verow, M., Atkins, E., Fishwick, C. W. G., Rowlands, D., Harris, M., & Griffin, S. (2009). Determinants of hepatitis C virus p7 ion channel function and drug sensitivity identified in vitro. *Journal of Virology*, *83*(16), 7970–7981. https://doi.org/10.1128/jvi.00521-09

StGelais, C., Tuthill, T. J., Clarke, D. S., Rowlands, D. J., Harris, M., & Griffin, S. (2007). Inhibition of hepatitis C virus p7 membrane channels in a liposome-based assay system. *Antiviral Research*, *76*(1), 48–58. https://doi.org/10.1016/j.antiviral.2007.05.001

Stouffer, A. L., Acharya, R., Salom, D., Levine, A. S., di Costanzo, L., Soto, C. S., Tereshko, V., Nanda, V., Stayrook, S., & DeGrado, W. F. (2008). Structural basis for the function and inhibition of an influenza virus proton channel. *Nature*, *451*(7178), 596–599. https://doi.org/10.1038/nature06528

Strebel, K., Klimkait, T., & Martin, M. A. (1988). A novel gene of HIV-1, vpu, and its 16-Kilodalton product. *Science*, *241*(4870), 1221–1223. https://doi.org/10.1126/science.3261888

Strtak, A. C., Perry, J. L., Sharp, M. N., Chang-Graham, A. L., Farkas, T., & Hyser, J. M. (2019). Recovirus NS1-2 has viroporin activity that induces aberrant cellular calcium signaling To facilitate virus replication. *mSphere*, *4*(5). https://doi.org/10.1128/msphere.00506-19

Sun, S., Karki, C., Aguilera, J., Lopez Hernandez, A. E., Sun, J., & Li, L. (2021). Computational study on the function of palmitoylation on the envelope protein in SARS-CoV-2. *Journal of Chemical Theory and Computation*, *17*(10), 6483–6490. https://doi.org/10.1021/acs.jctc.1c00359

Sunstrom, N. A., Premkumar, L. S., Premkumar, A., Ewart, G., Cox, G. B., & Gage, P. W. (1996). Ion channels formed by NB, an influenza B virus protein. *The Journal of Membrane Biology*, *150*(2), 127–132. https://doi.org/10.1007/s002329900037

Surya, W., Li, Y., & Torres, J. (2018). Structural model of the SARS coronavirus E channel in LMPG micelles. *Biochimica et Biophysica Acta - Biomembranes*, *1860*(6), 1309–1317. https://doi.org/10.1016/j.bbamem.2018.02.017

Surya, W., Li, Y., Verdià-Bàguena, C., Aguilella, V. M., & Torres, J. (2015). MERS coronavirus envelope protein has a single transmembrane domain that forms pentameric ion channels. *Virus Research*, *201*, 61–66. https://doi.org/10.1016/j.virusres.2015.02.023

Surya, W., Tavares-Neto, E., Sanchis, A., Queralt-Martín, M., Alcaraz, A., Torres, J., & Aguilella, V. M. (2023). The complex proteolipidic behavior of the SARS-CoV-2 envelope protein channel: Weak selectivity and heterogeneous oligomerization. *International Journal of Molecular Sciences*, *24*(15), 12454. https://doi.org/10.3390/ijms241512454

Surya, W., & Torres, J. (2022). Oligomerization-dependent beta-structure formation in SARS-CoV-2 envelope protein. *International Journal of Molecular Sciences*, *23*(21), 13285. https://doi.org/10.3390/ijms232113285

Suzuki, T., Orba, Y., Okada, Y., Sunden, Y., Kimura, T., Tanaka, S., Nagashima, K., Hall, W. W., & Sawa, H. (2010). The human polyoma JC

virus agnoprotein acts as a viroporin. *PLoS Pathogens*, *6*(3), e1000801. https://doi.org/10.1371/journal.ppat.1000801

Takeuchi, K., & Lamb, R. A. (1994). Influenza virus M2 protein ion channel activity stabilizes the native form of fowl plague virus hemagglutinin during intracellular transport. *Journal of Virology*, *68*(2), 911–919. https://doi.org/10.1128/jvi.68.2.911-919.1994

Tang, Y., Zaitseva, F., Lamb, R. A., & Pinto, L. H. (2002). The gate of the influenza virus M2 proton channel is formed by a single tryptophan residue. *The Journal of Biological Chemistry*, *277*(42), 39880–39886. https://doi.org/10.1074/jbc.M206582200

Tannock, G. A., Kim, H., & Xue, L. (2020). Why are vaccines against many human viral diseases still unavailable; an historic perspective? *Journal of Medical Virology*, *92*(2), 129–138. https://doi.org/10.1002/jmv.25593

Taube, R., Alhadeff, R., Assa, D., Krugliak, M., & Arkin, I. T. (2014). Bacteria-based analysis of HIV-1 Vpu channel activity. *PLoS ONE*, *9*(10), e105387. https://doi.org/10.1371/journal.pone.0105387

Thomaston, J. L., Alfonso-Prieto, M., Woldeyes, R. A., Fraser, J. S., Klein, M. L., Fiorin, G., & DeGrado, W. F. (2015). High-resolution structures of the M2 channel from influenza A virus reveal dynamic pathways for proton stabilization and transduction. *Proceedings of the National Academy of Sciences of the United States of America*, *112*(46), 14260–14265. https://doi.org/10.1073/pnas.1518493112

Thomaston, J. L., Konstantinidi, A., Liu, L., Lambrinidis, G., Tan, J., Caffrey, M., Wang, J., Degrado, W. F., & Kolocouris, A. (2020). X-ray crystal structures of the influenza M2 proton channel drug-resistant V27A mutant bound to a spiro-adamantyl amine inhibitor reveal the mechanism of adamantane resistance. *Biochemistry*, *59*(4), 627–634. https://doi.org/10.1021/acs.biochem.9b00971

Thomaston, J. L., Polizzi, N. F., Konstantinidi, A., Wang, J., Kolocouris, A., & DeGrado, W. F. (2018). Inhibitors of the M2 proton channel engage and disrupt transmembrane networks of hydrogen-bonded waters. *Journal of the American Chemical Society*, *140*(45), 15219–15226. https://doi.org/10.1021/jacs.8b06741

Thomaston, J. L., Samways, M. L., Konstantinidi, A., Ma, C., Hu, Y., Bruce Macdonald, H. E., Wang, J., Essex, J. W., DeGrado, W. F., & Kolocouris, A. (2021). Rimantadine binds to and inhibits the influenza A M2 proton channel without enantiomeric specificity. *Biochemistry*, *60*, 2471–2482. https://doi.org/10.1021/acs.biochem.1c00437

Thomaston, J. L., Woldeyes, R. A., Nakane, T., Yamashita, A., Tanaka, T., Koiwai, K., Brewster, A. S., Barad, B. A., Chen, Y., Lemmin, T., Uervirojnangkoorn, M., Arima, T., Kobayashi, J., Masuda, T., Suzuki, M., Sugahara, M., Sauter, N. K., Tanaka, R., Nureki, O., … DeGrado, W. F. (2017). XFEL structures of the influenza M2 proton channel: Room temperature water networks and insights into proton conduction. *Proceedings of the National Academy of Sciences of the United States of America*, *114*(51), 13357–13362. https://doi.org/10.1073/pnas.1705624114

Toft-Bertelsen, T. L., Jeppesen, M. G., Landbrug, A., Mujezinovic, A., Bentzen, B. H., Kledal, T. N., & Rosenkilde, M. M. (2022). Reply to: How many SARS-CoV-2 "Viroporins" are really ion channels? *Communications Biology*, *5*(1), 860. https://doi.org/10.1038/s42003-022-03670-9

Toft-Bertelsen, T. L., Jeppesen, M. G., Tzortzini, E., Xue, K., Giller, K., Becker, S., Mujezinovic, A., Bentzen, B. H., Andreas, B., Kolocouris, A., Kledal, T. N., & Rosenkilde, M. M. (2021). Amantadine inhibits known and novel ion channels encoded by SARS-CoV-2 in vitro. *Communications Biology*, *4*(1), 1347. https://doi.org/10.1038/s42003-021-02866-9

Tomar, P. P. S., Krugliak, M., & Arkin, I. T. (2021). Blockers of the SARS-CoV-2 3a channel identified by targeted drug repurposing. *Viruses*, *13*(3), 532. https://doi.org/10.3390/v13030532

Tomar, P. P. S., Krugliak, M., Singh, A., & Arkin, I. T. (2022). Zika M—A potential viroporin: Mutational study and drug repurposing. *Biomedicine*, *10*(3), 641. https://www.mdpi.com/2227-9059/10/3/641

Tomar, P. P. S., Oren, R., Krugliak, M., & Arkin, I. T. (2019). Potential viroporin candidates from pathogenic viruses using bacteria-based bioassays. *Viruses*, *11*(7), 632. https://doi.org/10.3390/v11070632

Torres, J., Maheswari, U., Parthasarathy, K., Ng, L., Liu, D. X., & Gong, X. (2007). Conductance and amantadine binding of a pore formed by a lysine-flanked transmembrane domain of SARS coronavirus envelope protein. *Protein Science*, *16*(9), 2065–2071. https://doi.org/10.1110/ps.062730007

Torres, J., Wang, J., Parthasarathy, K., & Liu, D. X. (2005). The transmembrane oligomers of coronavirus protein E. *Biophysical Journal*, *88*(2), 1283–1290. https://doi.org/10.1529/biophysj.104.051730

Tosteson, M. T., Caulfield, M. P., Levy, J. J., Rosenblatt, M., & Tosteson, D. C. (1988). The synthetic precursor specific region of pre-pro-parathyroid hormone forms ion channels in lipid bilayers. *Bioscience Reports*, *8*(2), 173–183. https://doi.org/10.1007/bf01116462

Tosteson, M. T., Pinto, L. H., Holsinger, L. J., & Lamb, R. A. (1994). Reconstitution of the influenza virus M2 ion channel in lipid bilayers. *The Journal of Membrane Biology*, *142*(1), 117–126. https://doi.org/10.1007/BF00233389

Townsend, J. A., Sanders, H. M., Rolland, A. D., Park, C. K., Horton, N. C., Prell, J. S., Wang, J., & Marty, M. T. (2021). Influenza AM2 channel oligomerization is sensitive to its chemical environment. *Analytical Chemistry*, *93*(48), 16273–16281. https://doi.org/10.1021/acs.analchem.1c04660

Troyano-Hernáez, P., Reinosa, R., & Holguín, Á. (2021). Evolution of SARS-CoV-2 envelope, membrane, nucleocapsid, and spike structural proteins from the beginning of the pandemic to September 2020: A global and regional approach by epidemiological week. *Viruses*, *13*(2), 243. https://doi.org/10.3390/v13020243

van Kuppeveld, F. J. M., Hoenderop, J. G. J., Smeets, R. L. L., Willems, P. H. G. M., Dijkman, H. B. P. M., Galama, J. M. D., & Melchers, W. J. G. (1997). Coxsackievirus protein 2B modifies endoplasmic reticulum membrane and plasma membrane permeability and facilitates virus release. *The EMBO Journal*, *16*(12), 3519–3532. https://doi.org/10.1093/emboj/16.12.3519

van Kuppeveld, F. J. M., Melchers, W. J. G., Kirkegaard, K., & Doedens, J. R. (1997). Structure–function analysis of Coxsackie B3 virus protein 2B. *Virology*, *227*(1), 111–118. https://doi.org/10.1006/viro.1996.8320

Varadi, M., Anyango, S., Deshpande, M., Nair, S., Natassia, C., Yordanova, G., Yuan, D., Stroe, O., Wood, G., Laydon, A., Žídek, A., Green, T., Tunyasuvunakool, K., Petersen, S., Jumper, J., Clancy, E., Green, R., Vora, A., Lutfi, M., … Velankar, S. (2022). AlphaFold protein structure database: Massively expanding the structural coverage of protein-sequence space with high-accuracy models. *Nucleic Acids Research*, *50*(D1), D439–d444. https://doi.org/10.1093/nar/gkab1061

Verdiá-Báguena, C., Nieto-Torres, J. L., Alcaraz, A., DeDiego, M. L., Enjuanes, L., & Aguilella, V. M. (2013). Analysis of SARS-CoV E protein ion channel activity by tuning the protein and lipid charge. *Biochimica et Biophysica Acta (BBA) - Biomembranes*, *1828*(9), 2026–2031. https://doi.org/10.1016/j.bbamem.2013.05.008

Verdiá-Báguena, C., Nieto-Torres, J. L., Alcaraz, A., DeDiego, M. L., Torres, J., Aguilella, V. M., & Enjuanes, L. (2012). Coronavirus E protein forms ion channels with functionally and structurally-involved membrane lipids. *Virology*, *432*(2), 485–494. https://doi.org/10.1016/j.virol.2012.07.005

von Heijne, G. (1989). Control of topology and mode of assembly of a polytopic membrane protein by positively charged residues. *Nature*, *341*(6241), 456–458. https://doi.org/10.1038/341456a0

von Heijne, G. (2006). Membrane-protein topology. *Nature Reviews. Molecular Cell Biology*, *7*(12), 909–918. https://doi.org/10.1038/nrm2063

Wang, C., Lamb, R. A., & Pinto, L. H. (1994). Direct measurement of the influenza A virus M2 protein Ion channel activity in mammalian cells. *Virology*, *205*(1), 133–140. https://doi.org/10.1006/viro.1994.1628

Wang, C., Lamb, R. A., & Pinto, L. H. (1995). Activation of the M2 ion channel of influenza virus: A role for the transmembrane domain histidine residue. *Biophysical Journal*, *69*(4), 1363–1371. https://doi.org/10.1016/S0006-3495(95)80003-2

Wang, J., Cady, S. D., Balannik, V., Pinto, L. H., DeGrado, W. F., & Hong, M. (2009). Discovery of spiro-piperidine inhibitors and their modulation of the dynamics of the M2 proton channel from influenza a virus. *Journal of the American Chemical Society*, *131*(23), 8066–8076. https://doi.org/10.1021/ja900063s

Wang, J., Ma, C., Fiorin, G., Carnevale, V., Wang, T., Hu, F., Lamb, R. A., Pinto, L. H., Hong, M., Klein, M. L., & DeGrado, W. F. (2011). Molecular dynamics simulation directed rational design of inhibitors targeting drug-resistant mutants of influenza A virus M2. *Journal of the American Chemical Society*, *133*(32), 12834–12841. https://doi.org/10.1021/ja204969m

Wang, J., Pielak, R. M., McClintock, M. A., & Chou, J. J. (2009). Solution structure and functional analysis of the influenza B proton channel. *Nature Structural & Molecular Biology*, *16*(12), 1267–1271. https://doi.org/10.1038/nsmb.1707

Wang, J., Wu, Y., Ma, C., Fiorin, G., Wang, J., Pinto, L. H., Lamb, R. A., Klein, M. L., & Degrado, W. F. (2013). Structure and inhibition of the drug-resistant S31N mutant of the M2 ion channel of influenza A virus. *Proceedings of the National Academy of Sciences of the United States of America*, *110*(4), 1315–1320. https://doi.org/10.1073/pnas.1216526110

Wang, K., Lu, W., Chen, J., Xie, S., Shi, H., Hsu, H., Yu, W., Xu, K., Bian, C., Fischer, W. B., Schwarz, W., Feng, L., & Sun, B. (2012). PEDV ORF3 encodes an ion channel protein and regulates virus production. *FEBS Letters*, *586*(4), 384–391. https://doi.org/10.1016/j.febslet.2012.01.005

Wang, Y., Hu, Y., Xu, S., Zhang, Y., Musharrafieh, R., Hau, R. K., Ma, C., & Wang, J. (2018). In vitro pharmacokinetic optimizations of AM2-S31N channel blockers led to the discovery of slow-binding inhibitors with potent antiviral activity against drug-resistant influenza A viruses. *Journal of Medicinal Chemistry*, *61*(3), 1074–1085. https://doi.org/10.1021/acs.jmedchem.7b01536

Wanitchang, A., Wongthida, P., & Jongkaewwattana, A. (2016). Influenza B virus M2 protein can functionally replace its influenza A virus counterpart in promoting virus replication. *Virology*, *498*, 99–108. https://doi.org/10.1016/j.virol.2016.08.016

Weerawardhana, A., Uddin, M. B., Choi, J. H., Pathinayake, P., Shin, S. H., Chathuranga, K., Park, J. H., & Lee, J. S. (2022). Foot-and-mouth disease virus non-structural protein 2B downregulates the RLR signaling pathway via degradation of RIG-I and MDA5. *Frontiers in Immunology*, *13*, 1020262. https://doi.org/10.3389/fimmu.2022.1020262

Wei, S., Hu, X., Du, L., Zhao, L., Xue, H., Liu, C., Chou, J. J., Zhong, J., Tong, Y., Wang, S., & OuYang, B. (2021). Inhibitor development against p7 channel in hepatitis C virus. *Molecules*, *26*(5), 1350. https://doi.org/10.3390/molecules26051350

Wei, S., Liu, C., Du, L., Wu, B., Zhong, J., Tong, Y., Wang, S., & OuYang, B. (2022). Identification of a novel class of cyclic penta-peptides against hepatitis C virus as p7 channel blockers. *Computational and Structural Biotechnology Journal*, *20*, 5902–5910. https://doi.org/10.1016/j.csbj.2022.10.035

Weis, N., Bollerup, S., Sund, J. D., Glamann, J. B., Vinten, C., Jensen, L. R., Sejling, C., Kledal, T. N., & Rosenkilde, M. M. (2023). Amantadine for COVID-19 treatment (ACT) study: A randomized, double-blinded, placebo-controlled clinical trial. *Clinical Microbiology and Infection*, *29*(10), 1313–1319. https://doi.org/10.1016/j.cmi.2023.06.023

Wetherill, L. F., Holmes, K. K., Verow, M., Müller, M., Howell, G., Harris, M., Fishwick, C., Stonehouse, N., Foster, R., Blair, G. E., Griffin, S., & Macdonald, A. (2012). High-risk human papillomavirus E5 oncoprotein displays channel-forming activity sensitive to small-molecule inhibitors. *Journal of Virology*, *86*(9), 5341–5351. https://doi.org/10.1128/jvi.06243-11

Whitfield, T., Miles, A. J., Scheinost, J. C., Offer, J., Wentworth, P. Jr., Dwek, R. A., Wallace, B. A., Biggin, P. C., & Zitzmann, N. (2011). The influence of different lipid environments on the structure and function of the hepatitis C virus p7 ion channel protein. *Molecular Membrane Biology*, *28*(5), 254–264. https://doi.org/10.3109/09687688.2011.581253

Wilkinson, J., Ewart, G., Luscombe, C., McBride, K., Ratanasuwan, W., Miller, M., & Murphy, R. L. (2015). A phase 1b/2a study of the safety, pharmacokinetics and antiviral activity of BIT225 in patients with HIV-1 infection. *Journal of Antimicrobial Chemotherapy*, *71*(3), 731–738. https://doi.org/10.1093/jac/dkv389

Willbold, D., Hoffmann, S., & Rösch, P. (1997). Secondary structure and tertiary fold of the human immunodeficiency virus protein U (Vpu) cytoplasmic domain in solution. *European Journal of Biochemistry*, *245*(3), 581–588. https://doi.org/10.1111/j.1432-1033.1997.t01-1-00581.x

Willey, R. L., Maldarelli, F., Martin, M. A., & Strebel, K. (1992). Human immunodeficiency virus type 1 Vpu protein induces rapid degradation of CD4. *Journal of Virology*, *66*(12), 7193–7200. https://doi.org/10.1128/jvi.66.12.7193-7200.1992

Wilson, L., Gage, P., & Ewart, G. (2006). Hexamethylene amiloride blocks E protein ion channels and inhibits coronavirus replication. *Virology*, *353*(2), 294–306. https://doi.org/10.1016/j.virol.2006.05.028

Wilson, L., McKinlay, C., Gage, P., & Ewart, G. (2004). SARS coronavirus E protein forms cation-selective ion channels. *Virology*, *330*(1), 322–331. https://doi.org/10.1016/j.virol.2004.09.033

Wilson, R. L., Fuentes, S. M., Wang, P., Taddeo, E. C., Klatt, A., Henderson, A. J., & He, B. (2006). Function of small hydrophobic proteins of paramyxovirus. *Journal of Virology*, *80*(4), 1700–1709. https://doi.org/10.1128/jvi.80.4.1700-1709.2006

Wingfield, W. L., Pollack, D., & Grunert, R. R. (1969). Therapeutic efficacy of amantadine HCl and rimantadine HCl in naturally occurring influenza A2 respiratory illness in man. *The New England Journal of Medicine*, *281*, 579–584. https://doi.org/10.1056/NEJM196909112811102

Wittlich, M., Koenig, B. W., Stoldt, M., Schmidt, H., & Willbold, D. (2009). NMR structural characterization of HIV-1 virus protein U cytoplasmic domain in the presence of dodecylphosphatidylcholine micelles. *The FEBS Journal*, *276*(22), 6560–6575. https://doi.org/10.1111/j.1742-4658.2009.07363.x

Wong, S.-S., Chebib, M., Haqshenas, G., Loveland, B., & Gowans, E. J. (2011). Dengue virus PrM/M proteins fail to show pH-dependent ion channel activity in Xenopus oocytes. *Virology*, *412*(1), 83–90. https://doi.org/10.1016/j.virol.2010.12.050

Wozniak, A. L., Griffin, S., Rowlands, D., Harris, M., Yi, M., Lemon, S. M., & Weinman, S. A. (2010). Intracellular proton conductance of the hepatitis C virus p7 protein and its contribution to infectious virus production. *PLoS Pathogens*, *6*(9), e1001087. https://doi.org/10.1371/journal.ppat.1001087

Wu, Y., Canturk, B., Jo, H., Ma, C., Gianti, E., Klein, M. L., Pinto, L. H., Lamb, R. A., Fiorin, G., Wang, J., & DeGrado, W. F. (2014). Flipping in the pore: Discovery of dual inhibitors that bind in different orientations to the wild-type versus the amantadine-resistant S31N mutant of the influenza A virus M2 proton channel. *Journal of the American Chemical Society*, *136*(52), 17987–17995. https://doi.org/10.1021/ja508461m

Xia, B., Shen, X., He, Y., Pan, X., Liu, F. L., Wang, Y., Yang, F., Fang, S., Wu, Y., Duan, Z., Zuo, X., Xie, Z., Jiang, X., Xu, L., Chi, H., Li, S., Meng, Q., Zhou, H., Zhou, Y., … Gao, Z. (2021). SARS-CoV-2 envelope protein causes acute respiratory distress syndrome (ARDS)-like pathological damages and constitutes an antiviral target. *Cell Research*, *31*(8), 847–860. https://doi.org/10.1038/s41422-021-00519-4

Xia, S., Fang, P., Pan, T., Xiao, W., Zhang, H., Zhu, X., Xiao, S., & Fang, L. (2022). Porcine deltacoronavirus accessory protein NS7a possesses the functional characteristics of a viroporin. *Veterinary Microbiology*, *274*, 109551. https://doi.org/10.1016/j.vetmic.2022.109551

Xia, X., Cheng, A., Wang, M., Ou, X., Sun, D., Mao, S., Huang, J., Yang, Q., Wu, Y., Chen, S., Zhang, S., Zhu, D., Jia, R., Liu, M., Zhao, X.-X., Gao, Q., & Tian, B. (2022). Functions of Viroporins in the viral life cycle and their regulation of host cell responses [review]. *Frontiers in Immunology*, *13*, 890549. https://doi.org/10.3389/fimmu.2022.890549

Xie, S., Wang, K., Yu, W., Lu, W., Xu, K., Wang, J., Ye, B., Schwarz, W., Jin, Q., & Sun, B. (2011). DIDS blocks a chloride-dependent current that is mediated by the 2B protein of enterovirus 71. *Cell Research*, *21*(8), 1271–1275. https://doi.org/10.1038/cr.2011.112

Yang, Y., Xiong, Z., Zhang, S., Yan, Y., Nguyen, J., Ng, B., Lu, H., Brendese, J., Yang, F., Wang, H., & Yang, X. F. (2005). Bcl-xL inhibits T-cell apoptosis induced by expression of SARS coronavirus E protein in the absence of growth factors. *The Biochemical Journal*, *392*(Pt 1), 135–143. https://doi.org/10.1042/bj20050698

Ye, Y., & Hogue, B. G. (2007). Role of the coronavirus E viroporin protein transmembrane domain in virus assembly. *Journal of Virology*, *81*(7), 3597–3607. https://doi.org/10.1128/jvi.01472-06

Yu, H.-G., Sizemore, G., Smoot, K., & Perrotta, P. (2021). Detecting SARS-CoV-2 Orf3a and E ion channel activity in COVID-19 blood samples. *Journal of Clinical and Translational Science*, *5*(1), e196. https://doi.org/10.1017/cts.2021.856

Zeba, A., Sekar, K., & Ganjiwale, A. (2023). M protein from dengue virus oligomerizes to pentameric channel protein: In silico analysis study. *Genomics Inform*, *21*(3), e41. https://doi.org/10.5808/gi.23035

Zhang, R., Wang, K., Lv, W., Yu, W., Xie, S., Xu, K., Schwarz, W., Xiong, S., & Sun, B. (2014). The ORF4a protein of human coronavirus 229E functions as a viroporin that regulates viral production. *Biochimica et Biophysica Acta (BBA) - Biomembranes*, *1838*(4), 1088–1095. https://doi.org/10.1016/j.bbamem.2013.07.025

Zhang, R., Wang, K., Ping, X., Yu, W., Qian, Z., Xiong, S., & Sun, B. (2015). The ns12.9 accessory protein of human coronavirus OC43 is a viroporin involved in virion morphogenesis and pathogenesis. *Journal of Virology*, *89*(22), 11383–11395. https://doi.org/10.1128/jvi.01986-15

Zheng, L., Liu, H., Tian, Z., Kay, M., Wang, H., Wang, X., Han, H., Xia, W., Zhang, J., Wang, W., Gao, Z., Wu, Z., Cao, H., Geng, R., & Zhang, H. (2022). Porcine epidemic diarrhea virus E protein inhibits type I interferon production through endoplasmic reticulum stress response (ERS)-mediated suppression of antiviral proteins translation. *Research in Veterinary Science*, *152*, 236–244. https://doi.org/10.1016/j.rvsc.2022.07.019

Zhou, H. X., & Cross, T. A. (2013). Influences of membrane mimetic environments on membrane protein structures. *Annual Review of Biophysics*, *42*, 361–392. https://doi.org/10.1146/annurev-biophys-083012-130326

Zhou, Y., Frey, T. K., & Yang, J. J. (2009). Viral calciomics: Interplays between Ca2+ and virus. *Cell Calcium*, *46*(1), 1–17. https://doi.org/10.1016/j.ceca.2009.05.005

Zhu, Z., Wang, G., Yang, F., Cao, W., Mao, R., Du, X., Zhang, X., Li, C., Li, D., Zhang, K., Shu, H., Liu, X., & Zheng, H. (2016). Foot-and-mouth disease virus viroporin 2B antagonizes RIG-I-mediated antiviral effects by inhibition of its protein expression. *Journal of Virology*, *90*(24), 11106–11121. https://doi.org/10.1128/jvi.01310-16

SUPPORTING INFORMATION

Additional supporting information can be found online in the Supporting Information section at the end of this article.

How to cite this article: Devantier, K., Kjær, V. M. S., Griffin, S., Kragelund, B. B., & Rosenkilde, M. M. (2024). Advancing the field of viroporins—Structure, function and pharmacology: IUPHAR Review 39. *British Journal of Pharmacology*, *181*(22), 4450–4490. https://doi.org/10.1111/bph.17317